

Thesis for the Master's
degree in chemistry

Kristine Solberg

**Heavy metal levels and
mercury speciation in water,
soil and sediments in a
highly contaminated mining
area in Khaidarkan,
Kyrgyzstan**

60 study points

DEPARTMENT OF CHEMISTRY

Faculty of mathematics and natural
sciences

UNIVERSITY OF OSLO 05/2009



Acknowledgements

This master study has been carried out at the department of chemistry at the University of Oslo in the period from August, 2007 to June, 2009. The study was made possible due to the Ministry of Foreign Affairs, Department for Security and the High North, Section for Global Security Issues and CIS and their funding of the TEMP-CA project over a five year period. Especial thanks goes to Senior Advisors Solveig Rossebø and Ole Johan Bjørnøy, and the Ambassador to Central Asia, Mette Kongshem for their support through the whole project period.

First of all I would like to thank Professor Rolf D. Vogt for his guidance and help through out this study. In addition I would also like to thank Professor Grethe Wibetoe for her help and support, especially for support and good advice when things were not going as we wished in the laboratory. I would also like to thank Professor Odd Eilertsen, for realizing my trips to Kyrgyzstan in October, 2007 and May, 2008 and for the opportunity of being a part of the TEMP-CA project.

I am grateful for advice and help with the laboratory work from the technical personnel Anne Marie Skramstad and Hege Lynne. My appreciation goes also to Professor Thorjørn Larssen for good advice and assistance.

This thesis would not have been possible without the help and support, and numerous coffee breaks with my fellow students at the environmental chemistry group, in particular Marthe-Lise Søvik, Goran Khalaf and Christian W. Mohr. I would also thank “the girls”, Pernille Bohn, Ihna Stallemo and Frøydis Meen Wærsted for their tremendous work and good effort in the laboratory. It was a pleasure working with you.

Last, but not least I would like to thank my family and my fiancé, Kjell-Ove Opoft. Thank you for you endless support.

Table of contents

Acknowledgements	2
Table of contents	3
List of figures	6
List of tables	9
Abbreviations and symbols	10
Abstract	12
1. Introduction	14
1.1 Heavy metals	15
1.2 Mercury	16
1.3 Background information about Kyrgyzstan and the TEMP-CA project.....	18
1.3.1 Khaidarkan Mercury Plant (KMP).....	19
1.4 The aim of the study.....	22
2. Theory	23
2.1 Soil classification and the composition of soil.....	23
2.2 Soil chemical parameters.....	26
2.2.1 Soil pH	26
2.2.2 Redox conditions.....	27
2.3 The physico-chemical behaviour of trace metals in soils	27
2.3.1 Cation Exchange	28
2.3.2 Specific adsorption.....	28
2.3.3 Co-precipitation.....	28
2.3.4 Organic complexation	28
2.4 Heavy metals – origin, transport and bioavailability	29
2.4.1 The origin of heavy metals in the environment.....	29
2.4.2 Transport of heavy metals	30
2.4.3 Speciation and bioavailability of trace metals.....	31
2.5 Pearson’s classification of metals	32
2.5.1 Hard metal ions	32
2.5.2 Soft metal ions	33
2.5.3 Borderline metal ions.....	35
2.6 Mercury – a metal of special concern	36
2.6.1 Toxicity of Hg.....	36
2.6.2 Sources of mercury	37
2.6.3 Natural and anthropogenic releases of Hg in the environment.....	37
2.7 Mobilisation of mercury from a mercury mine.....	38
2.7.1 Atmospheric emissions.....	40
2.7.2 Aqueous transport.....	40
2.8 Theoretical background on analytical techniques	42
2.8.1 DMA-80 Direct Mercury Analyzer.....	42
2.8.2 PSA 10.035 Millennium Merlin 1631 Hg Analyser	43
2.8.3 ICP-AES Inductively Coupled Plasma Atomic Emission Spectrometry.....	43
2.8.4 Ion-exchange chromatography (IC)	44
3. Materials and Methods	46

3.1 Description of samples, sites and procedures.....	46
3.1.1 Site description	46
3.1.2 Soil and sediment sampling procedure.....	52
3.1.3 Water sampling procedure	53
3.2 Sample preparation.....	56
3.2.1 Pre-cleaning procedure.....	56
3.2.2 Grinding and sieving.....	57
3.2.3 Homogenising procedures	57
3.2.4 Dilution.....	58
3.2.5 Filtering.....	58
3.3 Instrumentation and procedures	58
3.3.1 Determination of the content of Hg in solid samples with the DMA-80	58
3.3.2 Sequential extraction procedure	59
3.3.3 Determination of heavy metal content in soil, sediment and water with ICP-AES.....	60
3.3.4 Determination of the content of Hg in water with Millennium Merlin Hg analyser	61
3.3.5 Ion chromatography (IC)	61
3.3.6 Determination of soil colours.....	61
3.3.7 Determination of dry content	62
3.3.8 Determination of total alkalinity	62
3.3.9 Soil parameters.....	62
3.4 Software for data processing.....	63
3.5 Quality control	64
3.5.1 Validation and quality control of the DMA-80 method for Hg determination.....	64
3.5.2 Accuracy and precision of the IC method.....	66
3.5.3 ICP-AES method	66
3.5.4 Accuracy of the method for determination of Hg in water with Millennium Merlin Hg Analyser	66
4. Results and discussion	67
4.1 Results and observations in Gauyang.....	67
4.2 Results and observations in Khaidarkan	68
4.2.1 Major ions in the water sampled in Khaidarkan.....	68
4.2.2 Major components of the soil and sediments sampled in Khaidarkan	69
4.2.3 Total mercury.....	70
4.2.4 Results for other associated heavy metals in Khaidarkan	78
4.2.5 Sequential extraction.....	89
4.3 Statistical interpretation	92
4.3.1 Correlation.....	92
4.3.2 Cluster analysis.....	93
4.3.3 Principal Component Analysis	95
4.4 Method development of the methods.....	98
4.4.1 Development and validation of the homogenisation procedure.....	98
4.4.2 Selection of wavelengths used in the ICP-AES analysis.....	99
4.5 Validation and quality control.....	99
4.5.1 Validation of the DMA-80 method.....	99
4.5.2 Validation of the IC method.....	102
4.5.3 Validation of the PSA 1631 method for determination of Hg in water.....	103
4.5.4 Paired t-test for the comparison of Hg measurements with DMA80 and ICP-AES	104

5. Conclusions and further work	106
6. References.....	108

List of figures

Figure 1 Trend in emissions of Hg, Pb and Cd in Europe and Central Asia from 1990 to 2005 (Data from (msc-e, 2008b)).	16
Figure 2 The location of mercuriferous belts. The location of the Hg mine in Khaidarkan is indicated by a red cross (Gustin et al., 1999).	18
Figure 3 Production of Hg at Khaidarkan Mercury Plant from 1940-1993 (Stavinskiy et al., 2001).	19
Figure 4 Production of Hg at Khaidarkan Mercury Plant from 1994 - 2005 in metric tonnes. Figures from 1994-1999 from UNEP Chemicals (2002), figures from 2000-2005 from UNEP Chemicals (2006).	19
Figure 5 Spatial distribution of emissions of Hg from Kyrgyzstan in 2006 in $\text{g km}^{-2} \text{y}^{-1}$ (msc-e, 2008a)	20
Figure 6 A hypothetical soil profile (Kang and Tripathi, 1992)	25
Figure 7 Stability field diagram for Hg. Conditions as given in appendix M.	39
Figure 8 Dominant complex species at conditions found in drainage water from a tailing pond at the studied site (See appendix M for concentrations). DNOM is omitted as this is not an important species at the site. The blue shaded area represents normal pH values in the Khaidarkan area.	41
Figure 9 Principal sketch of the DMA-80 instrumentation (Milestone, 2003)	43
Figure 10 Principal sketch of ICP-AES	44
Figure 11 Map of Kyrgyzstan. Khaidarkan is marked with a black square. Modified from ENVSEC (2007).	46
Figure 12 Filtering of metallic mercury to remove impurities after distillation	47
Figure 13 Tailing pond (left) and slag heaps (right) associated with KMP in Khaidarkan.	47
Figure 14 Satellite photo of Khaidarkan sampling site. Red dots are soil samples and blue dots are sediment samples. The red triangles represent the tailing pond (left) and slag heap (right). The purple dots represent metallurgical facilities of the Khaidarkan Mercury plant (KMP) (Google Earth, 2009b).	49
Figure 15 Satellite photo of the monitoring site, Gauyang. In this study only samples from macroplots 1, 5, 9 and 10 were used. The blue dot marked Site 1 is water sampled from the main river. The ephemeral stream dividing the monitoring field was dry during sampling and could therefore not be sampled (Google Earth, 2009a).	51
Figure 16 Installation of macroplot (left picture) and microplots (right picture).	52
Figure 17 Drainage water from slag heaps (left picture) and tailing pond (middle picture) and water used as drinking water by the locals (right picture)	54
Figure 18 Sample site location of the water sampled in Khaidarkan (Google Earth, 2009b).	54
Figure 19 Schematic presentation of the sequential extraction procedure for Hg in soil and sediment samples	60
Figure 20 Hg concentration in horizon A, horizon B and horizon C in soil sampled in the monitoring field, Gauyang. The first number in the sample name correspond to the macroplot, the second number correspond the microplot (See section procedure for description of the sampling procedure).	67
Figure 21 Hg concentration in soil and sediment samples in Khaidarkan (circles), median value (middle line) and quartiles (box ranges). The vertical black line gives the reference value for uncultivated soil ($0.1 \mu\text{g g}^{-1}$) presented by (Bradl, 2005). The purple area represents background	

values for the area ($0.15 - 0.93 \mu\text{g g}^{-1}$) (The sample “1 sed up” (8.8 mg g^{-1}) is omitted from the plot to give a better picture of the variation in the Hg levels in the other samples). The outlier in the plot is from the tailing sediments.	71
Figure 22 Total Hg concentration in soil samples in the elevation gradient up-valley and downstream from the slag heaps (situated near sample 4) and tailing pond (situated upstream of sample 6) in the Khaidarkan area.	72
Figure 23 Loss on ignition (LOI %) compared to the Hg concentration in soil samples in the spatial gradient up and downstream from the slag heaps and tailing pond in the Khaidarkan area.	73
Figure 24 Sampling sites 2 sed down (left picture) and 5 sed down (right picture).....	74
Figure 25 Apple garden irrigated with water from the nearby river (1downstream).....	75
Figure 26 Hg concentration in water samples in Khaidarkan (circles), median value (middle line,) and quartiles (box ranges). The vertical line is a reference value for streams reported by (Bradl, 2005). The concentration in the stream draining the slag heaps is omitted from the plot. The outlier in the plot is the water draining the tailing pond.....	77
Figure 27 Major complex species in the tailing water sample determined by the speciation programme medusa (Conditions is given in appendix M). The blue shaded area represents normal pH in the Khaidarkan area.	77
Figure 28 Concentration of selected heavy metals in the tailing pond sediments. The black lines represent the average background level in the area.	78
Figure 29 Concentration of selected heavy metals in the sediments in stream draining the slag heaps. The black lines represent the average background level in the area.	79
Figure 30 Concentrations of selected heavy metals in 3 sed down (left) and 4 sed down (right). Sediments sampled in the small tributary streams (2 – and 3 downstream respectively). The black lines represent average background level in the area.	81
Figure 31 Concentration of selected heavy metals in sediment sampled in the river bed of a dry flooding area (5 sed down). The black lines represent average background level in the area.....	82
Figure 32 Concentration of selected heavy metals in sediments sampled in a stream used for irrigation of the apple garden (2 sed down). The black lines represent the average background level in the area.....	83
Figure 33 Concentration of selected metals in horizon A _p (light green bar) and B _p (dark green bar) in soil sampled from an apple garden downstream from the tailing. The black lines represent the average background level of the area.	84
Figure 34 Concentration of selected heavy metals in horizon A (light green bar) and horizon B (dark green bar) in sample 6 downstream. The black lines represent the average background level of the area.	85
Figure 35 Heavy metal levels in the upper horizon of sample 1, 2, 3 and 4 sampled in an elevation gradient up-valley from the slag heaps.....	86
Figure 36 Heavy metal levels in the lower horizon of sample 1, 2, 3 and 4 sampled in an elevation gradient up-valley from the slag heaps.....	86
Figure 37 Boxplots showing concentrations of selected heavy metals in soil and sediment sampled in the Khaidarkan area (circles) median value (middle line) and quartiles (box ranges). The vertical black line gives the reference value for uncultivated soil given by (Bradl, 2005) for the respective heavy metals. The brown area represents background values for the area. See appendix N for reference and background values.....	88
Figure 38 Results from the sequential extraction procedure. In the upper figure, the fractionation of Hg is shown in percentages. The lower figure gives the total Hg concentration (The concentration of	

all the fractions added up). The letter in the sample names denotes the horizon of the soil sample. The number denotes the sample site (see Figure 14)..... 90

Figure 39 Dendogram of the soil and sediment samples in Khaidarkan based on the similarities of the heavy metals and some soil parameters..... 94

Figure 40 Dendogram of the soil and sediment samples in Khaidarkan based on the similarities of the different samples. 95

Figure 41 Loading plot of PC1 vs. PC2 for the soil and sediment samples in Khaidarkan with two clear clusters marked in the figure. 96

Figure 42 Score plot of PC1 vs. PC2 for the soil and sediment samples in Khaidarkan. Red dots represent soil samples, blue dots represent sediment samples. The green dot represents the tailing sediments. 97

Figure 43 Hg recoveries for San Joaquin soil analyzed by DMA80 99

Figure 44 Hg recoveries of San Joaquin, 280R and 277R..... 101

Figure 45 Recovery of the main anions for Fluka reference solution analyzed by IC 103

Figure 46 Recovery of Hg in four different control solutions analysed by PSA 1631 Hg analyser. 103

List of tables

Table 1 Selected metal ions classified by Pearson's classification of metal ions	32
Table 2 Short description of the soil samples	55
Table 3 Short description of the sediment samples	56
Table 4 Short description of the water samples	56
Table 5 pH and concentration of the major ions in four water samples from Khaidarkan and Gaiyang (site 1) in $\mu\text{eq L}^{-1}$	69
Table 6 Soil parameters in soil and sediments in Khaidarkan and Kara Koi	70
Table 7 Total Hg concentration in soil (i.e. not stream water sediments) collected in an elevation gradient up-valley and downstream from the slag heaps and tailing pond in the Khaidarkan area. The values are given in $\mu\text{g Hg g}^{-1}$	72
Table 8 Hg concentration in sediment samples up- and downstream from the slag heaps and tailing pond in the Khaidarkan area. The values are given in $\mu\text{g Hg g}^{-1}$	74
Table 9 Hg concentration in samples from the tailing pond sediments and of soil from a cultivated area downstream from the tailing pond. Concentrations are given in $\mu\text{g g}^{-1}$	75
Table 10 Dissolved Hg concentration in water samples in the Khaidarkan area. Concentrations are given in $\mu\text{g L}^{-1}$	76
Table 11 World average level in stream and concentration of heavy metals in water near slag heaps	80
Table 12 Result for uncertainty test when comparing measured values for the certified reference material with given concentrations of the certified reference material (CRM). Mean and STD are given in $\mu\text{g kg}^{-1}$	100
Table 13 Result for uncertainty test when comparing measured values for three certified reference materials with given concentrations of the certified reference materials (CRM). Mean and STD are given in $\mu\text{g kg}^{-1}$	101
Table 14 LOD and MDL for the DMA-80 method during total Hg analysis and analysis of fractions of the sequential extraction procedure	102
Table 15 LOD for the PSA 1631 method for Hg determination in water	104
Table 16 Comparison of Hg measurements from analysis with DMA80 and ICP-AES	104

Abbreviations and symbols

ATSDR	Agency for Toxic Substances and Disease Registry
BEC	Background Equivalent Concentration
CEC	Cation Exchange Capacity
CRM	Certified Reference Material
DDL	Diffusive Double Layer
DMA	Direct Mercury Analyzer
DNOM	Dissolved Natural Organic Material
DOM	Dissolved Organic Matter
FAO	Food and Agricultural Organization
ha	hectare (1 ha = 10,000 m ²)
IC	Ion Chromatography
ICP-AES	Inductively Coupled Plasma Atomic Emission Spectrometry
IRMM	Institute for Reference Materials and Measurements
IUPAC	International Union of Pure and Applied Chemistry
KMP	Khaidarkan Mercury Plant
LD50	Lethal Dose-50 % of population killed
MAC	Maximum allowable Concentration
MeHg	Methyl mercury
msc-e	Meteorological Synthesizing Centre - East
NFG	Norwegian Forestry Group
NFLI	Norwegian Forest and Landscape Institute
NIST	National Institute of Standards and Technology
NOM	Natural Organic matter
OC	Organic Carbon
OM	Organic matter
PCA	Principal Component Analysis
PEC	Probable Effect Concentration
PESAC	Privatisation and Enterprise Sector Adjustment Credit
PET	polyethylene tetra phthalate

PP	polypropylene
ppm	parts per million
ppma	parts per million atoms
ppt	parts per trillion
PSA	P S Analytical
SMW	Soil Map of the World
SRB	Sulphate Reducing Bacteria
STP	Standard Temperature and Pressure
TEMP-CA	Terrestrial Environmental Monitoring Project in Central Asia
UNECE	United Nations Economic Commission for Europe
UNEP	United Nations Environment Programme
USDA	United States Department of Agriculture
US EPA	United States Environmental Protection Agency
USGS	United States Geological Survey
USSR	Union of Soviet Socialist Republics
WHO	World Health Organization
Ω	ohm

Abstract

The world second largest mercury (Hg) mine and smelter, the Khaidarkan Mercury Plant (KMP) is located in Khaidarkan, a small city in a valley in Batken oblast, Kyrgyzstan. The smelter roasts locally mined cinnabar and captures the mercury by condensation. At the plant there are several slag deposits with over 500 millions tonnes of exhausted ores as well as quarry material from the mines, containing traces of Hg and associated contaminants, such as arsenic, antimony, cadmium, lead and zinc. A large tailing pond containing wastes from the smelter has also been generated. Slag heaps and tailing pond are open and exposed, potentially leading to the spread of pollutants and regional contamination of soils and waters. Lack of fences allows animals to access contaminated sites for drinking and grazing. Seepage water from the tailing drains into a tributary of the Syr Darya River, the Shaktnaya River.

Soil samples were collected along an elevation gradient on the main valley slope, and soil, sediments and water were sampled downstream from the Hg tailing area. Background samples were collected from a monitoring site located more than 10 km upstream (south) of the plant. In this study the levels of Hg in water, sediments and soil has been measured with a direct mercury analyser (DMA-80). A sequential extraction procedure was conducted in order to measure the main pools of Hg in the soil and thereby assess main mechanisms governing Hg mobility and transport. Water samples were collected in streams in the area. The water samples and extracts from the sequential extraction were analysed for concentration of Hg with a Millennium Merlin Hg analyser. In addition, the levels of heavy metals in the soil, sediment and water samples were measured with ICP-AES.

The level of Hg in soil and sediment in Khaidarkan is high, ranging from 0.4 to 8 795 $\mu\text{g g}^{-1}$. The highest value, which is somewhat extreme, was found in sediments in a small stream draining the slag heaps. Up the valley slope, values from 0.4 to 53 $\mu\text{g g}^{-1}$ were found, while downstream from the tailing pond the level of Hg ranged from 3.5 to 217 $\mu\text{g g}^{-1}$. The concentration of Hg in the tailing pond sediments was 353 $\mu\text{g g}^{-1}$. This concentration of Hg is quite high and exemplifies the poor efficiency of the waste management at the facility. The levels of other associated heavy metals are generally high, especially for antimony, cadmium and arsenic. Enhanced levels were found also for lead and zinc. It is hypothesised that the contamination of these heavy metals in the area is a result

of the anthropogenic activity of the KMP. Interpretation of statistical analysis of the data (correlation matrixes, cluster analysis and Principal Component Analysis (PCA) supports this postulation.

The sequential extraction procedure revealed that Hg is mainly present as residual Hg (as HgS or bound in silicates) in the soil and sediments. The soil samples up-valley from the slag heaps contain in addition a significant amount of strongly bound Hg (i.e. acid soluble). As the levels of Hg decrease as a function of distance from the source up-valley from the burners and slag heaps it is apparent that atmospheric emission and transport of Hg is significant. Even though a few of the downstream sediment samples contain some elemental Hg, it appears as Hg is mainly mobilised and transported from the slag heaps and tailing pond as residual Hg, in the form of colloids or particles. High level of Hg in a flooding area indicates that Hg is mobilised and transported in periodic peak flow events. The high level of dissolved Hg that was found in the drainage waters indicate that solved Hg species are also mobilised from the waste areas to the surrounding environment.

1. Introduction

Problematic definitions

The concept “heavy metal” is a somewhat problematic term. It has never been defined by an authoritative body such as International Union of Pure and Applied Chemistry (IUPAC), but many have attempted to give a definition. The term is often used when addressing potentially toxic metals. None of the following definitions takes this into account. The term has been widely and inconsistently used since Bjerrum was the first to define heavy metals according to the Oxford English Dictionary as “metals with a density greater than 7 g cm^{-3} ” in Bjerrum’s *Inorganic Chemistry* in 1936 (Duffus, 2002). Other definitions have been presented, e. g. by the United Nations Economic Commission for Europe (UNECE) as “those metals or, in some cases, metalloids which are stable and have a density greater than 4.5 g cm^{-3} and their compounds” (UNECE, 1998). Definitions have also been made according to atomic number, atomic weight and chemical properties (Duffus, 2002). Nevertheless the scientific community does not seem to come to any consensus. A more relevant classification of metals can be the Pearson’s classification of hard, borderline and soft metals which will be presented later in this study. In spite of its inconsistency, the traditional term “heavy metals” will be applied in this study as defined by UNECE.

“Speciation” is another term that is used inconsistently in the scientific community. It is often used when addressing “fractionation”. In this study the definition given by IUPAC will be employed: “Distribution of an element amongst defined chemical species in a system” where chemical species is defined as: “specific form of an element defined as to isotopic composition, electronic or oxidation state, and/or complex or molecular structure” (IUPAC, 2000). “Fractionation” is defined as a “process of classification of an analyte or a group of analytes from a certain sample according to physical (e.g., size, solubility) or chemical (e.g., bonding, reactivity) properties” (IUPAC, 2000).

1.1 Heavy metals

Heavy metals have been used by mankind for thousands of years and consequently there have been large anthropogenic releases to the environment. Some of the elements e. g. mercury (Hg), can be transported long distances by air masses and therefore pose a threat even to living beings far from any emission source (Clarkson, 2002).

Heavy metals associated with the most adverse health effects to the human population are lead (Pb), mercury (Hg), cadmium (Cd) and arsenic (As). Pb has been used for at least 5000 years in building materials, as pigment on ceramics and in welding pipes used for transport of water. In ancient Rome, lead acetate was used to sweeten old wine and may have contributed to the fall of the Roman Empire. During the last century the use of Pb as an additive in petrol has led to large emissions to the environment. This trend has decreased during the last few decades due to the introduction of unleaded petrol (Figure 1) (Järup, 2003). Hg is a metal that has fascinated mankind for millenniums. Due to its unique physical properties it has found many application areas. There is archaeological evidence that Hg has been used for at least 3 500 years (Nriagu, 1979). This highly toxic metal was e. g. for a long time used as a treatment for syphilis as well as other medicinal applications, for instance as a preservative for vaccines (Hylander and Meili, 2003; Järup, 2003; Steinnes, 1995). Even though the hazards related to the use of heavy metals have been known for a long time, the global uses and exposure of heavy metals have steadily increased since the middle of the 19th century until the end of the 20th century where the trend has reversed in most developed and some developing countries (Järup, 2003). Figure 1 shows an example of the declining trend in emissions of Hg, Cd and Pb by giving the emission in Europe and Central Asia after 1990.

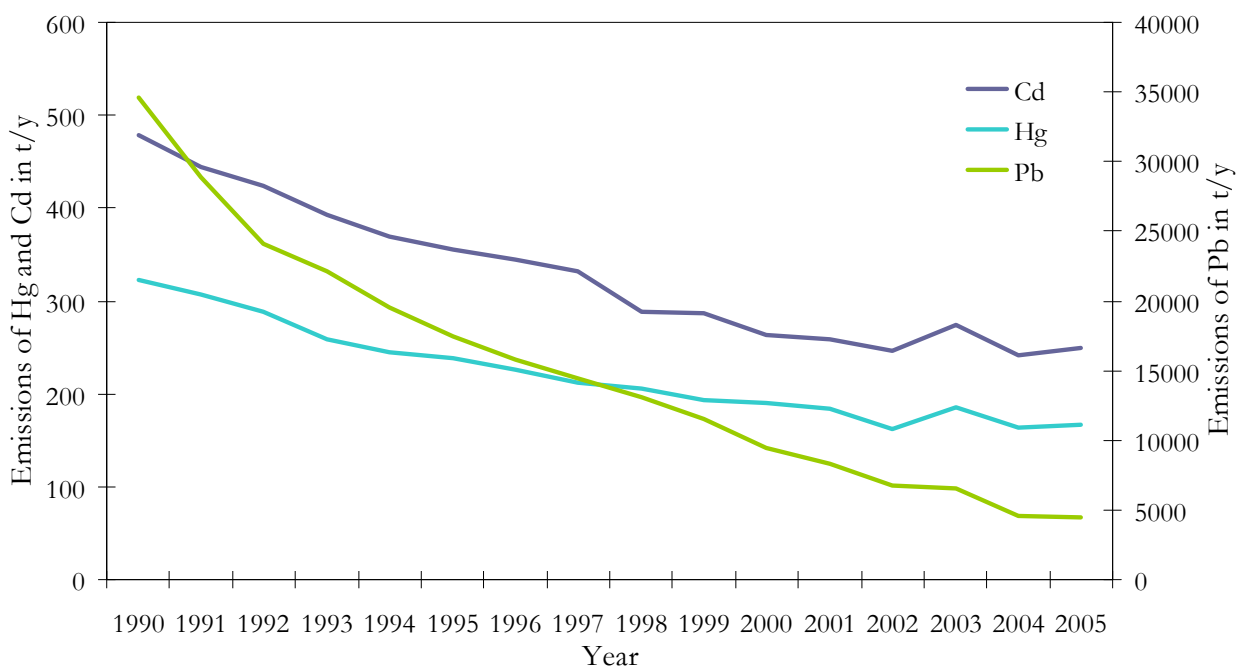


Figure 1 Trend in emissions of Hg, Pb and Cd in Europe and Central Asia from 1990 to 2005 (Data from (msc-e, 2008b)).

1.2 Mercury

Hg is a heavy metal of global concern due to its long residence in the atmosphere (up to one year) (Clarkson, 2002; Krabbenhoft et al., 2005). Hg released to the atmosphere from a point source can therefore travel great distances before being deposited. Once deposited the Hg may be readily re-emitted after volatilisation. This re-volatilization is temperature dependant and is less prone to occur in colder regions. Hg will therefore have a tendency to accumulate in colder regions were the re-emission is slower and the condensation from the atmosphere is favoured. This repeated re-emission is called the grasshopper-effect (Wania and Mackay, 1996).

Hg is potentially one of the most toxic metals to organisms. Hg occur in three oxidation states; elementary Hg^0 , mercurous Hg^+ and mercuric Hg^{2+} . The toxicity and mobility of Hg depends on the state. In the organism it can induce severe damage to the central nervous system as well as the kidney. Its effect on the central nervous system makes it especially toxic to developing foetuses

(Clarkson and Magos, 2006). Toxic Hg compounds are found in all three of the oxidation states, but the most toxic Hg compound is found as mercuric Hg (Clarkson and Magos, 2006). The most toxic Hg compounds is considered to be the organomercurials and especially methyl mercury (CH_3Hg^+), often referred to as MeHg, and dimethylmercury (Clarkson and Magos, 2006; Gochfeld, 2003). The toxicity of Hg has been known for years, but it was first in 1956, after the terrible incident in Minamata, Japan where thousands of people were poisoned, that the extent of the problem was really understood. MeHg, produced as a by-product of acetaldehyde synthesis, was released from a chemical factory to the Minamata bay for several years causing MeHg to accumulate in fish and other seafood in the bay. Thousands of inhabitants were thereby poisoned by MeHg since the local seafood was the staple food source for the local communities, so MeHg poisoning of the inhabitants was the result. This was later referred to as the Minamata disease. Another serious event involving Hg took place in Iraq in 1971. This incident was a result of the human consumption of grain treated with organomercurials fungicides (Gochfeld, 2003; Honda et al., 2006).

As the awareness of Hg's toxicity has increased the use and production has been given restrictions. Norway was the first nation to get a ban against the use of Hg in products with a few exceptions in 2008 (Ministry of the Environment, 2007) and is followed by Sweden in June 2009 (Ministry of the Environment, 2009). Today, the main global uses of Hg are as a catalyst in the production of chlorine gas and caustic soda, as an amalgamator in the extraction of gold, and in batteries and electrical switches. Although banned in many countries (e.g. Norway, Sweden and Denmark), Hg is still used worldwide as amalgams in dental fillings (ATSDR, 1999; Ministry of the Environment, 2007).

In some parts of the world there are natural enriched levels of Hg in the ground. These areas are located in areas that are called mercuriferous belts and are associated with plate tectonic boundaries (Gustin et al., 1999). An overview of the mercuriferous belts are shown in Figure 2. In these areas all mineralogical activities as well as burning of fossil fuels will lead to enhanced emissions of Hg compared to similar activities in other parts of the world.

Releases of Hg related to the primary Hg production have historically been substantial, but have recently decreased as many of the Hg mines have shut down. Hylander and Meili (2003) estimated accumulated historic Hg emissions to roughly 10 000 tonnes and recent annual Hg emissions to the

atmosphere associated with Hg mines to be only 10-30 tonnes. This estimate is only considering direct emissions to the atmosphere. The total emissions of Hg as a result of Hg mining are larger due to the indirect emissions originating from the mining operations. Hg may be mobilised from mine tailings and other waste areas and volatilisation of elemental Hg and other volatile Hg compound from soil and surface waters may be a result. There are in addition large emissions related to waste incineration (Hylander and Meili, 2003).

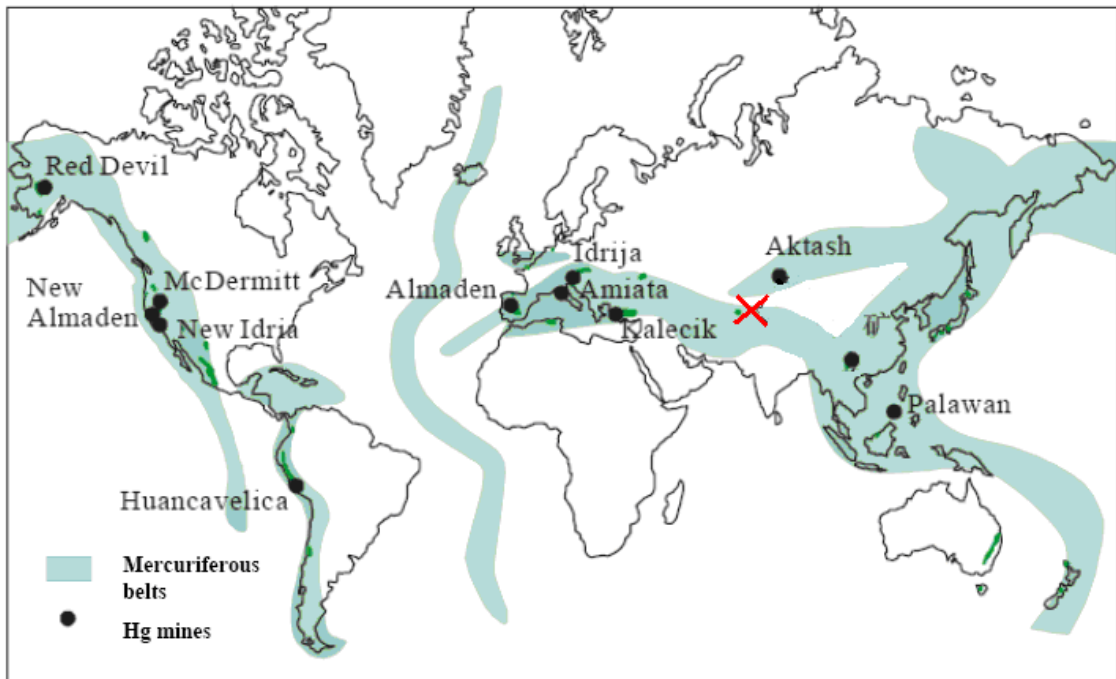


Figure 2 The location of mercuriferous belts. The location of the Hg mine in Khaidarkan is indicated by a red cross (Gustin et al., 1999).

1.3 Background information about Kyrgyzstan and the TEMP-CA project

Kyrgyzstan is a small mountainous country located in Central Asia. The young country has been independent since the liberation from the Soviet Union in 1991. At present Kyrgyzstan is the second largest producer of primary Hg and the only major Hg mine still operating in the world is located here (Marked with a red cross in Figure 2) (USGS, 2008).

1.3.1 Khaidarkan Mercury Plant (KMP)

In 1914 the world's second largest antimony-mercury deposit was discovered in Khaidarkan. The KMP was built on the base of this deposit in 1942. KMP has until now extracted 40 000 tonnes Hg accounting for 40-100% of the total production of Hg in the former USSR (64% in the late 1980s) (Stavinskiy et al., 2001; Zozulinsky, 2007). The production of Hg from KMP is given in Figure 3 and Figure 4. The figures represent the period before and after the collapse of the USSR, respectively.

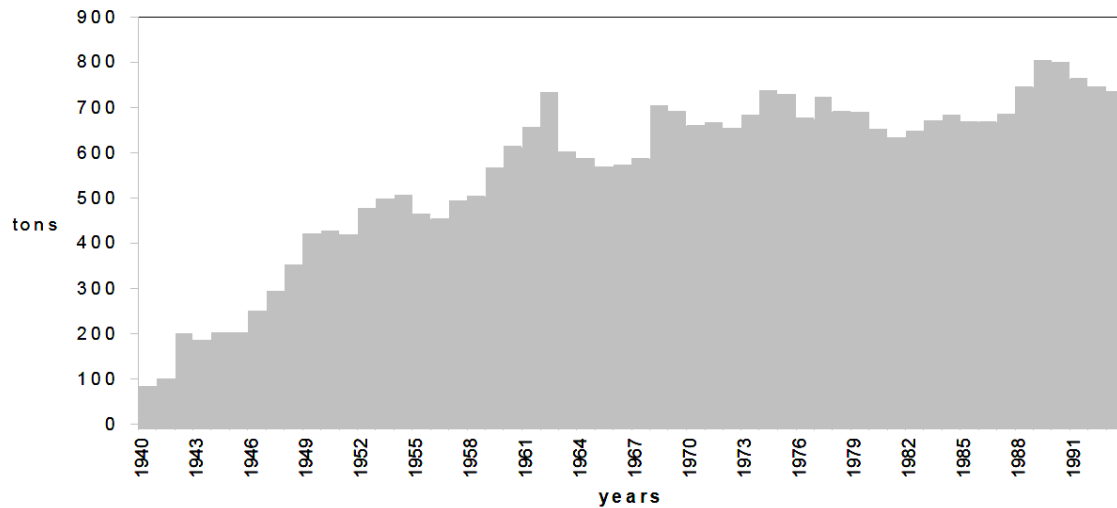


Figure 3 Production of Hg at Khaidarkan Mercury Plant from 1940-1993 (Stavinskiy et al., 2001)

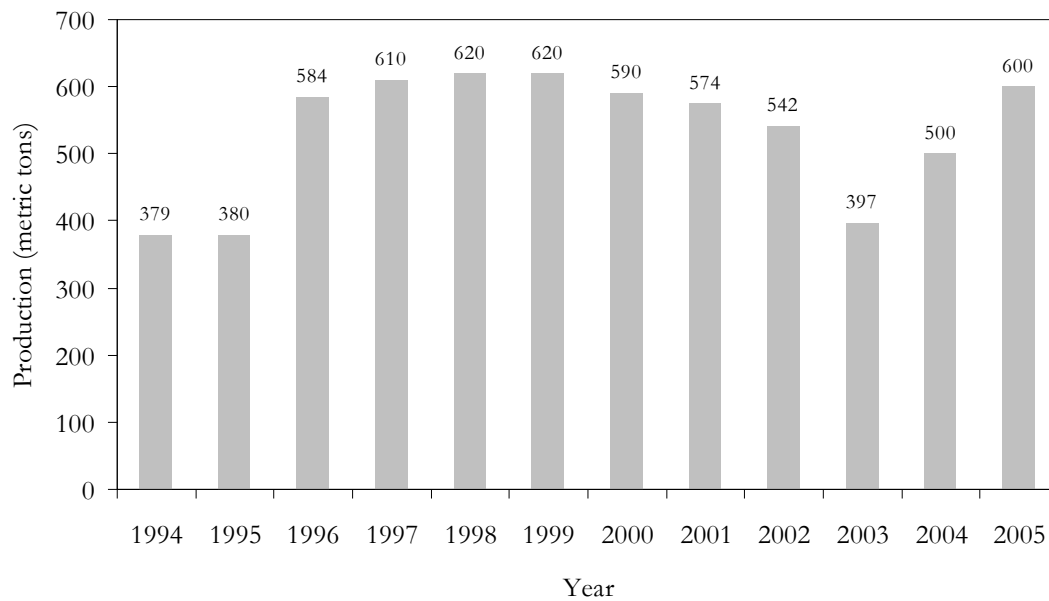


Figure 4 Production of Hg at Khaidarkan Mercury Plant from 1994 - 2005 in metric tonnes. Figures from 1994-1999 from UNEP Chemicals (2002), figures from 2000-2005 from UNEP Chemicals (2006).

After the collapse of the USSR the plant lost its financiers, the production fell drastically and the plant was declared bankrupt. In 1994 the plant became competitive again due to the support from PESAC International Program and the production rose to around 600 metric tons annually from 1996 (Stavinskiy et al., 2001).

Due to lack of monitoring data on releases of Hg from Kyrgyzstan it is difficult to conclude on Kyrgyzstan's contribution to the global anthropogenic releases of Hg. Some estimates have been made, but the uncertainties of the estimates are large and probably underestimated. An assessment of the spatial distribution of Hg emissions from Kyrgyzstan in 2000 is presented in Figure 5. The total Hg emission from Kyrgyzstan in 2000 was estimated to 2.1 tonnes (msc-e, 2008a). By comparison, China emitted 605 tonnes Hg in 2000. This represented 28% of the total Hg emissions (Pacyna et al., 2006). Another estimate by Kakareka et al. (2004), states that the Kyrgyz republic emitted 36.1, 19.2 and 30.8 tonnes Hg per year in 1990, 1995 and 1997 respectively.

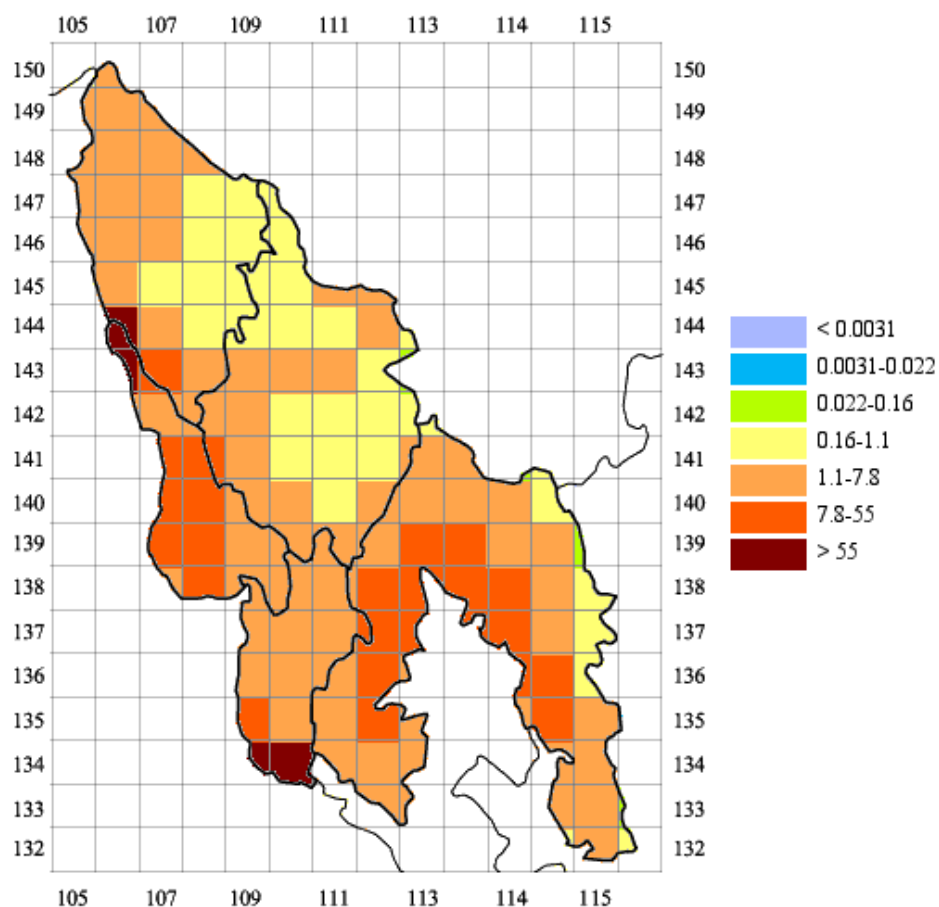


Figure 5 Spatial distribution of emissions of Hg from Kyrgyzstan in 2006 in g km⁻² y⁻¹ (msc-e, 2008a)

A previous study of Hg contamination by Sharshenova et al. (1995) in the area around the KMP plant in Khaidarkan showed levels 13 times higher than the Maximum Allowable Concentration (MAC) of Hg in soil. The concentrations of Hg in vegetables and fruit grown within the city of Khaidarkan exceeded the MAC with a factor of 10. The concentrations in atmospheric air and drinking water did not exceed the MAC. The study reports background values of Hg in soil, drinking water and air of 0.39 mg kg^{-1} , $0.075 \text{ } \mu\text{g L}^{-1}$ and 0.95 ng m^{-3} respectively (Sharshenova et al., 1995).

Terrestrial Environmental Monitoring Project in Central Asia (TEMP-CA)

The TEMP-CA project is a cooperation project between NFG – Norwegian Forestry Group and the forest- and environmental authorities in Central Asia (Kyrgyzstan, Tajikistan, Uzbekistan and Kazakhstan). The project is funded by Ministry of Foreign Affairs, section of Global Security and Issues and CIS. Kyrgyz scientists at the National Academy of Sciences and different universities are responsible for coordination of the activities within Central Asia through a non-profit public foundation. “Relascope” together with the Norwegian lead institute, NFLI, the Norwegian Forest and Landscape Institute. University of Oslo, Department of Chemistry, participate in the project as lead partner on the working package of environmental chemistry. The main goal of the project is to establish a forest- and environmental monitoring program for environmental assessments in Central Asia around Ferghana Valley. The project will give a scientific basis for future decision making on abating land degradation and pollution control and may contribute to an enlarged focus on the soil and water management. The project has four main focus areas; soil structure, soil chemistry biodiversity and forest vitality. This study is related to the soil chemistry part. The focal point of this study has been on the levels of contaminants, with emphasis on Hg, near and around the industrial Hg processing area, the KMP and its associated waste areas.

1.4 The aim of the study

As described in section 1.3.1, the TEMP-CA project has four focus areas. In this study only one of the focus areas will be addressed, namely the soil chemical part. Khaidarkan is a relatively unexplored area regarding heavy metal levels, despite that it is likely highly contaminated as indicated by previous studies. The main objective of the study is therefore to generate a better measure of the heavy metal levels and their spatial distribution in the vicinity of the operating Khaidarkan Mercury Plant (KMP) with special attention on Hg. A remote TEMP-CA monitoring site (Kara Koi) has been used as a reference on the heavy metal levels. At the Gauyang monitoring site some samples were sampled with the purpose to be analysed for Hg and give a background level of Hg in the area. This pilot study of one of many heavy metal hotspots in the area has been conducted in order to get the attention to the problem and hopefully result in funding for an environmental audit and appropriate remediation actions.

Around the KMP tailing area the environment is expected to be highly contaminated by Hg, especially downstream from the tailing area and near the slag heaps due to leaching of Hg with seepage water. The levels of Hg are also expected to be higher than the world average at the TEMP-CA monitoring sites due to the areas situation in the mercuriferous belt. The levels in Gauyang are probably higher than in Kara Koi as a result of shorter distance from the anthropogenic emission sources. Other heavy metals often found associated with sulphur (soft metals) are similarly expected to be higher than background values in these areas as the Hg is mined from a sulphide deposit. It is hypothesised that the Hg levels in the environment are high close to the point sources and that the concentration in the soil is high downstream of the KMP tailing where leaching of Hg with seepage water comes in addition to emissions to air.

Data on the size of pools of Hg in the soil and the speciation of Hg is important in order to assess the mobility and transportation of Hg. A sequential extraction of Hg in some of the soil and sediment samples has been conducted in order to try to conclude on how Hg is mobilised and transported from the point source to the surroundings, deposited and accumulated in the local environment.

2. Theory

2.1 Soil classification and the composition of soil

Soil is what covers the uppermost part of the earth except on bare rock, ice and glaciers and waters. It is a natural media for plant growth and consists of solids, in the form of minerals and organic matter, liquid and gases. It is characterised by having soil horizons or layers that is different from that of the parent material as a result of additions, losses, transfers and transformations of energy and matter and/or by the ability to support rooted plants in a natural environment (USDA, 1999).

Pedogenesis is the concept of soil formation. The development of soil is influenced by some soil forming factors were the most important are climate, vegetation and time. Human influences, topography and parent material can also influence the process. These factors will contribute in the development of different soil profiles which is characterised by certain horizons or layers. The Food and Agricultural Organization of the United Nation (FAO) has developed a system¹ of classification of the different soil profiles and published in 1974 a Soil Map of the Wold (SMW) which consists of soil information from all over the world organised in 26 different major soil groupings or soil profiles. In 1990 this system was revised to the globally applicable FAO-Unesco Soil Classification System (FAO, 2001). The main soil profiles in the sampling areas in Khaidarkan and Gauyang are umbrisol and cambisol.

Umbrisols are defined as acid soils with a thick, dark topsoil rich in organic matter. Umbrisols occur mostly in cool, humid and mountainous regions with little moisture deficit. The soil profile can be AC or A(B)C and the characteristic feature of the soil is that it is has good drainage, is medium-textured with a dark, acid surface horizon rich in organic matter (FAO, 2001). Appendix Q-1 gives the soil colour of the samples from Gauyang and Khaidarkan. It is a clear trend of dark coloured topsoil (sample names containing A). The texture of some of the soil samples is given in

¹ The FAO-Unesco soil classification system is only one of many soil classification systems such as USDA Soil Taxonomy and Canadian system of soil classification among others.

Table 2 and is medium textured. It was also observed a large content of organic matter in the topsoil during sampling.

Cambisols are defined as weakly to moderately developed soils. The occurrence of cambisols is worldwide, but it is mostly found in temperate regions. The profile has typically an ABC horizon sequence with an A-horizon of ochric, mollic or umric type over a cambic² B-horizon. The colour of the B-horizon is normally yellowish-brown or in some cases intense red. The soil texture is loamy to clayey. Most cambisols have good drainage, good water holding capacity, a high porosity and good structural stability (FAO, 2001). In Gauyang and Khaidarkan the soil colours are typically yellowish or greyish brown in the B- and C layers (Appendix Q-1) and the soil texture is loamy to clayey (Table 2).

It is important to differentiate between organic soil and mineral soil in order to understand mobility and transport of heavy metals in soils. Organic soil layers are mostly found in the uppermost part of a soil profile (Figure 6). Some natural organic material (NOM) can be present in mineral horizons as well, but for a soil to be characterised as organic soil material it must contain more than 20 % organic matter (OM) by weight (FAO, 2001). The amount of NOM depends on climatic conditions, topography and the inorganic soil components. Humus is an important intermediate product in the decay of organic substances. Humus is subdivided in three categories; humin, humic acids and fulvic acids. These differ in molecular size and number of functional groups, hence in solubility (vanLoon and Duffy, 2005). Fulvic and humic acids and humins contribute to the cation-exchange capacity (CEC) of the soil (see section 2.3.1) and to the binding of heavy metal ions and other environmental toxins, due to functional groups such as phenol-, carboxyl- and hydroxyl groups (Fergusson, 1990). These processes will be further addressed in section 2.3.

² An **ochric** horizon is a surface horizon lacking fine stratification and which is either light coloured, or thin, or has a low OC content, or is massive and hard when dry. A **mollic** horizon is a well structured, dark coloured surface horizon with a high base saturation and a moderate to high content in OM. An **umbric** horizon is a thick, dark coloured, base-desaturated surface horizon rich in OM. A **cambic** horizon is a subsurface horizon showing evidence of alteration relative to the underlying horizons. **FAO.** (1998). Food and Agriculture Organization. Word reference base for soil resources, (ed. J. A. Deckers O. C. Spaargaren F. O. Nachtergaele L. R. Olderman and R. Brinkman).

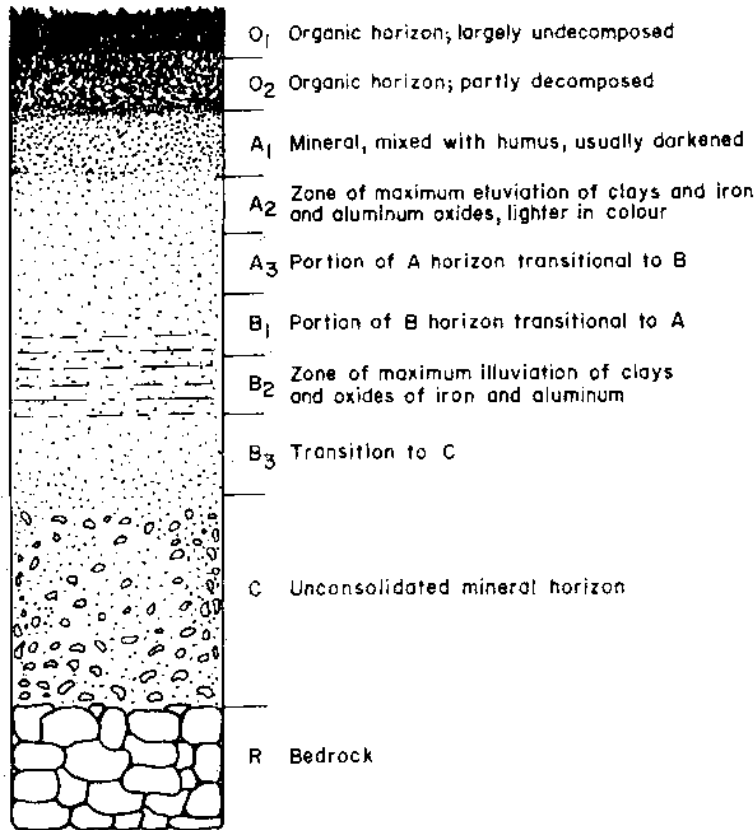


Figure 6 A hypothetical soil profile (Kang and Tripathi, 1992)

Most soils are dominantly mineral material. Mineral soil is soil that contains less than 20 % OM by weight (FAO, 2001) (A-, B- and C-horizons in Figure 6). The mineral soil consists of primary minerals, clays, oxides and hydroxides, carbonates and other minerals. In the Khaidarkan area the bedrock is mainly sedimentary minerals with conglomerate, limestone and sandstone. These minerals contain large amounts of carbonates. The carbonates will contribute to a rise of the pH of the soil due to the dissolution of carbonates (see section 2.2.1) The pH in the study area is indeed in the neutral to alkaline range (Appendix H-1).

The clay minerals represent a small, but important component of soils. They are important in regards to the fate of heavy metals in the environment because the large surface area of clays and the negative charges leads to a high metal binding capacity. There are three main types of clays that differ in their structural arrangement of octahedral AlO_6 -sheets and tetrahedral SiO_4 -sheets; 1:1 clays, such as kaolinite, 2:1 clays, such as montmorillonite and 2:2 clays such as chlorite.

Clays have the ability to adsorb metal ions by their outer hydroxyl groups according to equilibrium equation 1



The clay surface is negatively charged due to isomorphic substitution and may also be negatively charged due to protonation and deprotonation of pH sensitive functional groups resulting in adsorption sites for heavy metal ions (Equation 2) (Fergusson, 1990).



The surface negative charge will lead to electrostatic attraction of cations to form a diffusive double layer (DDL). These counter-ions can be replaced by the major cations in the soil solution (such as calcium (Ca^{2+}), magnesium (Mg^{2+}), sodium (Na^+) and potassium (K^+)) (vanLoon and Duffy, 2005).

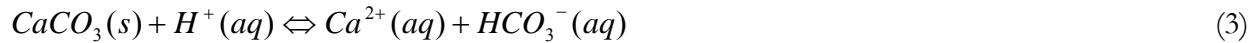
Soil also consists of an amount of water and air that fill up the interstitial spaces between the soil colloids (Fergusson, 1990). Soil pore water is important governing both the transport of heavy metals and the bioavailability of heavy metals. Plants take up most nutrients from the soil pore water and the content of heavy metals in the soil solution is therefore of great importance. It is often therefore assumed that dissolved heavy metals are readily available to organisms and the soluble metal complexes are important when addressing mobility of metals (Cancès et al., 2003).

2.2 Soil chemical parameters

2.2.1 Soil pH

Soil pH is one of the key parameters governing and explaining chemical behaviour of metals and other constituents in the soil. Soil pH is a measure of soil acidity and applies to the H^+ concentration in solution present in soil pores which is in dynamic equilibrium with ions in the DDL (Alloway, 1995c). Base cations (such as Ca^{2+} , Mg^{2+} , Na^+ and K^+) in the DDL will increase the pH when released to the soil solution (Alloway, 1995c; Fergusson, 1990). Soil pH depends on the composition

of soil. Soils rich in carbonates will usually have a high soil pH because carbonates have the ability to neutralize acidity (Equation 3). Soils with large fraction of humic substances will have a lower pH because humic acids have a wide variety of functional groups as phenols and carboxyl groups (Alloway, 1995c; vanLoon and Duffy, 2005).



Generally heavy metal cations are more mobile under acid conditions than neutral to alkaline conditions. It has been found that high pH favours the retention of e.g. cinnabar, being more stable at high pH (Higuera et al., 2003).

2.2.2 Redox conditions

Soil pH and redox conditions are closely related. Changes in redox potential will lead to changes in pH. Reducing condition will normally result in an increase in soil pH and the pH will decrease under oxidising conditions. Redox conditions are important when considering the mobility of heavy metals due to difference in mobility at different oxidation states. HgS is e.g. very stable in most conditions, but is more soluble in oxidizing than reducing conditions (Lottermoser, 2003). The release of Hg from cinnabar may occur under the combined conditions of oxidising conditions, low pH and a high concentration of Cl⁻. The solubility of HgS may also increase somewhat under extreme reducing conditions and a high pH (Piao and Bishop, 2006; Wollast et al., 1975). Redox conditions are also important regarding the microbial methylation of certain metallic and metalloid pollutants such as As, Hg, Sb and selenium (Se). Anoxic conditions will enhance the microbial activity of microorganisms with anaerobic respiration and can lead to the formation of e.g. the very toxic compound, MeHg (Alloway, 1995c; Celo et al., 2006).

2.3 The physico-chemical behaviour of trace metals in soils

The behaviour of heavy metals in soil is highly dependant on the soil processes and the properties of the soil. Metal ions can be adsorbed from the liquid phase by soil constituents by many different

mechanisms and this has a large influence on the mobility and the bioavailability of the metal (Alloway, 1995c). These processes will be addressed in the following subchapters.

2.3.1 Cation Exchange

The adsorption of metal cations to soil constituent depends on the negative charge on the surfaces of the soil colloids. Exchange between counter-ions in the DDL and the metal ions in solution is referred to as ion exchange (Alloway, 1995c). The Cation Exchange Capacity (CEC) of a soil is a quantitative assessment of the ability of a soil to interact with cations in the solution. CEC is defined as the sum of positive charge associated with the negative surface colloids of a soil. Of organic and mineral soil, organic soils have the largest contribution on the CEC value of the soil. 2:1 clays contribute most to a large CEC of the different types of clay (Alloway, 1995c).

2.3.2 Specific adsorption

Heavy metal cations and anions can be partly covalently bound to lattice negatively charged functional groups. This is referred to as specific adsorption. The metal ions will form inner-sphere complexes with surface ligands (Alloway, 1995c). The CEC of the soil is a good indication of the extent of adsorption occurring in the soil, but due to specific adsorption, the adsorption is often far greater than what is to be expected by the CEC value of the soil (Alloway, 1995c).

2.3.3 Co-precipitation

Co-precipitation is the simultaneous precipitation of a chemical agent in combination with other elements. The co-precipitation is not dependent on mechanism or rate (Alloway, 1995c). A relevant example of co-precipitation is the precipitation of Hg and other elements on suspended particles in streams.

2.3.4 Organic complexation

Humic substances are strong complexing agents of metal ions. In addition to cation exchange reactions, the solid-phase humic matter can form specific chelate complexes with metals. These coordinate complexes are formed with the functional groups of the humic matter. This can lead to

an accumulation of heavy metals in the organic forest floor horizon. Some metals have a higher affinity to complexation to organic matter than others. This will be further addressed in section 2.4. Also the dissolved natural organic matter (DNOM) can bind metal ions and thereby prevent the metal from being adsorbed to the soil organic matter or precipitated, which will lead to an enhanced mobility of the metal (Alloway, 1995c). DNOM plays an important role in the mobilisation of Hg from soil (Ravichandran, 2004).

2.4 Heavy metals – origin, transport and bioavailability

2.4.1 The origin of heavy metals in the environment

Heavy metals occur naturally in the earth's crust. They are incorporated in primary minerals by isomorphic substitution of the major ions in the crystal lattice during the cooling of the magma (Alloway, 1995b; Bradl, 2005). Sedimentary rocks, such as sandstone, shale and limestone, are formed by the lithification of primary minerals, secondary minerals as clays or chemical precipitates such as CaCO_3 . The sedimentary rocks comprise almost 75% of the rocks at the earth's surface and are important soil parent materials. Their content of heavy metals is determined by the rocks adsorptive properties as well as the mineralogical properties. The concentration of heavy metals in the water where the sediments were deposited is also of importance. Soil will naturally contain an amount of heavy metals given mainly by the concentration in the parent material. As described in section 1.2, Hg is enriched in the bedrock in certain parts of the world as a result of tectonic activities. This is the case in Khaidarkan where Hg is found in ores in sedimentary deposits as HgS. Hg is a chalcophile³ element and are likely to occur in sulphide deposits (Alloway, 1995b).

Apart from natural contribution of heavy metals in soil there is a significant anthropogenic contribution, mainly from industrial and agricultural activities. The anthropogenic component is in some regions and for some metals larger than the contribution from natural sources (Bradl, 2005). The major industrial drivers of anthropogenic releases of heavy metals are fossil fuel combustion, mining activities, metallurgical and chemical industries, waste disposal, electronics, shooting and

³ A chalcophile element is a sulphur-loving element. It will have a high affinity for sulphur and normally occur in sulphide deposits. Chalcophile metals are a part of the Goldschmidt's geological classification from 1922.

military operations. Agricultural activities contribute to the overall heavy metal loading to the environment through the spreading of fertilisers, pesticides and wood preservatives and sewage sludges (Alloway, 1995b; Bradl, 2005).

2.4.2 Transport of heavy metals

Even though a toxic metal is present in a significant amount in the environment it does not necessarily pose a risk. If an element is present in a stable form (e.g. it is buried in the crystal silicate lattice of a mineral or strongly bound to e.g. sulphide) it will not affect the surroundings markedly. The potential for or actual transport of metals is therefore important from an environmental point of view.

Water is an important medium for transport of metals. The water chemistry in surface waters is to a large degree influenced by the type of rock and soil in the watershed. Key parameters that influence the composition of the water are pH and redox conditions. Climate (esp. temperature and precipitation), adsorption or desorption processes (esp. cation exchange), dilution, evaporation and organisms present are important governing processes and factors controlling the chemistry of the surface water system. (Bradl, 2005) The pH is a key parameter determining the mobility of a metal due to its control on the extent of hydrolysis. In low pH environments most metals are in a more aqueous form and hence will be more mobile than in neutral to alkaline environments. The soil influences the pH of the water in the watershed. If the water passes through soil rich in limestone (CaCO_3) the pH of the water will be strongly buffered to a pH around 8 due to carbonate solubility and bicarbonate buffering (Equation 4 and 5).



If, however, it has drained through soils rich in poorly weatherable granite minerals or quartz sandy deposits, it will develop a pH closer to 6 (Bradl, 2005). Dissolved natural organic material (DNOM), rich in fulvic and humic acids will lead to a pH decrease in the stream water if the water body is poorly buffered. In some streams the pH may drop to around 4 during high discharge periods. The acidic character of humic material is mainly associated with the functional groups and then especially

carboxylate and phenolic groups. The carboxyls will be deprotonated to a large degree in natural waters due to its pK values in the range between 2.5 and 5 (vanLoon and Duffy, 2005).

In the soil and groundwater there are several possible fates for metal ions that have entered the aqueous system. Solved metal ions are easily taken up by plants, but can also be sorbed onto mineral phases, by complexation or sorption on to oxides, clay minerals and organic matter (OM). DNOM is mobile in groundwater systems. Complexation of heavy metal ions by DNOM will therefore increase the mobility of the metal ions. At the soil surface a further route of transport can be by surface soil erosion or as wind-blown dust (Bradl, 2005). Volatile metals, especially Hg, but also metalloids such as As and antimony (Sb) can be liberated to the atmosphere by vaporisation from land and surface waters. This is particularly an important transport mechanism during forest fires.

When in the atmosphere heavy metals can be long-range transported as gases, aerosols or particulates by prevailing air currents. The residence time, and thereby the transport distance in the atmosphere vary, depending on reactivity and state (gas or particle). In the atmosphere the metals may be transformed through chemical reactions and will ultimately be precipitated, either by wet or dry deposition over water or land (Bradl, 2005).

2.4.3 Speciation and bioavailability of trace metals

The elements ability to be mobilised and transported between the environmental compartments and made potentially available is directly related to its speciation. The species that are available for uptake in organisms are considered to be the bioavailable fraction. The term bioavailability reflects the rate and amount of toxic substances that may be taken up in an organism. The elements speciation is therefore an important issue regarding both mobility and the metals toxicity. Soluble heavy metal complexes and organometallics like HgCl_2 and MeHg, respectively, are examples of more bioavailable species of Hg than e.g. silicate bound Hg or HgS in ore deposits.

2.5 Pearson's classification of metals

The Hard-soft acid-base principle was presented by Pearson already in 1963. Cations can be classified as hard, borderline or soft acids according to this principle (Table 1). The principle classifies Lewis acids by taking into account the compounds binding preferences towards different types of Lewis bases. Hard acids will tend to bind to hard or nonpolarisable bases and soft acids to soft or polarisable bases. The features that bring out hard acid behaviour are small size and high positive oxidation state. Soft acids are often large and have low or zero oxidation state (Pearson, 1963). In Table 1 the heavy metal ions that will be addressed in this study have been classified according to the hard-soft acid-base principle and the following subchapters gives a short theoretical basis on these heavy metals.

Table 1 Selected metal ions classified by Pearson's classification of metal ions⁴

Hard	Borderline	Soft
As ³⁺	Ni ²⁺	Cu ⁺
VO ²⁺	Cu ²⁺	Ag ⁺
	Zn ²⁺	Hg ⁺ , Hg ²⁺ , CH ₃ Hg ⁺
	Pb ²⁺	Cd ²⁺
		RSe ⁺

2.5.1 Hard metal ions

Due to their preference to hard Lewis bases, the following metals and metalloids have a high affinity for oxygen and F-containing ligands (vanLoon and Duffy, 2005).

Arsenic

As is a highly toxic metalloid. Probably one of the biggest cases of mass poisoning in history came as a result of high levels of As in groundwater used for drinking water in Bangladesh (Appelo and Postma, 2007). In soils, As occurs mainly as arsenate, AsO₄³⁻ under oxic conditions. As species is strongly sorbed to clays, oxides and hydroxides of iron and manganese and OM. The mobility of the metalloid increases under reducing conditions. This can be partly due to dissolution of iron oxyhydroxides that will lead to release of sorbed As species (O'Neill, 1995).

⁴ Pearson (1973)

The largest anthropogenic input of As is due to smelting of copper (Cu) (As minerals is found associated in Cu-ores) while coal combustion is the next most significant driver (O'Neill, 1995). High levels of As have also been recorded in soils in the vicinity of metal processing plants, in soils where As compounds has been used as pesticides and where arsenic ores are mined (Fergusson, 1990). As can undergo methylation to organometallic compounds, but in contrast to other metals forming organometallic compounds (e.g. HgCH_3^+ and SeCH_3^+), the majority of the organic As compounds are less toxic than the inorganic compounds (O'Neill, 1995).

Vanadium (V)

The main anthropogenic emissions of V to the atmosphere are from fossil fuel combustion. Soil and water receives the largest anthropogenic burden from certain fertilisers and from slag heaps or mine tailings.

The transport and partitioning of V between water and soil is strongly influenced by pH, redox potential and the presence of particulates. Contrary to most other heavy metals V is more mobile in neutral to alkaline conditions (ATSDR, 1992). With a typical hard metal behaviour, the most common species of V in fresh water are associated with oxygen. VO^{2+} and $\text{VO}(\text{OH})^+$ are the main vanadyl species present under reducing conditions and H_2VO_4^- and HVO_4^{2-} are the most common vanadate ions under oxidising conditions (Wehrli and Stumm, 1989).

2.5.2 Soft metal ions

Since soft metal ions prefer bonding with soft bases, the following metals will bind strongly to sulphur and prefer nitrogen ligands over oxides. Soft metal ions can often be found as organometallic complexes (vanLoon and Duffy, 2005).

Cadmium

The main anthropogenic releases of Cd to the environment is a result of non-ferrous metal mining and refining (especially Pb-Zn mining and smelting), manufacture and application of phosphate fertilisers, fossil fuel combustion and waste incineration. The major sources of Cd to soils are deposition from the atmosphere as well as direct discharges from phosphate fertilisers and sewage sludges (Alloway, 1995a; ATSDR, 2009).

Cd tends to be more mobile in soils than other heavy metals, such as Pb, Hg and Cu and is therefore more available to plants. Contamination of Cd in soils will therefore always be of environmental concern because Cd is highly toxic to plants and animals (Alloway, 1995a). The mobility is dependant on pH and on the amount of OM present. Cd is strongly adsorbed to OM. Sorption of Cd to different soil constituents is found to be more important in controlling the metals mobility than the solubility of Cd compounds (Fergusson, 1990). Cd is therefore often found concentrated in the surface soil, but it has a stronger tendency to move downward than Pb, Hg and Cu (Alloway, 1995a).

Copper

In nature, Cu forms sulphides, sulphates, sulphosalts, carbonates and other compounds. The abundance of Cu is greater in basaltic rocks than in granitic rocks and is very low in carbonate rocks (Baker and Senft, 1995). Elevated levels of Cu are often found near mines, smelters, industrial sites, landfills and waste disposals. Cu has a typical soft metal behaviour and binds strongly to OM and other components such as Fe/Mn oxides and clays and is therefore mainly concentrated in the top soil rich in OM. Cu is not a particularly mobile metal and will stay adsorbed in the vicinity of the point source. Water soluble Cu compounds can be transported in surface waters and then preferably associated with suspended particles (ATSDR, 2004; Baker and Senft, 1995).

Silver (Ag)

The major sources of anthropogenic releases of Ag to the environment are from the processing of ores, steel refining, cement manufacture, fossil fuel combustion and municipal waste incineration. The main anthropogenic source of Ag to agricultural soil is by the application of sewage sludges. The mobility of Ag in soils is affected by drainage, pH, redox conditions and amount of OM which will adsorb Ag (ATSDR, 1990).

Antimony (Sb)

Sb is not defined in the Pearson classification. It is put together with the soft metals because of its high affinity to sulphur as a chalcophile element⁵.

⁵A chalcophile element is a sulphur-loving element. It will have a high affinity for sulphur and normally occur in sulphide deposits. Chalcophile metals are a part of the Goldschmidt's geological classification from 1922.

Sb is a fairly volatile metalloid and is toxic to organisms. Natural releases are through wind-blown dust, volcanic eruption, forest fires and biogenic sources. Most of the anthropogenic releases are as a result of metal smelting and refining, coal-fired power plants and refuse incinerations. Sb's adsorption to soil and sediments is primarily associated with the Fe, Mn and Al content of the soil as it co-precipitates with the hydroxylated oxides of these elements (ATSDR, 2008).

Mercury

Hg is one of the most toxic heavy metals and is the main heavy metal of interest in this study. See section 2.6 for comprehensive theoretical basis on Hg.

2.5.3 Borderline metal ions

The following metals exhibit both hard and soft metal behaviour and can not be said to be one or the other. They are therefore classified as borderline metal ions.

Zinc

Zinc is an essential element for humans, but too much Zn can have negative health effects. Zn is abundant in the earth's crust and is most often found as ZnS in the natural ores. Most reactive Zn enters the environment as a result of Zn mining and smelting operations and the use of commercial products where Zn is contained. Soil is the greatest sink for Zn. Zn usually stays adsorbed to soil, but some leaching may occur. Zn is not a volatile element and will not vaporise from waters, but will primarily be deposited in sediments, hence will Zn contamination of soil and water not normally pose a large environmental threat to the surroundings (ATSDR, 2005).

Lead

Lead is probably the least mobile of the heavy metals and has a low bioavailability, but due to its long residence time in the soil it can be of environmental concern if the levels are high (Davies, 1995). Pb is often found accumulated in topsoil due to the low mobility and sorption to OM. Sorption is an important mechanism for Pb in soil and Pb is found associated with Fe/Mn- and Al-oxides, clays and OM. Pb has the ability to be methylated to more toxic organocompounds. Anthropogenic releases of Pb leading to enhanced levels in soils are metallurgical industry, traffic (lead as an additive in petrol), paint and from mining of lead (Fergusson, 1990).

2.6 Mercury – a metal of special concern

Due to its special physico-chemical properties Hg is the only metal that is a liquid under standard temperature and pressure (STP). The element is a heavy metal in the true sense with a density of 13.5 g cm^{-3} (Schroeder and Munthe, 1998). The high vapour pressure makes the element highly volatile. This distinguishes the metal from other heavy metals. The elemental Hg^0 vapour is toxic to organisms if inhaled and is a global environmental problem due its ability to travel long distances in the atmosphere and its tendency to accumulate in colder regions (Wania and Mackay, 1996).

2.6.1 Toxicity of Hg

Hg is as previously stated a metal of primary concern due to its high toxicity. The compounds of most worry are the organometallic compounds and then especially MeHg. MeHg is a neurotoxin and selectively damages the brain as a result of its ability to readily transverse the blood-brain barrier. The fact that MeHg and other organomercurials have both a lipophilic part and a hydrophilic part enables it to dissolve both in fatty tissue and in more polar body fluids in organisms due to its high affinity for sulphur. MeHg forms water-soluble complexes in body tissues attached to thiol (-SH) groups in proteins, certain peptides, and amino acids and is highly mobile in the body (Clarkson and Magos, 2006).

MeHg is especially of concern also due to its bioaccumulation capabilities. In marine environments the concentration of MeHg in organisms at the top of the aquatic food chain can be up to 100 000 times larger than in the surrounding waters (WHO, 1990). In the environment Hg can be methylated and demethylated by several different pathways, but it is generally accepted that methylation is principally a biological process where sulphate reducing bacteria (SRB) are the most important methylators (Mason and Benoit, 2003).

Metallic Hg is not particularly toxic if inhaled, with a gastro-intestinal adsorption of only approximately 0.01 % (in rats) (WHO, 2000). Hg^0 vapour is, however, far more toxic to humans if inhaled. Hg^0 vapour is absorbed through the lungs and may be taken up by the red blood cells and transported through the body. Since Hg vapour is a monoatomic uncharged gas it may readily

transverse the blood-brain and placental barrier and reach the brain where it can effect the central nervous system (Clarkson and Magos, 2006).

2.6.2 Sources of mercury

Hg is mainly extracted from limestone ores containing the mineral cinnabar with the chemical formula HgS. A number of other Hg-containing minerals are also found naturally (e.g. livingstonite (HgSb₄S₈), corderoite (Hg₃S₂Cl₂), metacinnabar (cubic HgS) and metallic Hg), but they are not as common as the cinnabar mineral.

One means of processing Hg from cinnabar is to roast the mineral ore at 500 - 600°C. The Hg is then liberated as elemental Hg according to the redox reaction in equation 6 (Navarro, 2008)



The Hg vapour, together with other exhaust gases, rises up and passes through a water-cooler condenser. Hg is the first of the products to condense as a liquid, so it can be collected while the other exhaust gases are released or further treated. Impurities are commonly removed by filtration. Apart from primary Hg production a large part of the produced Hg is achieved as a bi-product in the production of other metals and compounds, e. g. other chalcophilic metals such as Pb and Zn (Rytuba, 2003; UNEP Chemicals, 2006).

2.6.3 Natural and anthropogenic releases of Hg in the environment

The natural releases of Hg are estimated to be about one third of the total releases. The resulting two thirds are anthropogenic (Honda et al., 2006; Mason et al., 1994). There is, however, a disagreement in the scientific community about this size of this number. The natural emissions are released during outburst from volcanoes, forest fires, degrading of minerals and by degasification from land and water surfaces (Gochfeld, 2003; Jitaru and Adams, 2004; UNEP Chemicals, 2002). As previously stated, some Hg occur naturally in the soil and also in minor amounts in the oceans and in water on land, but some of the Hg released by the processes stated above is actually a re-mobilisation of historically deposited anthropogenic Hg. It is therefore difficult to estimate natural

versus anthropogenic releases correctly (UNEP Chemicals, 2002; WHO, 2000). An average natural emission rate has nevertheless been estimated to be about $1.5 \text{ ng Hg m}^{-2} \text{ h}^{-1}$ (Gustin et al., 2000; Krabbenhoft et al., 2005).

The main source of anthropogenic emission of Hg is the burning of fossil fuels with coal combustion as the biggest contributor due to Hg impurities in the coal. Various mining industry also contributes significantly, and especially the extraction of gold in small-scale artesian gold mining leads to large emissions of Hg. Hg is namely used as an extraction agent in the gold mining industry as a result of its capability of forming amalgams with gold. Other sources are the chloro-alkali industry where HgCl_2 is used as a cathode in the production, non-ferrous metal production, cement production and other industries, waste disposal, from crematoriums due to old amalgams in teeth and by primary Hg production (Jitaru and Adams, 2004; Pacyna et al., 2006).

Hg is mostly emitted in gaseous elemental form contributing 53 % of the total emissions. Gaseous divalent Hg follows with 23 %, while particulate Hg only contributes with 10 % of the emissions to the atmosphere (Pacyna and Pacyna, 2002).

The releases of Hg are not evenly spread to the environmental compartments land, water and air. 45 % is emitted to air, 7 and 48 % is released to water and land respectively (Steinnes, 1995).

2.7 Mobilisation of mercury from a mercury mine

Hg mining activities produce Hg mine waste with varying content of Hg. The waste is mainly composed of calcine (produced during roasting of carbonate rock), quarry (waste rock) and low-grade ore rock. The waste products are often stored in large heaps. Waste management differs from mine to mine. The waste dumps at the KMP are uncovered and exposed to the surrounding environment (see Figure 13 for pictures of the waste areas).

The mobilisation of Hg from a mining area is dependant on many factors, but is mainly determined by the speciation of the metal (Navarro, 2008). It is therefore important to determine the form of

Hg in the tailings when assessing the risk for environmental contamination associated with Hg mining activity.

Once in solution, the stability of Hg species and the behaviour of Hg in aqueous environments can be described by a pH-Eh diagram (Figure 6). The diagram gives the stable species under a set of given conditions (Given in appendix M) and was conducted with the speciation program Medusa⁶. The most stable species under normal conditions is Hg⁰. Hg⁰ released from mining operations may therefore be stable in a near-surface environment and persist in groundwater or surface-soils for quite some time, but is also readily available for evaporation to air (Navarro, 2008).

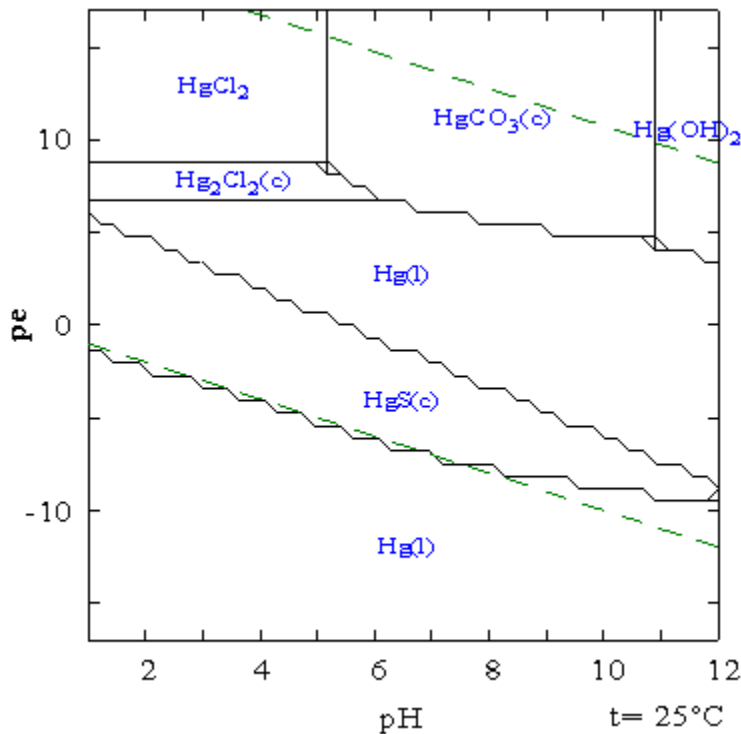


Figure 7 Stability field diagram for Hg. Conditions as given in appendix M.

The aqueous discharge of Hg is together with atmospheric emission the most important paths of transport. The mobility and transport is governed by complex formation, pH- and redox conditions and the presence of OM and iron oxyhydroxides. Natural episodes such as periods with heavy

⁶ Medusa is a species distribution program developed by Ignasi Puigdomenech. Available from <http://w1.156.telia.com/~u15651596/>

precipitation can enhance the leaching of Hg from waste material and hence the mobilisation (Navarro, 2008; Qiu et al., 2006).

2.7.1 Atmospheric emissions

One important transport pathway of Hg pollution from Hg smelters is by atmospheric emissions. Hg is easily vaporised or emitted to the atmosphere after the reduction of Hg^{2+} to elemental Hg^0 (Navarro, 2008; Rytuba, 2005). Atmospheric emissions from Hg smelters are a result of poor distillation and capture of the elemental Hg. In the atmosphere, Hg can be transported long distances depending on the oxidation state, but most of the Hg^0 released during mining activities will deposit near the mineralised area as wet deposition after oxidation to the more water soluble Hg^{2+} (Gochfeld, 2003; Rytuba, 2005). This deposited Hg, along with Hg emitted through runoff (see section 2.7.2) is still a part of the global Hg cycling as it may again be reduced and vaporise and thereby be transported via the atmosphere.

2.7.2 Aqueous transport

Water is also an important transport media by leaching of Hg from a mining area to its surrounding environment. It can be mediated by surface runoff over and through mine waste deposits, and by mine drainage and leachate that percolates through solid mine wastes. This Hg leaching is mainly associated with periodically peak flow events where Hg is washed out in particulate form or as highly-soluble secondary Hg phase forms produced as a result of inefficient and incomplete cinnabar retorting (Kim et al., 2000; Navarro, 2008; Qiu et al., 2006; Rytuba, 2003). The main processes governing the mobility, transport and re-sedimentation in the aqueous phase are dissolution of solids, followed by complex formation and redox reactions and co-precipitation or adsorption, respectively. In the porous media of the tailings and smelters, sorption reactions and the movement of mobile colloidal particles are important processes governing the fluxes of Hg in the drainage (Navarro, 2008; Rytuba, 2003).

The species of Hg present in aqueous solution can be predicted by specie distribution models when the levels of important ligands are known. Figure 8 below, is a model of the aqueous species distribution of Hg that will be present under a set of environmental conditions. The selected

concentrations of the important ligands are what are commonly found at the studied site. The blue shaded area represents the normal pH range in surface waters in Khaidarkan, Kyrgyzstan. The speciation analysis has been conducted with the speciation program Medusa⁷.

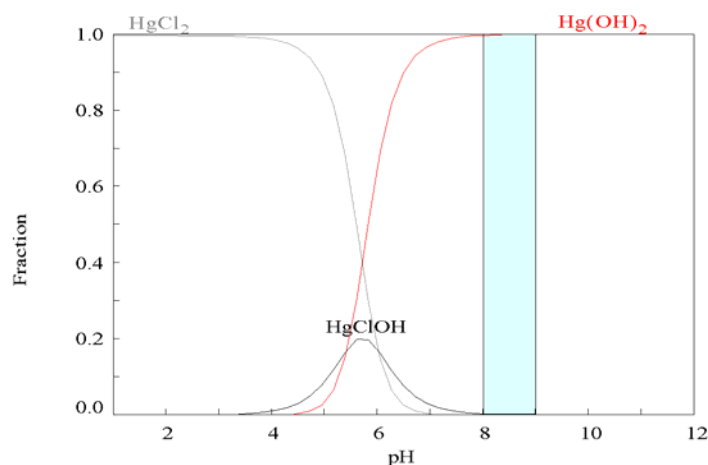


Figure 8 Dominant complex species at conditions found in drainage water from a tailing pond at the studied site (See appendix M for concentrations). DNOM is omitted as this is not an important species at the site. The blue shaded area represents normal pH values in the Khaidarkan area.

Hg is bound strongly to different complexing ligands. This may lead to enhanced mobilisation or immobilisation of the metal depending on the solubility of the complex. A complex-binder that in many sites will be of special importance is OM. Complexes of Hg with OM or DNOM lead to immobilisation or mobilisation of Hg respectively, and OM may also enhance the methylation and reduction of Hg^{2+} . OM is specially important controlling the sorption of Hg in soils and sediments in chloride deficient systems where Hg-hydroxy species dominate (Davis et al., 1997). Hg may also be bound to chloride and carbonates depending on the pH, redox conditions (Figure 7) and concentration of these ligands. In Khaidarkan the pH is high (from 8 to 9). The role of Cl as a complexing ligand is therefore less important (Figure 7 and Figure 8). In waste areas of mines where limestone is the parent material, the calcine produced during the roasting of the ore material produces a high pH and there is a high concentration of carbonates (mainly as bicarbonate at the pH in question). It would be plausible to assume that the carbonates may contribute to an enhanced solubility of HgS by complexation with Hg^{2+} . Carbonates have, however, been found to have little effect on the solubility of HgS (Piao and Bishop, 2006), but a somewhat enhanced solubility may

⁷ Medusa is a species distribution program developed by Ignasi Puigdomenech. Available from <http://w1.156.telia.com/~u15651596/>

occur. As previously mentioned the solubility of HgS is highest under acid, oxic conditions (mainly due to complexation with Cl⁻ (Davis et al., 1997)). In excess sulphide conditions and high pH (>10) the solubility of HgS may increase due to the formation of soluble mercury bisulphide species (Piao and Bishop, 2006; Wollast et al., 1975).

An important transport mechanism in the aqueous environment is colloidal transport. This has been demonstrated by various column experiments (Gray et al., 2002). Studies of leachates from calcines from Hg mining indicated that transport of Hg-bearing soluble colloids were important. Most Hg in water samples in the vicinity of Hg mines in Nevada has been found to be associated with particulate Hg or attached to suspended particles (Gray et al., 2002). Similar results are found in Wanshan in China (Qiu et al., 2006). This would lead to high levels of Hg in stream sediments downstream from mine waste hot spots. Due to gravitational forces the colloids will settle and the concentration of Hg in the stream water normally decreases rapidly from the point source.

2.8 Theoretical background on analytical techniques

2.8.1 DMA-80 Direct Mercury Analyzer

The DMA-80 is an instrument that measures the Hg content of a solid or liquid sample with no pre-treatment step. Hg is determined with atomic absorption spectrometry (Milestone, 2003). The sample is first dried and subsequently thermally and chemically decomposed by controlled heating in an oxygenated environment. The decomposition products are then carried by an oxygen flow to the catalytic section of the furnace. The oxidation is completed and halogens nitrate and sulphide oxides are trapped in this area. At last the Hg vapour is lead to the amalgamator and trapped in a gold amalgamator trap. The cell is flushed to remove other decomposition products. Then the amalgamator is thermally heated and the Hg vapour is desorbed and detected by the spectrophotometer (Figure 9). The spectrophotometer is an atomic absorption spectrometer that measures the absorbance at 253.7 nm as a function of Hg concentration (US EPA, 2007).

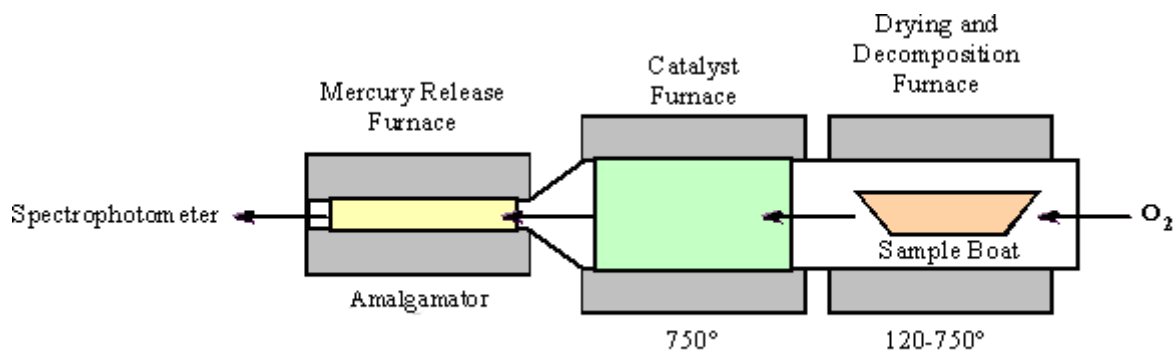


Figure 9 Principal sketch of the DMA-80 instrumentation (Milestone, 2003)

2.8.2 PSA 10.035 Millennium Merlin 1631 Hg Analyser

PSA 10.035 Millennium Merlin 1631 Hg Analyser (Millennium Merlin Hg Analyser) is an instrument that applies the atomic fluorescence technique in combination with cold vapour technology and amalgamation. This combination leads to improved sensitivity and lower detection limits. Hg can be detected in the parts per trillion (ppt) range. Prior to the analysis the aqueous sample is filtered through a 0.45 μ m filter. If the sample is not in an aqueous form it must be decomposed. The sample is preserved by adding HCl. All Hg in the sample is then oxidised by adding a potassium bromide/potassium bromate reagent. In order to destroy the excess of bromine $\text{NH}_2\text{OH} \cdot \text{HCl}$ is added. The sample solution is then applied to the instrument and all Hg^{2+} is reduced to volatile Hg^0 with SnCl_2 . The vapour is separated from the solution by purging it with Ar through a gas-liquid separator and the vapour is trapped in a gold trap as a pre-concentration step. The Hg is carried in a steam of inert gas to the cold-vapour atomic fluorescence spectrometer (CV-AFS) where the concentration of Hg is detected with atomic fluorescence spectrometry at 253.7 nm (US EPA, 2005).

2.8.3 ICP-AES Inductively Coupled Plasma Atomic Emission Spectrometry

ICP-AES is a widely used tool for determining the concentration of a wide range of elements in the periodic table (most metals and semi-metals). In atomic emission spectrometry the concentration of an element is determined by measuring the intensity of the light emitted at characteristic wavelengths (Boss and Fredeen, 2004). The atomisation source is the inductively coupled plasma. Plasma is an electrical conducting gaseous mixture containing a significant concentration of cations and electrons.

Said in a simpler way, plasma is ionised gas. The plasma is activated by a spark from a Tesla coil. A radio-frequent generator gives a power up to 2kW at about 27 or 41 MHz (Skoog et al., 1998).

Most samples are liquids and are nebulised into an aerosol (Figure 10). A fraction of the sample (1-2 %) is then carried in a stream of argon to the ICP torch, punching a hole in the plasma. The atomisation and ionisation (equation 7) of the sample aerosol takes place in this central channel of the plasma where the temperature can be up to 10000K (The temperature range is from 6000 to 10000K in the plasma).



A principal sketch of the instrument is given in Figure 10.

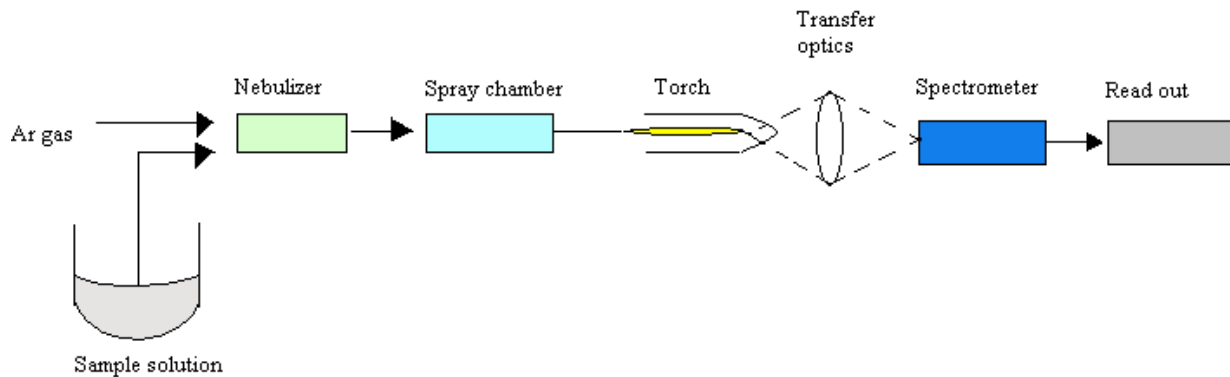


Figure 10 Principal sketch of ICP-AES

2.8.4 Ion-exchange chromatography (IC)

Ion-exchange chromatography is a separation method for the determination of ions. The ions are separated due to different retention on an ion-exchange resin and detected with a conductivity detector. The principle of the technique is based on the exchange equilibrium between ions in a solution and ions of like sign on a stationary phase (Skoog *et al.*, 1998). The most common active sites on a cation-exchange resin are the sulphonic acid group $-\text{SO}_3\text{H}^+$. For the anion-exchange resin, the tertiary ammonium group $-\text{N}(\text{CH}_3)_3^+\text{OH}^-$ is most often the functional group (Fritz, 1987; Skoog

et al., 1998). When a mobile phase enters the column carrying a cation M^{x+} an exchange-equilibrium can take place on the cation-exchanger. The exchange can be described as in equation 8 below.



The same sort of exchange-equilibrium takes place on an anion-exchanger if an anion is to be detected. Different ions are separated due to different affinity to the exchanger. Polyvalent ions are for example more strongly held to the stationary phase than singly charged ions (Skoog *et al.*, 1998). For this work suppressed-ion anion chromatography was performed. The anions are then separated by ion-exchange and detected by electrical conductivity. Since the mobile phase itself has a substantial signal the method uses a suppressor column that removes unwanted electrolytes prior to the conductivity measurement (Harris, 2003).

3. Materials and Methods

3.1 Description of samples, sites and procedures

3.1.1 Site description

Khaidarkan

Khaidarkan is located southwest in Kyrgyzstan in the Batken oblast (province) (Figure 11). Batken oblast was established in 1999 and is one of the poorest regions in Kyrgyzstan (Martino et al., 2005).



Figure 11 Map of Kyrgyzstan. Khaidarkan is marked with a black square. Modified from ENVSEC (2007).

The small city hosts the Khaidarkan Mercury Plant (KMP) and the community is totally dependent on the Hg mine and metallurgical plant through its employment of the majority of the citizens; 1500 people in total (Frattini and Borroni, 2006).

In one of the KMP facilities metallic mercury is processed by the mechanism described in section 2.6.2 (Figure 12). In addition there is a metallurgical plant that enriches the concentration of calcium

fluoride (CaF), Hg and Sb raw materials for further industrial workings. Sb is further enriched at the Kadamjai Antimony facility located in Kadamjai, about 40 km northeast of Khaidarkan.



Figure 12 Filtering of metallic mercury to remove impurities after distillation

Associated with the KMP is an open tailing area where solid waste from the mining and processing as well as waste water is deposited. The waste water is transported through 6 km long pipelines to the tailing pond (Figure 13). The same waste pond has been applied since 1967 and covers an area of 38.2 ha with a maximum depth of 27 metres (Frattini and Borroni, 2006).



Figure 13 Tailing pond (left) and slag heaps (right) associated with KMP in Khaidarkan.

Burnt calcine slag from the Hg roasting deposited together with quarry material from the mines in large heaps approximately 1 km from the centre of Khaidarkan. As shown in Figure 13 both the tailing pond and slag heaps are open and not sealed in any way and hence exposed to the

surrounding environment. The tailing pond has an overflowing system in order to avoid flooding. Overflowing water is discarded outside the pond directly on the ground and is draining in the nearby Shaktanya river (Frattini and Borroni, 2006). There are no protective installations, like fences around neither of the waste areas. Cattle were observed nearby the tailing pond during sampling. The Khaidarkan sampling area is shown in Figure 14.

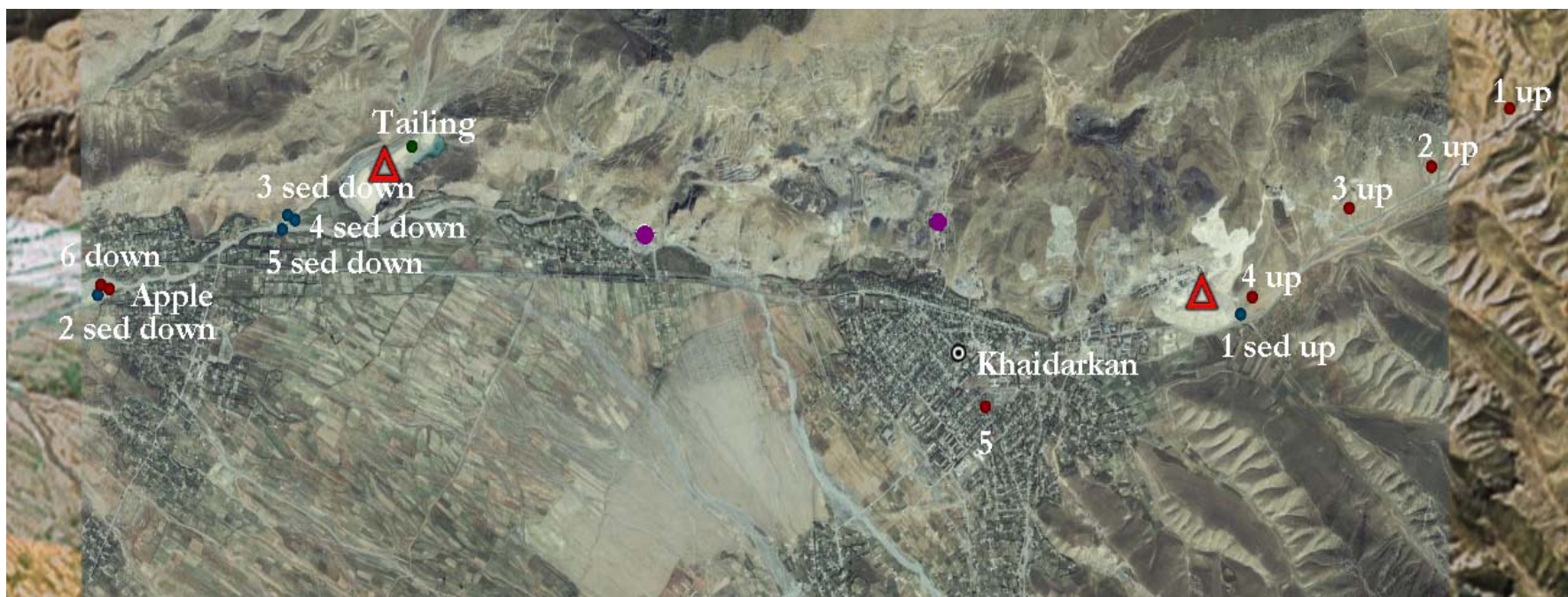


Figure 14 Satellite photo of Khaidarkan sampling site. Red dots are soil samples and blue dots are sediment samples. The red triangles represent the tailing pond (left) and slag heap (right). The purple dots represent metallurgical facilities of the Khaidarkan Mercury plant (KMP) (Google Earth, 2009b).

The routes of exposure of Hg from the KMP facilities are many. From the roasting process, elemental Hg can be emitted to the atmosphere due to poor distillation. The metallurgical plant that enriches the concentration of CaF, Hg and Sb raw materials releases waste water directly to the surrounding environment. Transportation of pollutants via this water to soil and groundwater is a possibility. Wind-blown dust carrying contaminants is a potential problem regarding especially the tailing pond, but also the slag heaps. Leaching of Hg and associated heavy metals with drainage water from the tailing pond and slag heaps may also be a significant route for Hg to the environment. The overflowing system in the tailing pond is probably one of the biggest contributors to release of Hg and other pollutants to the surroundings.

Ferghana Valley is a large valley that covers an area of 22 000 km² and is located downstream from Kyrgyzstan. The valley is mainly located in the neighbouring Uzbekistan. The area is one of the most fertile areas in Central Asia and is very important regarding the agricultural production for the region. The possibility of spreading of contaminants from KMP to the Ferghana Valley is real and is of special concern. The region is also situated in an area of quite high seismic activity so there is a large possibility of earthquakes in the area. An earthquake could be disastrous regarding the spreading of Hg and associated pollutants especially from the tailing pond connected to KMP.

In the Soviet time an extensive irrigation infrastructure was established along the Syr-Daria basin. This included the area of interest. Water is taken from the rivers and used inefficiently as irrigation water (Martino et al., 2005).

Gauyang

Gauyang is situated approximately 10 km south of Khaidarkan. A monitoring field in the TEMP-CA was established here with a system of macroplots (See section 3.1.2) The macroplots were situated on steep mountain ridges divided by a river valley (Figure 15). The small river draining the watershed containing the monitoring plots was dry during sampling. The forest type is juniper forest. The vegetation on the north slope is richer and has more biodiversity than the south slope. The soil type of the north slope is mainly umbrisol with thick organic profiles. The south slope is dominated with cambisol rich in carbonates. The parent material in the area is mainly limestone and granite. The weather on the days of sampling was dry, sunny and warm. There had been a snowfall prior to the

sampling, but the snow had recently melted. The climate for this area is mountain climate of continental type (Stavinskiy et al., 2001).



Figure 15 Satellite photo of the monitoring site, Gauyang. In this study only samples from macroplots 1, 5, 9 and 10 were used. The blue dot marked Site 1 is water sampled from the main river. The ephemeral stream dividing the monitoring field was dry during sampling and could therefore not be sampled (Google Earth, 2009a).

Kara Koi

Kara Koi is a TEMP-CA monitoring area established in 2005. The samples were analysed by Alex Stewart Laboratory in Kara Balta, Kyrgyzstan the same year. Kara Koi is situated 110 km east of Khaidarkan in Batken oblast. The climate and vegetation in the Kara Koi monitoring area resembles that of Gauyang. The Kara Koi site is situated on steep slopes bordering a deep valley. The soil depth varies from deep soils in the valley to very shallow soil at the top of the slopes. The parent material is mainly limestone. The soils therefore had typically a deep A layer with soil types of

Phaeozem⁸ and Umbrisols. The Kara Koi area is used for grazing purposes during spring and summer. The levels of heavy metals and soil parameters from Kara Koi will be used as background values for the area.

3.1.2 Soil and sediment sampling procedure

Soil sampling procedure at Gauyang

In the monitoring field ten macroplots of 10m x 10m (Figure 16) were chosen subjectively so as to span variation of important ecological gradients. The macroplots were placed in the centre of 30m x 30m plots where important tree parameters were recorded. Within the macroplots, five 1 m² microplots (Figure 16) were chosen at random by a statistical method. A total of 50 microplots were therefore selected. Around most of the microplots two or more generic mineral soil horizons were sampled using an Edelman auger. The samples were collected 20-30 cm at the left, right and down-slope side of the microplot to avoid disturbance of the seepage of water through the plot. The TEMP-CA project has established seven monitoring sites in Kyrgyzstan and data from two of these sites are used in this thesis (Kara Koi and Gauyang).



Figure 16 Installation of macroplot (left picture) and microplots (right picture)

⁸ Phaeozem is a dark soil rich in OM with no secondary carbonates in the upper meter of the soil. It is a fertile soil which is a porous well-aerated with good structural stability (FAO, 2001).

Soil sampling procedure at Khaidarkan

In Khaidarkan soil samples were sampled to span the spreading of contaminants from the waste sites. Soil samples were collected in an elevation gradient down the valley side to the slag heaps near the city Khaidarkan (1-, 2-, 3- and 4 up in Figure 14). The samples were collected with an Edelman auger in approximately 1 km intervals from the slag heaps. At all the sites two soil horizons were collected. A soil sample was also collected in the city centre (5 in Figure 14) and a soil sample was collected downstream from the tailing area (6 down in Figure 14). It was also collected a soil sample in a cultivated area (Apple in Figure 14, see Figure 25 for picture of the apple garden) downstream from the tailing area that was irrigated with water from the nearby stream (1 downstream in Figure 18). A short description of the soil samples is given in Table 2.

Sediment sample procedure

Sediment samples were collected in the stream draining the slag heaps (1 sed up, see Figure 17), of the tailing pond sediments and in streams downstream from the Hg mine tailing pond. A sediment sample was also collected in the ephemeral stream that divided the monitoring site in Gauyang monitoring area (see Figure 15). A short description of the sediment samples is given in Table 3

3.1.3 Water sampling procedure

The water that was sampled for analysis of Hg were sampled in pre-cleaned PET bottles (section 3.2.1) and conserved by adding 2 mL concentrated HCl (see appendix A) These samples were also analysed for heavy metal concentrations with ICP-AES. At four of the sites (the streams that had sufficient volume of water) an additional sample was sampled in a glass flask for the determination of redox potential. The flasks were not able to prevent the intrusion of air during the trip so the redox potential was not determined, but the samples were used for analysis of anions and alkalinity. The sampling procedure was to first rinse the bottle in the water to be sampled. This rinse water was discarded downstream from the sampling spot. This procedure was repeated three times. The water was then sampled by holding the bottle completely under water. The bottles were top filled. A short description of the water samples collected is given in Table 4. The sample location is shown in Figure 18. After arrival at the laboratory all water samples were transferred to PP flasks that are recommended for storage of samples to be analysed for Hg.



Figure 17 Drainage water from slag heaps (left picture) and tailing pond (middle picture) and water used as drinking water by the locals (right picture)



Figure 18 Sample site location of the water sampled in Khaidarkan (Google Earth, 2009b).

Table 2 Short description of the soil samples

Site	Sample name	Comments	Horizon	Depth (m)	Soil type	Texture	Vegetation	Parent material	Wetness during sampling
Khaidarkan	1A up	Highest point in elevation gradient	A	0-15	Mineral		Shrubs	Conglomerate	Dry
Khaidarkan	1B up	Highest point in elevation gradient	B	15-32	Mineral		Shrubs	Conglomerate	Dry
Khaidarkan	2A up		A	0-12	Mineral		Shrubs	Conglomerate	Dry
Khaidarkan	2C up		C		Mineral		Shrubs	Conglomerate	Dry
Khaidarkan	3B1 up		B1	0-15	Mineral		Shrubs	Conglomerate	Dry
Khaidarkan	3B2 up		B2	15-30	Mineral		Shrubs	Conglomerate	Dry
Khaidarkan	4A up	Near slag heaps	A	0-10	Mineral		Grass		Dry
Khaidarkan	4B up	Near slag heaps	B	10-30	Mineral		Grass		Dry
Khaidarkan	5A	Garden soil in Khaidarkan. Diffuse boarder	A	0-5	Mineral		Pine trees, grass		Dry
Khaidarkan	5B	Garden soil in Khaidarkan. Diffuse boarder	B	5-30	Mineral		Pine trees, grass		Dry
Khaidarkan	6A down	Pocket of soil in mountain slide. Diffuse boarder	A	0-5	Mineral		Shrubs	Limestone, Granite	Dry
Khaidarkan	6B down	Pocket of soil in mountain slide. Diffuse boarder.	B	5-30	Mineral		Shrubs	Limestone, Granite	Dry
Khaidarkan	Ap apple	Cultivation area. Irrigation with river water?	A	0-10	Mixed		Apple trees		Dry
Khaidarkan	Bp apple	Cultivation area. Irrigation with river water?	B	10-20	Mixed		Apple trees		Dry
Khaidarkan	Tailing	Tailing pond material					No		Dry
Gauyang	1-3A	Dark humus rich. South slope	A	0-20	Mineral	silty loam	Bushes	Limestone, Granite	Dry
Gauyang	1-3B	South slope	B	20-70	Mineral	clay	Bushes	Limestone, Granite	Dry
Gauyang	1-3C	South slope	C	70-	Mineral	clay	Bushes	Limestone, Granite	Dry
Gauyang	5-22A	Brownish humus layer. South slope	A	0-20	Mineral	silty loam	Bushes	Limestone, Granite	Dry
Gauyang	5-22B	South slope	B	20-70	Mineral	silty loam	Bushes	Limestone, Granite	Dry
Gauyang	5-22C	South slope	C	70-	Mineral	silty loam	Bushes	Limestone, Granite	Dry
Gauyang	9-42A	Brownish humus layer. North slope	A	0-10	Mineral	silty loam	Juniper forest	Limestone, Granite	Dry
Gauyang	9-42B	North slope	B	10-25	Mineral	sandy loam	Juniper forest	Limestone, Granite	Dry
Gauyang	9-42C	North slope	C	25-	Mineral	sandy clay	Juniper forest	Limestone, Granite	Dry
Gauyang	10-46A	Dark humus rich. North slope	A	0-25	Mineral	loam	Juniper forest	Limestone, Granite	Dry
Gauyang	10-46B	North slope	B	25-45	Mineral	loam	Juniper forest	Limestone, Granite	Dry
Gauyang	10-46C	North slope	C	45-	Mineral	sandy clay	Juniper forest	Limestone, Granite	Dry

Table 3 Short description of the sediment samples

Site	Sample name	Comments	Wetness
Khaidarkan	1 sed up	In small stream draining the slag heaps	Wet
Khaidarkan	2 sed down	In river next to apple garden.	Wet
Khaidarkan	3 sed down	In small stream coming from tailing	Wet
Khaidarkan	4 sed down	In small stream alongside tailing pond	Wet
Khaidarkan	5 sed down	In flooding area	Dry
Gauyang	6 sed field	In ephemeral stream in Gauyang	Dry

Table 4 Short description of the water samples

Site	Sample name	Comments
Khaidarkan	Drinking water	Water sampled from a leaking water pipe. The water was collected for drinking water purposes by the local community.
Khaidarkan	1 downstream	River next to apple garden, downstream from tailing pond. Water used for irrigation of apple garden
Khaidarkan	2 downstream	Stream running from tailing pond
Khaidarkan	3 downstream	Stream alongside tailing pond
Khaidarkan	Waste water KMP	Waste water from KMP
Khaidarkan	Tailing	Stream draining tailing pond
Khaidarkan	Slag heap	Small stream draining slag heaps
Gauyang	Site 1	Main river near monitoring area, Gauyang

3.2 Sample preparation

3.2.1 Pre-cleaning procedure

The PET and PP bottles used for water samples were cleaned in a Miele Mielabor G 7783 Mutitronic washing machine (Miele, Germany) which is run with 5 % (w/w) HNO₃ and type II water. The bottles were also cleaned with diluted HCl over night. Unless otherwise stated all glass equipment used in the experimental work had been top filled or soaked in 5 % (w/w) HNO₃ and then rinsed with type II and type I water prior to analysis. The glass bottles used for analysis of Hg with Millennium Merlin Hg analyser had been rinsed with type II water three times and type I water one time and then heated to at least 550 °C for two hours in a Naber furnace prior to analysis. The zirconium oxide (ZnO₂) grinding cups and balls were rinsed with type II and type I water between the runs and was additionally cleaned by immersing all parts in type I water in an ultrasonic bath for ten minutes.

3.2.2 Grinding and sieving

By collecting the fraction passing a 2 mm sieve the sand, silt and clay fraction of the soil is collected. Sieving is an essential part of homogenising the sample and is consistent with the internationally accepted standard for chemical analysis (Tan, 1996). The soil samples were sieved through a 2 mm sieve and then dried at room temperature for three weeks on cardboard plates covered with aluminium foil. The wet sediment samples were first dried at room temperature and then manually ground with an agate mortar and sieved through a 2 mm sieve. The dry sediment samples were handled as the soil samples (described above). When grinding the sample it is important not to crush the individual soil minerals, but large aggregates should be broken (Tan, 1996).

3.2.3 Homogenising procedures

The analytical precision of the soil analysis was limited due to difficulties achieving good homogeneity of the soil samples. In order to get best possible results three different homogenising procedures were tested.

Homogenising with grinding and sieving

The first homogenising procedure tested was simply homogenising by the sample pre-treatment of grinding and sieving. The soil and sediment samples were measured directly with the DMA-80 (section 3.3.1) after grinding and sieving (see section 3.2.2). The soil and sediment samples were stored in plastic cups until analysis.

Homogenising with quartering and mixing with a Retsch Mixer Mill type MM 2000

The second homogenising procedure tested was homogenising the soil and sediment samples with quartering followed by mixing of the sample in a Retsch Mixer Mill type MM 2000. The quartering step is a subsample procedure that gives each particle of the sample an equal chance of being subsampled and analysed (Tan, 1996). The sample was shaped like a cone and divided into quadrants. The top left and bottom right quadrants were discarded and the other two was mixed. This procedure was repeated three times on all the samples. The subsamples were further homogenised by thoroughly mixing in the Mixer Mill with amplitude set to position 40 for 6 minutes. The homogenised samples were stored in plastic zip-lock bags until analysis with the DMA-80 (section 3.3.1).

Homogenising with quartering and cryogenic grinding with a Retsch Mixer Mill type MM 2000

The third homogenising procedure tested was homogenising with cryogenic grinding after quartering. Prior to grinding in the Retsch Mixer Mill, the soil and sediment samples were cooled in liquid nitrogen for two minutes to prevent volatilisation of elemental Hg due to the heat increase during the mixing procedure. The homogenised samples were stored in plastic zip-lock bags until analysis with the DMA-80.

3.2.4 Dilution

The soil and sediment samples with highest levels of Hg needed to be measured in very small amounts (as low as 2 mg) to fit within the working range of the instrument (Hg content of 0.05 – 600 ng). The uncertainty of the balance and inhomogeneity in the samples lead to large standard deviations in the measurements. This was solved by diluting the samples that contained high concentrations of Hg from two to hundred times (most of the samples were diluted ten times) with high purity graphite prior to analysis on the DMA-80. The mixture was thoroughly mixed with the Retsch Mixer Mill type MM 2000.

3.2.5 Filtering

The water samples were filtered through a 0.45 µm filter prior to analysis with ICP-AES, IC, PSA and alkalinity analysis.

3.3 Instrumentation and procedures

3.3.1 Determination of the content of Hg in solid samples with the DMA-80

The total Hg concentration of the homogenised soil and sediment samples were measured with the DMA-80. The calibration curve used is given in appendix C-3. The calibration curve was prepared by dilution of prepared standards. Two standards were prepared with the dilution of a 1000 ± 0.5 mg l⁻¹ Hg stock solution (mercury(II) chloride, Teknolab AS, Kolbotn, Norway): A 10 µg g⁻¹

standard for the upper calibration curve from 35-600 ng and a $1 \mu\text{g g}^{-1}$ standard for the lower calibration curve from 0.05 - 35 ng. Instrumental specifications are given in appendix C-1. The heating programme used (appendix C-2) was recommended for soil samples and tested on a reference material with acceptable recovery (see Figure 43).

3.3.2 Sequential extraction procedure

The sequential extraction procedure used was a slightly modified version of the protocol developed by Lechler et al. (1996). The pyrolysis step in the procedure was performed somewhat different. It has been shown that heating the samples over $80 \text{ }^{\circ}\text{C}$ may cause the amount of elemental Hg to be highly overestimated (Sladek and Gustin, 2003). In stead of heating the sample to 180°C for 48 hours as described by the Lechler-procedure the samples were heated to $80 \text{ }^{\circ}\text{C}$ for 8 hours. A schematic presentation of the sequential extraction procedure is given in Figure 19 below. After the first step (pyrolysis) the Hg concentration in the solid sample was measured with DMA-80. The amount of elemental Hg was then estimated by subtraction the measured value from the total concentration of Hg. The Hg concentration in the residual sample was also measured with DMA-80. The Hg content of the extracts obtained after step 2, 3 and 4 was measured with Millennium Merlin Hg analyser. The sequential extraction procedure was performed by three bachelor students supervised by the candidate.

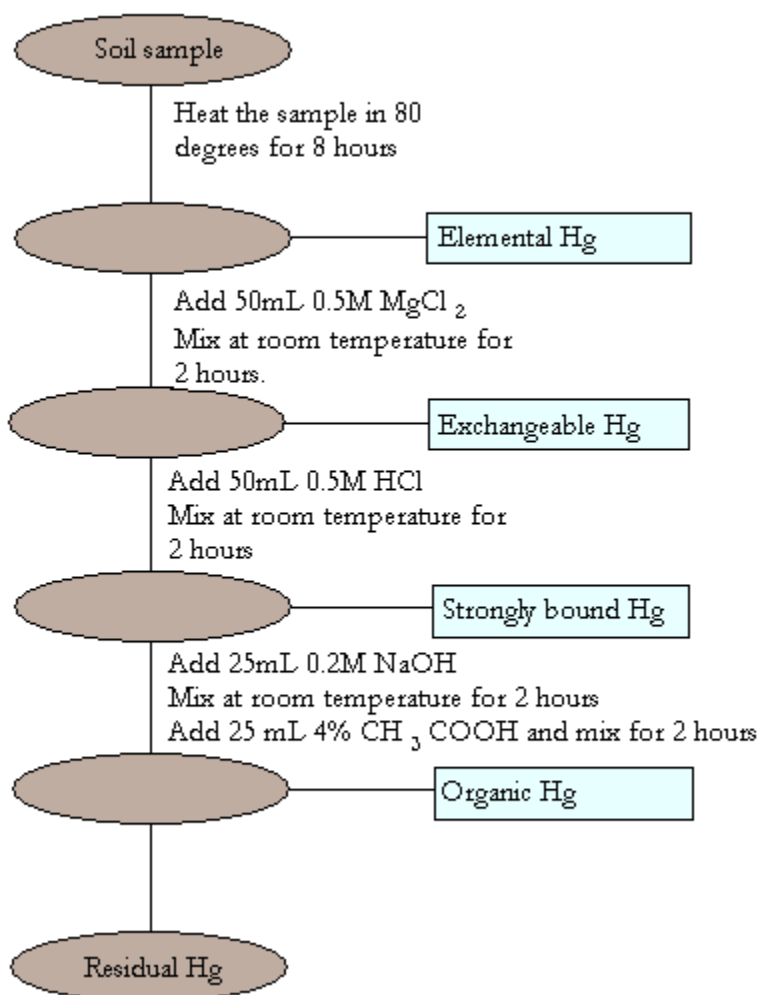


Figure 19 Schematic presentation of the sequential extraction procedure for Hg in soil and sediment samples

3.3.3 Determination of heavy metal content in soil, sediment and water with ICP-AES

Selected heavy metals and the main cations in the water samples were analysed with a Varista Varian ICP-AES. The instrument was calibrated using four standards in the range from 0-600 $\mu\text{g/L}$ for As, Sb, Se, Cd, Cu, Mn, Ni and Zn, 0-1.2 mg/L for V and Pb and 0-150 mg/L for Ca and Mg (Appendix D-5). The multistandards were prepared from single- and multi- ICP standards (see appendix A). Calibration curves are given in appendix D-6. Results are given in appendix D-4. Na and K in water were analysed with a Sherwood Flame Photometer 410. The standards prepared for

the ICP-AES analysis were applied for the calibration curve. Calibration curves and results are given in appendix P

Selected heavy metals and the main cations (Ca, Mg, Na and K) in the soil and sediment samples from the Khaidarkan site were in addition analysed with an Optima 5300DV ICP-AES at Alex Stewart Laboratory in Kara Balta, Kyrgyzstan. The results are given in appendixes D-1, D-2 and D-3.

3.3.4 Determination of the content of Hg in water with Millennium Merlin Hg analyser

The analysis of Hg in the water samples was performed with the Millennium Merlin Hg analyser. Calibration curve, concentration of standard solutions and results are given in appendix I.

The content of Hg in the extracts obtained from the 2-, 3- and 4.step in the sequential extraction procedure (section 3.3.2) was also determined with the Millennium Merlin Hg Analyser. The results are given in appendix K.

3.3.5 Ion chromatography (IC)

Main anions (F^- , Cl^- , NO_3^- , NO_2^- and SO_4^{2-}) were determined with a DIONEX 2000 IC. The instrument was calibrated with four standard solutions with concentrations in the range from 0.4-10 $mg L^{-1}$ for F^- , 2-50 $mg L^{-1}$ for Cl^- , NO_2^- , Br^- , NO_3^- and SO_4^{2-} and 4-100 $mg L^{-1}$ for PO_4^{3-} (Appendix F-1). The standards were run for every 15 sample to correct for possible instrumental drift. Quality control was provided by running a reference standard solution. The recovery of the anions in the standards is given in Figure 45.

3.3.6 Determination of soil colours

The soil colours given in appendix Q were determined by using the Munsell soil colour charts, 1992 Revised Edition from Macbeth. The determination of the soil colour was performed by two independent persons (the candidate and a co-worker).

3.3.7 Determination of dry content

In order to make the results comparable with other results it is common to report the results normalised to the unit of dry mass of the sample. The dry weight of the samples was determined by a standard procedure (Krogstand, 1992) slightly modified though in accordance with ISO11465. A pre-weighed aliquot of the sample was heated for at least six hours or to constant weight at 105 ± 5 °C. It was assumed sufficient to heat the samples for six hours since the samples had been dried at room temperature. Based on experience of little deviation and variance from co-workers it was assumed that it was sufficient to measure only one replicate of each sample. The water content in percent was then calculated and is given in appendix B-2. All results by the candidate have been corrected for the water content and are given on a dry weight basis. See appendix B-1 for equations for calculations.

3.3.8 Determination of total alkalinity

The alkalinity of the water samples was determined as according to ISO 9963-1. Procedure, equation for calculation and results are given in appendix E.

3.3.9 Soil parameters

The following soil parameters were analysed at Alex Stewart Laboratory in Kara Balta, Kyrgyzstan⁹.

Soil pH

Soil pH of soil and sediment sampled in Khaidarkan was determined according to the procedure of ISO10390. The pH of a suspension of soil that is made up in five times its volume of water is measured with a pH meter (Mettler Toledo, Seven Easy).

Loss on Ignition (LOI)

Loss on Ignition was measured by a standard procedure (Krogstand, 1992) slightly modified though in accordance with ISO10694. A pre-weighed aliquot (3 to 5 g air-dried soil passed through a 2 mm aperture sieve) of the samples was heated in a furnace at 550 ± 25 °C in a Carbolyte Muffle furnace for more than 3 hours. The sample was then cooled in an exicator in at least 30 minutes before

⁹ See <http://www.alexstewart.kg/>

weighing. The LOI in percent was then calculated and is given in Appendix B-2. See appendix B-1 for equations for calculations.

For organic soil the LOI is a fairly good estimate of the amount of organic matter in the soil. For mineral soil the LOI has to be corrected for content of clay (Krogstand, 1992).

Total carbon (C tot)

The measurement of total carbon was conducted according to ISO10694. The total C includes both carbonates and OC. This is a dry combustion technique on a LECO carbon analyser. The soil sample is heated to 940 °C in a flow of oxygen-containing gas that is free from carbon dioxide. Carbon in the sample is thereby oxidised to CO₂. The released CO₂ is determined using an infrared (IR) detector.

The potential cation exchange capacity (CEC)

CEC was measured according to ISO 13536 using BaCl₂ buffered at pH = 8.1 using triethanolamine. The soil was first saturated with respect to barium by treating the soil three times with buffered barium chloride solution. A known excess of 0.02 mol L⁻¹ magnesium sulphate solution was then added. All barium present is precipitated as highly insoluble barium sulphate and the sites with exchangeable ions are then readily occupied by magnesium. The excess magnesium was determined with an Optima 5300DV ICP-AES.

3.4 Software for data processing

Principal Component Analysis (PCA)

Principal Component Analysis (PCA) was computed with the Minitab statistical program (Minitab 15, 2007). PCA is a multivariable analysis that has a purpose of decomposing a dataset into principal components (PC) and revealing “hidden phenomena” in a large data set. This is often referred to as a parameter reducing routine. Variance is an important concept of PCA analysis and the variance of a variable is defined as “a measure of the spread of the variable values” (Esbensen et al., 1994). A principal component is a variable computed to describe the covariance, or linear association, of the data set. The first principal component (PC1) describes the largest part of the variation in the data

set (often around 40%) and is positioned along the direction of maximum variance. The second principal component (PC2) is situated in a direction that is orthogonal to the first PC and in the direction of the second largest variation, and so on for PC3, PC4 etc (Esbensen et al., 1994). In this study the first two principal components described around 66 % of the variation and were used to describe the dataset.

Cluster Analysis

Cluster analysis was also performed with the Minitab statistical programme. Cluster analysis is a method of modelling groupings, or clusters of similar parameters or objects. The clusters are presented with a dendrogram, a two-dimensional chart where the y-axis shows the similarity (where 100 % is very similar and 0 % is very unlike) between the clusters and the horizontal lines denotes the clusters (Esbensen et al., 1994).

3.5 Quality control

Prior to making any of the following control- and standard solutions the variable automatic pipettes used were calibrated by comparing volume to weight. The pipettes had to be within the acceptable limits of precision and accuracy for both the smallest and the largest volume of the automatic pipette.

3.5.1 Validation and quality control of the DMA-80 method for Hg determination

As a quality control for the accuracy of the DMA-80 method for Hg determination and as a check of the calibration curve a certified reference material (CRM) was run along with the samples for each analysis run. The maximum acceptable deviation from the certified value was set arbitrarily to no more than ± 10 %. The recovery of the CRM is a measure of the accuracy of the method. The recovery of the CRM was found by measuring the CRM on three separate days. The recovery was calculated according to equation 9.

$$\text{Recovery}\% = \left(\frac{\text{Measured_value}}{\text{Certified_value}} \right) \cdot 100 \quad (9)$$

In addition the accuracy of the method was tested by comparing the expanded combined uncertainties (U_{Δ}) of the measured values and certified value with the difference between their means (Δ_m). If $U_{\Delta} \geq \Delta_m$, the difference between the measured value and the certified value is not significant ($P = 0.05$) (Linsinger, 2005). Additional information is given in appendix G-3.

As an additional validation of the method, control solutions were run in occasional runs. The measured concentration was not accepted to deviate from the known concentration with more than $\pm 10\%$. Control solutions prepared from an external standard (different from the standard used to prepare the calibration solutions) were also run periodically to validate the Hg-standard used to prepare the calibration curve.

To minimise the memory effect in the DMA-80 method empty boats were run after each sample. Two empty boats were run in the beginning of every run to clean the system of any residual Hg. If the empty boat did not get a satisfactory blank value, empty boats were run till this was achieved. An absorbance of < 0.01 was considered satisfactory. It was not found necessary to run empty boats between replicates of the same sample.

To validate the purity of the graphite used for the dilution of the samples several replicates of pure graphite was measured with the DMA-80.

Limit of detection (LOD) and method detection limit (MDL) for the DMA-80 method.

The limit of detection is “the smallest quantity of analyte that is “significantly different” from the blank” (Harris, 2003). Significantly different can be defined in many ways, hence can the LOD be defined in many ways. A widely used definition and the definition used in this study is the definition presented in equation 10

$$LOD = 3 \cdot s_{blank} \tag{10}$$

where s_{blank} is the standard deviation (in ng) of a blank solution measured n times ($n > 10$)

Method detection limit (MDL) is a measure of the smallest quantity possibly obtained by the method in question. In this study the MDL was measured by dividing the LOD with the highest possible mass of sample that can be applied to the instrument (Equation 11).

$$MDL = \frac{LOD}{m_{highest}} \quad (11)$$

3.5.2 Accuracy and precision of the IC method

As a validation of the stock solution used to prepare the calibration standards, an additional stock solution was run. It was run with original concentration and diluted five times. This was also a validation of the accuracy of the method. The maximum deviation of the measured concentrations from the known concentrations was arbitrarily set to $\pm 10\%$. To correct for instrumental drift the calibration solutions were run for every 15 samples.

3.5.3 ICP-AES method

As a correction for possible instrumental drift a new calibration curve was recorded for every 20 samples.

3.5.4 Accuracy of the method for determination of Hg in water with Millennium Merlin Hg Analyser

As a validation of the accuracy of the method and the stock solution used to prepare the calibration standards, a control solution prepared from a different stock solution were run together with the samples. Maximum acceptable deviation was arbitrarily set to $\pm 10\%$ from the known value.

Limit of detection was determined for the method in the same way as for the DMA-80 method (described in section 3.5.1).

4. Results and discussion

4.1 Results and observations in Gauyang

The samples from Gauyang were only analysed for concentration of Hg. Concentrations of Hg are given in Figure 20. The average concentration ($0.4 \mu\text{g g}^{-1}$) has been used as a background level for the area in the following sections. The samples in the monitoring field have Hg concentrations far above the average for uncultivated soil ($0.045 - 0.16 \mu\text{g g}^{-1}$). Enhanced levels of Hg compared to the world average concentration are, however, expected due to the areas situation in the mercuriferous belt. Some of the Hg may, however be of anthropogenic origin (from KMP).

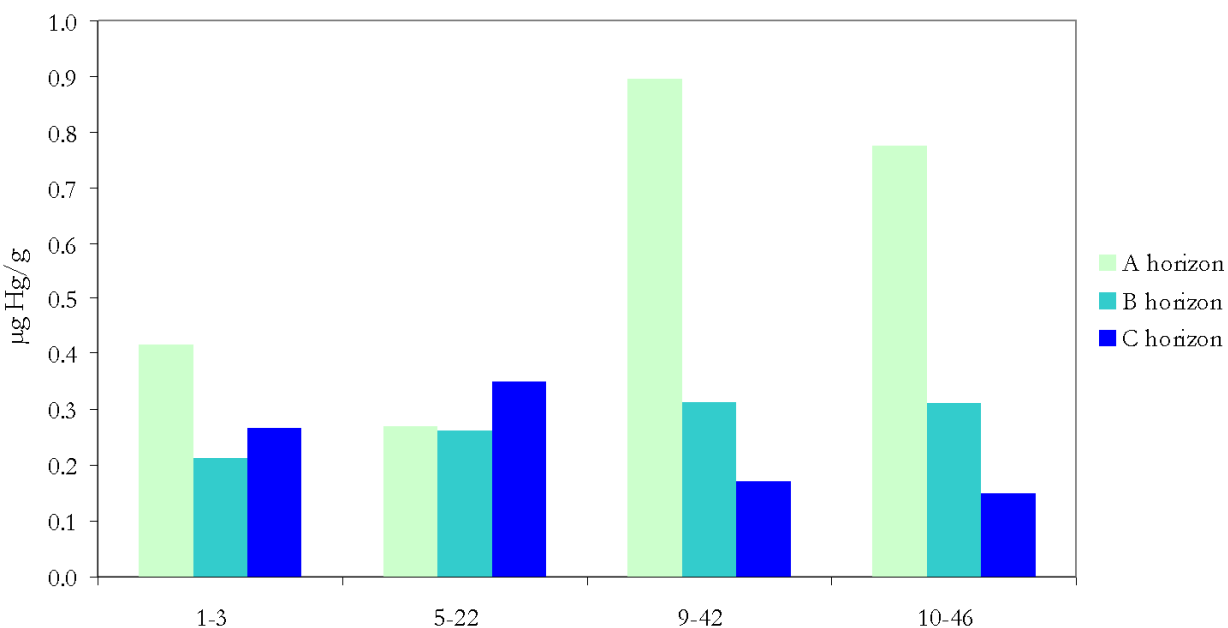


Figure 20 Hg concentration in horizon A, horizon B and horizon C in soil sampled in the monitoring field, Gauyang. The first number in the sample name correspond to the macroplot, the second number correspond the microplot (See section procedure for description of the sampling procedure).

Macroplots 1 and 5 are situated along the south slope. Macroplots 9 and 10 are situated along the north slope. The north slope has a much richer fauna than the south slope with more and more varied vegetation. The north slope does not receive as much sunlight as the south slope which can explain some of these differences. The soil on the north slope has a dark top soil more rich in OM

than the soil on the south slope. In the soil in macroplots 1 and 5 there are no clear trend in the Hg concentration between the horizons. There is, however, a clear trend in decreasing Hg concentration down the profile in macroplot 9 and 10 Figure 20. This trend is largely explained by the high adsorptive capacity of organic matter towards Hg. The accumulation of Hg in the topsoil may also be an indication of anthropogenic origin of Hg as a result of atmospheric deposition.

4.2 Results and observations in Khaidarkan

In the following section the results from Khaidarkan will be presented. The main anion and cations and soil parameters will be presented first, the levels of Hg in soil, sediment and water will then be addressed at all the different sampling sites. The levels of selected heavy metals will then be presented in the waste areas, downstream from the tailing pond and then up-valley from the slag heaps. In the following subchapter will the results from a sequential extraction analysis be presented and a statistical interpretation of the data is given. For sample site locations see Figure 14 in section 3.1.1.

4.2.1 Major ions in the water sampled in Khaidarkan

The concentration of anions in the water samples is given in appendix F-3. Concentration of cations is given in appendix D-4 and P-3. The main anions and cations are given in Table 5.

For sample site locations see Figure 15 and Figure 18.

The dominant anions in the study area are sulphate ($\text{SO}_4^{2-}(\text{aq})$) and bicarbonate ($\text{HCO}_3^- (\text{aq})$) while the dominating cations in the water are $\text{Ca}^{2+}(\text{aq})$ and $\text{Mg}^{2+}(\text{aq})$ (Table 5). The dominance of bicarbonate together with Ca^{2+} and Mg^{2+} is a result of the carbonaceous bedrock in the area. This also explains the high pH in the area. At the pH range measured in the samples, alkalinity can be equalled to the bicarbonate concentration in the water as this is the expected species at the pH in question. In mine tailing areas the burning of limestone will liberate lime, CaO , and also this will contribute to an enhanced pH.

Table 5 pH and concentration of the major ions in four water samples from Khaidarkan and Gauyang (site 1) in $\mu\text{eq L}^{-1}$

	Site 1	1 downstream	Waste water KMP	Tailing
pH	8.57	8.60	8.62	8.07
SO ₄ ²⁻	858	1131	1179	2513
HCO ₃ ⁻ (Alkalinity)	2427 ^a	2003	1644	2297
Ca ²⁺	1404	2465	3434	2191
Mg ²⁺	841	1864	1657	1575

^a the value is probably overestimated (see appendix E)

The dominance of SO₄²⁻(aq) in the waters is likely from the oxidation of sulphides during the roasting process (HgS is burned in the presence of air (see section 2.6.2)) SO₂ (g) is released and may be further oxidised to sulphate and dissolve in the surrounding waters.

The concentration of ions is higher in the water sampled in Khaidarkan compared to in the water sampled in the monitoring field Gauyang (Site 1). The highest concentrations of SO₄²⁻ (aq) and HCO₃⁻ (aq) are found in the drainage water from the tailing pond. The waste water from KMP has quite high Ca²⁺ concentration compared to other ions in the sample. CaF is one of the products in the refining process and this may explain this high value. There should, however, then be an excess of F⁻ as well. This is not found (see appendix F-3, table F-3).

4.2.2 Major components of the soil and sediments sampled in Khaidarkan

The most abundant oxide forming elements in the soil sampled in Khaidarkan are Ca and iron (Fe) followed by aluminium (Al) and Mg. The average Fe-content of the area is 2.2 (%). The high content of Ca and Mg is a result of the carbonaceous bedrock in the area. An overview of the concentration of other parameters in soil and sediments in the area are presented in table L-1 in appendix L, average values and ranges of soil parameters in Khaidarkan and Kara Koi are presented in Table 6.

Table 6 Soil parameters in soil and sediments in Khaidarkan and Kara Koi

Sampling site			pH	LOI (%)	C tot (%)	Fe (%)	CEC (cmol/kg)
Khaidarkan	A	Average	7.7	12.5	6.0	2.5	12.2
		Range	7.6 - 7.8	9.2 - 17.0	3.2 - 9.1	1.3 - 3.5	6.1 - 16.9
	B	Average	7.6	10.8	5.2	2.3	10.6
		Range	7.4 - 8.1	7.6 - 13.4	2.5 - 8.6	1.3 - 3.6	3.9 - 16.8
Kara Koi	A	Average	7.1	17.1	5.7	3.5	N/A
		Range	6.1 - 7.6	8.7 - 35.8	1.9 - 19.8	2.3 - 4.9	N/A
	B	Average	7.4	10.8	3.9	3.5	N/A
		Range	6.1 - 8.0	5.7 - 24.7	1.5 - 11.3	1.4 - 5.0	N/A

In Khaidarkan there are slightly higher pH values and higher content of C tot than in the background area, Kara Koi. The LOI and Fe content are lower in Khaidarkan.

4.2.3 Total mercury

The levels of Hg in Khaidarkan are generally high, but vary considerably as a result of distance from the point source, exposure to transport media and sample material characteristics. All values are above the reference value for uncultivated soil of $0.1 \mu\text{g g}^{-1}$ (Bradl, 2005) and all but one (2C up) are above the background values for the area.

The boxplot in Figure 21 shows the large variation of total Hg in the area with levels of Hg ranging from 0.4 to $8795 \mu\text{g g}^{-1}$ within an area of 15 km in diameter.

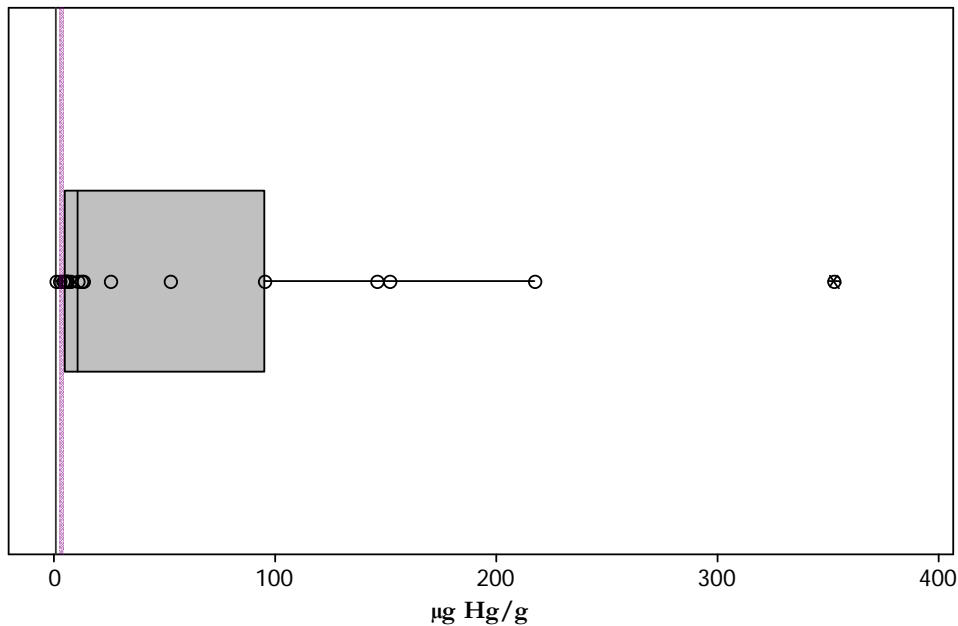


Figure 21 Hg concentration in soil and sediment samples in Khaidarkan (circles), median value (middle line) and quartiles (box ranges). The vertical black line gives the reference value for uncultivated soil ($0.1 \mu\text{g g}^{-1}$) presented by (Bradl, 2005). The purple area represents background values for the area ($0.15 - 0.93 \mu\text{g g}^{-1}$) (The sample “1 sed up” (8.8 mg g^{-1}) is omitted from the plot to give a better picture of the variation in the Hg levels in the other samples). The outlier in the plot is from the tailing sediments.

The highest concentration of Hg in the Khaidarkan area found in this study is 8.8 mg g^{-1} and is found in a sediment sample in a small stream draining the large slag heaps (1 sed up). This concentration exceeds the second largest concentration ($353 \mu\text{g g}^{-1}$), that was found in the tailing pond by 25 times and is almost 90 000 times larger than the background value for uncultivated soil. High values in these samples are to be expected when comparing with other similar studies of Hg mining areas where up to 46 mg Hg g^{-1} have been detected in calcine mine-waste and in directly contaminated soil in southwest Alaska (Gray et al., 2004). Nevertheless, the extremely high concentration is disturbing when considering the open access to the waste area and is in the upper range of Hg concentrations reported for Hg in sediments. The high value clearly indicates that leaching from the slag heaps occur. The results for soil collected in an elevation gradient up-valley (1 – 4) and downstream (6) from the slag heaps and tailing pond and in the city centre (5) are also high (exceeds the reference value for uncultivated soil by 4 to 500 times) (Table 7).

Table 7 Total Hg concentration in soil (i.e. not stream water sediments) collected in an elevation gradient up-valley and downstream from the slag heaps and tailing pond in the Khaidarkan area. The values are given in $\mu\text{g Hg g}^{-1}$.

1A up	1B up	2A up	2C up	3B ₁ up	3B ₂ up	4A up	4B up	5A	5B	6A down	6B down
4.9	3.2	9.8	0.4	12.9	5.6	52.3	7.0	5.6	2.2	11.9	4.3

Hg levels in the soil are shown in order of distance from the sources in Figure 22. (Sample 1 is furthest away up-valley from the slag heaps and 6 is farthest downstream of the tailing pond) There is a clear trend in a rise in concentration with closeness to the slag heaps which are situated 50 meters from sample 4. The concentration in the upper A horizon of sample 4 is especially high implying that the source of the high Hg levels is external and not due to high intrinsic levels in the soil material itself. The closeness to the slag heaps is most likely the explanation for the high concentration. The concentration decreases in the centre of the city (sample 5) while it increases again downstream from the tailing pond (sample 6). There is an overall clear trend of higher Hg concentration in the upper layers of the soil compared to underlying horizons. But also in the lower horizon there is a trend of rise in concentration of Hg towards the slag heaps (The drop in concentration in sample 2 is because the lower horizon of sample 2 is a C horizon while the lower concentration in the other samples is B horizon).

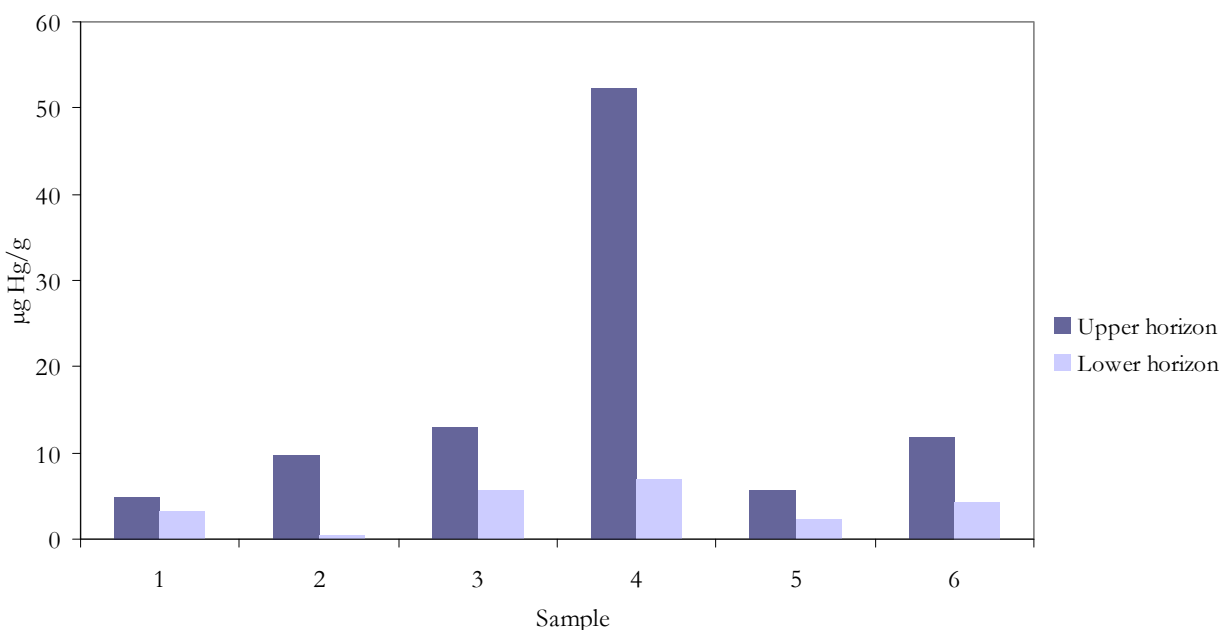


Figure 22 Total Hg concentration in soil samples in the elevation gradient up-valley and downstream from the slag heaps (situated near sample 4) and tailing pond (situated upstream of sample 6) in the Khaidarkan area.

The higher level of Hg in upper horizons can be explained by adsorption to organic matter in the soil which is present in the upper horizons. The accumulation of Hg in the topsoil is also likely if Hg has been deposited from the atmosphere or by irrigation. If the amount of OM in the top soil is low, the Hg will be transported down to the B horizon with time. Figure 23 is a plot of Loss on ignition (LOI %) versus Hg concentration in the soil samples. LOI is a measure of the organic content of the soil (see section 3.3.9). There seems to be a slight correlation between the LOI and Hg concentration in the soil samples, with an increase in Hg concentration of the soil with increasing organic content. This may imply that some of the accumulation of Hg in the more organic rich top soil is due to the complexation by OM, though it may also be due to a simple co-variation of high Hg content and organic content in the A horizon. Especially since the trend is somewhat vague it is likely that it also reflects that there is a transportation of Hg in the atmosphere and irrigation water (only for sample 5 since the other samples are not irrigated) and that much Hg is deposited near the emission source.

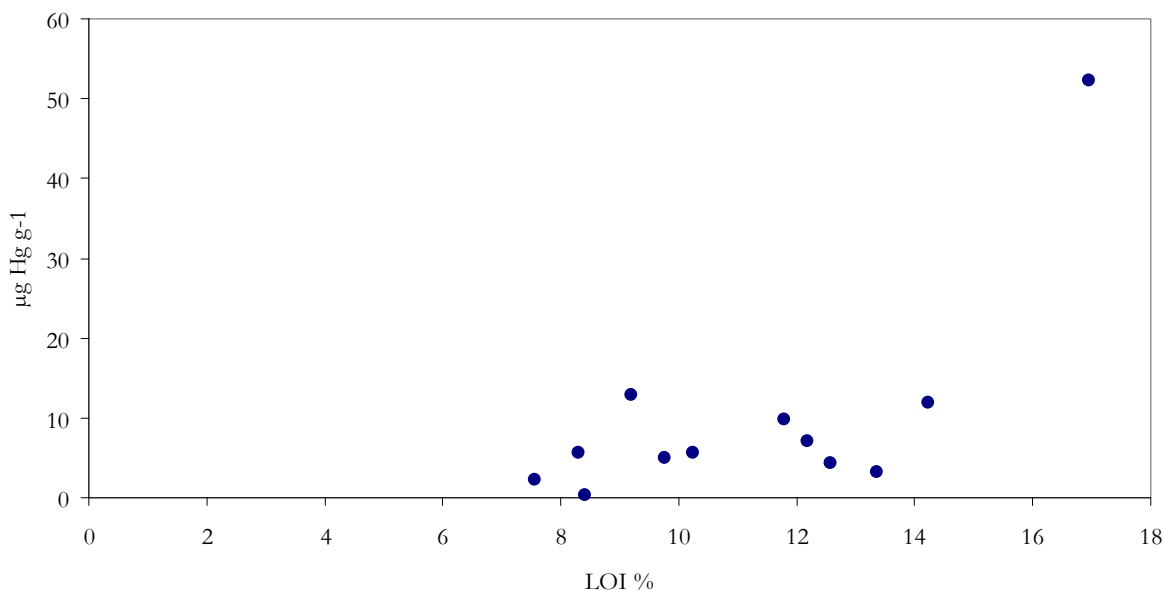


Figure 23 Loss on ignition (LOI %) compared to the Hg concentration in soil samples in the spatial gradient up and downstream from the slag heaps and tailing pond in the Khaidarkan area.

When disregarding the extreme sediment sampled next to the slag heaps, the sediments sampled in a wide flooding area (5 sed down) and in the stream next to an apple garden (2 sed down) (Figure 24) has the highest level of Hg (Table 8). All sediments sampled in the Khaidarkan area have Hg concentration above the Probable Effect Concentration (PEL) of 1.06 µg g⁻¹ for Hg in sediments,

were harmful effects are likely to be observed in sediment dwelling organisms (MacDonald et al., 2000).

Table 8 Hg concentration in sediment samples up- and downstream from the slag heaps and tailing pond in the Khaidarkan area. The values are given in $\mu\text{g Hg g}^{-1}$.

1 sed up	2 sed down	3 sed down	4 sed down	5 sed down
8795	146	3.5	25	217



Figure 24 Sampling sites 2 sed down (left picture) and 5 sed down (right picture)

These levels are remarkably high, and considerably higher than found in most of the soil samples. This indicates that most of the Hg released from the smelter and tailings is mobilised and transported in streams, preferably associated with particles, and deposited rapidly in the river bed. It would have been interesting to sample a transect a few kilometres further down along the flooding area. Most likely the Hg concentration will decrease rapidly as a function of distance from the tailing pond as a result of settlement of Hg-associated particles. The sediment sampled further downstream (2 sed down) has a higher Hg concentration than the sediments sampled closer to the tailing pond (3 sed- and 4 sed down). This refutes the previous assumption that the Hg levels will decrease rapidly from the source. The reason for this may be that colloids and suspended particles are leached from the tailing into these streams and first settle further downstream. The high level of Hg in the flooding river bed indicates that Hg is largely mobilised from the Hg mine tailing pond during periodical peak flow events.

A sample of the soil in an apple garden situated next to the river downstream from the tailing pond (Figure 25) was analysed and contains high levels of Hg (Table 9). The apple garden is irrigated with water from the contaminated river (1 downstream). The levels are disturbingly high (95 and 152 $\mu\text{g g}^{-1}$ in the A_p and B_p layer respectively) when considering the use as agricultural soil where food is harvested.

Table 9 Hg concentration in samples from the tailing pond sediments and of soil from a cultivated area downstream from the tailing pond. Concentrations are given in $\mu\text{g g}^{-1}$.

A_p apple	B_p apple	tailing
95	152	353



Figure 25 Apple garden irrigated with water from the nearby river (1downstream)

The Hg level in the material collected in the tailing pond (Figure 13) is high with total Hg concentration of 353 $\mu\text{g g}^{-1}$ (Table 9). The high concentration of Hg in the tailing pond sediments indicate that the roasting process at the KMP is inefficient and incomplete.

The level of dissolved Hg in waters in the Khaidarkan area are from low to extreme, ranging from 0.016 – 6 679 $\mu\text{g L}^{-1}$ (Table 10). However, the high values are directly associated with the slag heap and tailing.

Table 10 Dissolved Hg concentration in water samples in the Khaidarkan area. Concentrations are given in $\mu\text{g L}^{-1}$.

Drinking water	1 downstream	2 downstream	3 downstream	Waste water KMP	Tailing	Slag heap
0.109	0.091	0.071	0.016	0.020	0.752	6 679

Four of the water samples in Khaidarkan have values exceeding the world average for streams which is 0.07 $\mu\text{g L}^{-1}$ presented by Bradl (2005) (Figure 26). The drinking water sample and 1 downstream (furthest away from the sources) have concentrations just above the world average and are not much of concern. The level in the small stream draining the tailing is 100 times the world average and the concentration in the stream draining the slag heap is almost 100 000 times higher than the world average. Hg in water is more mobile than Hg adsorbed in soil and sediment and hence of more concern. All levels are however below the guideline value for drinking water of 6 $\mu\text{g L}^{-1}$ (WHO, 2006) except the level in the water stream near the slag heaps which is over 1000 times the guideline value. The lowest concentrations are found in the small tributary stream below the tailing pond (0.016 $\mu\text{g L}^{-1}$) and in waste water released from the metallurgical plant (0.020 $\mu\text{g L}^{-1}$). The extreme concentrations in the streams near the waste areas are of great concern and may be among the highest concentrations reported for dissolved Hg in streams. There is apparently a large fraction of dissolved material draining from the slag heap and tailing. The dissolved Hg is more mobile than particulate Hg. Hg in streams has in previous studies of similar areas been reported to be mainly associated with particles and colloids (Kim et al., 2000; Rytuba, 2003). Particle bound Hg was not analysed in this study, though likely captured by the samples of stream water sediment. The large level of dissolved Hg in the drainage water from the tailing and slag heap is disturbing. There is an obvious need for further research on how Hg is mobilised from slag heaps and tailings that consist mainly of insoluble HgS. As previously mentioned HgS is most soluble under acid conditions, but extreme basic conditions may also enhance the solubility. As neither of these conditions is found (the pH of the drainage water from tailing and water are 8.1 and 8.8 respectively) it is not likely that the high concentration of dissolved Hg arise from the dissolution of HgS. A more likely explanation may be that inefficient and incomplete roasting of the ore material has lead to the formation of

secondary Hg-roasting products, much more soluble than the parent cinnabar. The dissolved Hg may also be colloidal particles of HgS and other Hg-bearing minerals.

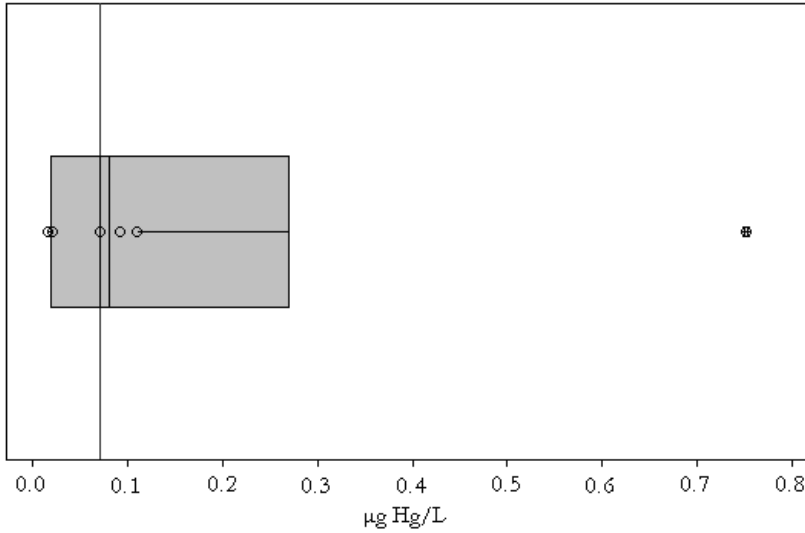


Figure 26 Hg concentration in water samples in Khaidarkan (circles), median value (middle line,) and quartiles (box ranges). The vertical line is a reference value for streams reported by (Bradl, 2005). The concentration in the stream draining the slag heaps is omitted from the plot. The outlier in the plot is the water draining the tailing pond

Figure 27 is a distribution diagram including the major species present in the tailing water sample as a function of pH. The pH in the tailing water is 8.1. Dissolved Hg will then almost solely be present as $\text{Hg}(\text{OH})_2$.

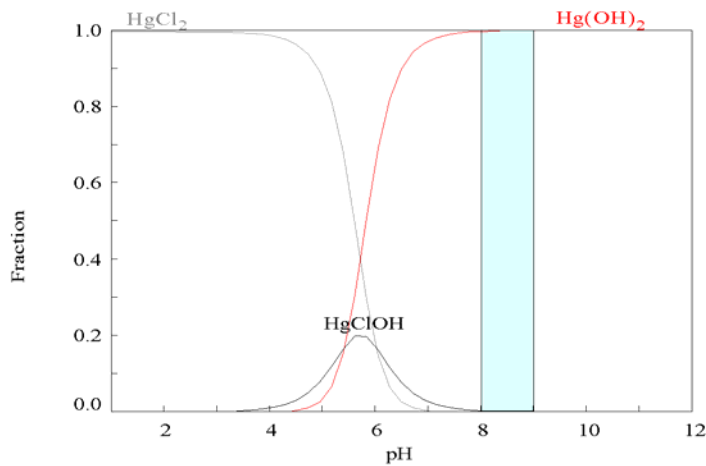


Figure 27 Major complex species in the tailing water sample determined by the speciation programme medusa (Conditions is given in appendix M). The blue shaded area represents normal pH in the Khaidarkan area.

4.2.4 Results for other associated heavy metals in Khaidarkan

The heavy metal concentration in soil and sediments presented in the following section has been determined by the Alex Stewart Laboratory in Kara Balta, Kyrgyzstan, except for the concentration of Hg that was analysed with DMA-80 at UiO. Presented is also the heavy metal concentration in water that was determined with ICP-AES at UiO. Raw data, calibration curves and additional information is given in appendix D. The results are compared with average background levels from the TEMP-CA monitoring site, Kara Koi (see section 3.1.1). These values are given in table N-1. As a background level of Hg is the average concentration from the TEMP-CA monitoring site, Gauyang used (see section 3.1.1). The results from Gauyang are presented and discussed in section 4.1.

Other heavy metal levels in the tailing pond

The concentration of heavy metals in the tailing pond material is very high for some of the metals, especially chalcophilic metals such as Pb, Sb and Cd, but the levels for As and Zn also exceeds the background level greatly (Figure 28). The concentration of Cu and V in the tailing pond is lower than the background levels in the area.

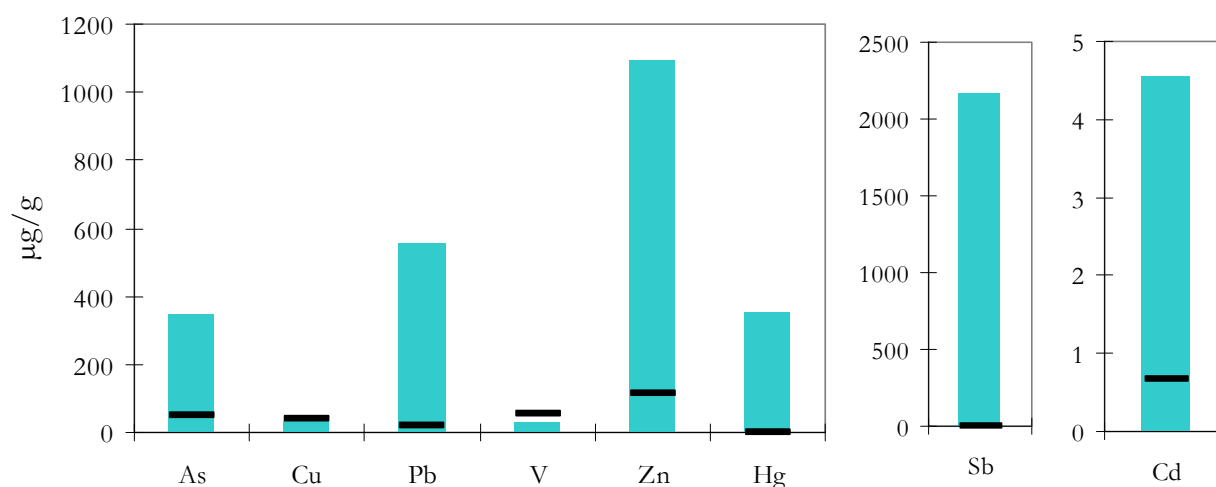


Figure 28 Concentration of selected heavy metals in the tailing pond sediments. The black lines represent the average background level in the area.

In the small stream draining the tailing pond the concentrations of heavy metals are generally low. The concentration of Mn is $26 \mu\text{g L}^{-1}$, somewhat above the average level in streams reported to $7 \mu\text{g}$

L⁻¹ by Bradl (2005). The concentration of Cu is 10 µg L⁻¹, slightly above the average level in streams (7 µg L⁻¹). The concentration of Sb is higher than the linear range of the method and was not detected but by comparing with the signal of the sample by the signal of the strongest standard, it was somewhat higher than of the strongest standard with a concentration of 0.6 mg L⁻¹. The level of Hg in the stream is as previously mentioned high (Table 10).

Other heavy metal levels in the sediments near the slag heap

The concentration of other heavy metals in the sediment near the slag heaps is also high, but somewhat lower than the levels in the sediments of the tailing pond (Figure 29), except for Hg where extreme values are found (not given in the figure) and Sb that has a slightly higher level than in the tailing pond. The concentration of As, Pb, Zn, Cd, Se and Sb exceeds the background levels manifold and the As and Hg concentration is way above the PEC (The PEC is 33 µg g⁻¹ for As and 1.06 µg g⁻¹ for Hg) where harmful effects are likely to occur for the sediment dwelling organisms (MacDonald et al., 2000). The levels for Cu and V are below the background levels in the area.

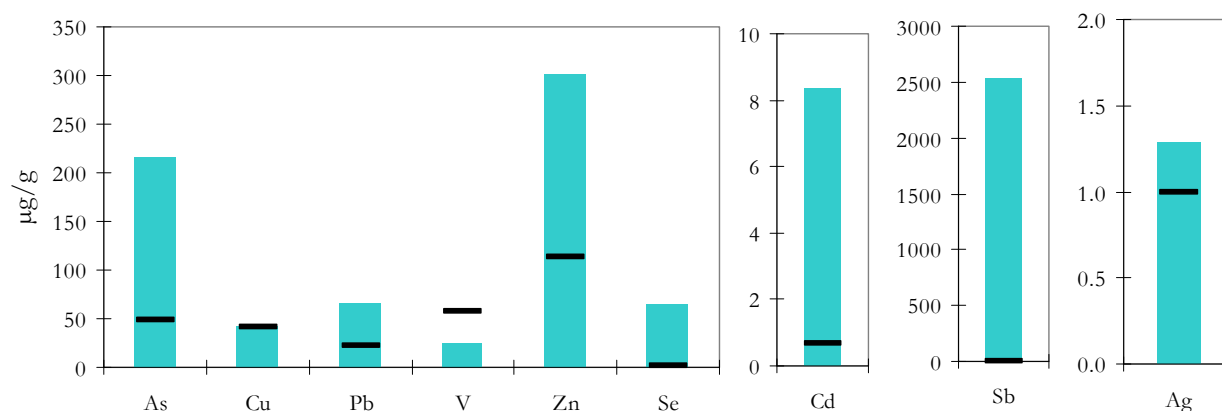


Figure 29 Concentration of selected heavy metals in the sediments in stream draining the slag heaps. The black lines represent the average background level in the area.

The concentration of heavy metals in the water in the stream draining the slag heaps is high for some metals (Table 11), especially Cd, with a concentration 1400 times larger than the average level for streams. The concentration of Cu, Mn and Zn is also highly elevated compared to the average level for streams while the concentration of Pb is below detection limit. The concentration of Sb was above the methods linear range and was not detected, but by comparing with the signal of the

strongest standard, the signal was approximately twice the signal of the strongest standard of 0.6 mg L⁻¹.

Table 11 World average level in stream and concentration of heavy metals in water near slag heaps

	World average level in streams (µg L ⁻¹)	Slag heap (µg L ⁻¹)
Cd	0.01	14
Cu	7	341
Mn	7	174
Pb	1	<d.l.
Sb	0.07	> l.r.
Zn	20	466

> l.r. = above linear range

< d.l. = below detection limit

The high concentrations of toxic heavy metals such as Pb, Cd, As and Hg, as well as Zn, Sb and Se in the tailing and slag heap indicate that the mining activity is a significant anthropogenic contributor to heavy metal contamination in the area. Some of the metals (such as As, Sb, Se and Hg) may be mobilised and long-range transported and contribute to the global pool of toxic heavy metals while other (such as Pb, Cd and Zn) may be of more concern to the local and regional environment.

The high levels of heavy metals in the tailing sediments and the sediments of a stream draining the slag heaps are, however, not surprising as they are waste areas for the KMP facility. The high levels of As, Pb, Hg and Cd are still disturbing if there is a mobilisation of these metals to the surrounding area because of the metals adverse health effects. It must also be held in mind that no protective fences were installed around the waste areas. Accidental consumption of the tailing or slag heap sediments or especially drainage water by grazing cattle is a possibility. To get a clearer view of the fate of the heavy metals, heavy metal levels in the surrounding soil and sediments are presented in the following sections

Heavy metal levels downstream from the tailing

Downstream from the tailing pond high levels of some heavy metals are found in stream sediments and in soil sampled from an apple garden. The heavy metal level in uncultivated soil downstream is high for Hg and Sb. See Figure 14 for an overview of the soil and sediment samples. An overview of the location of the water samples is given in Figure 18.

In the sediments sampled in the small tributary streams closest to the tailing pond downstream, low heavy metal levels were detected except for Sb and Hg (Figure 30). The concentration of Pb in the sample called 4 sed down is somewhat higher than the background level for the area.

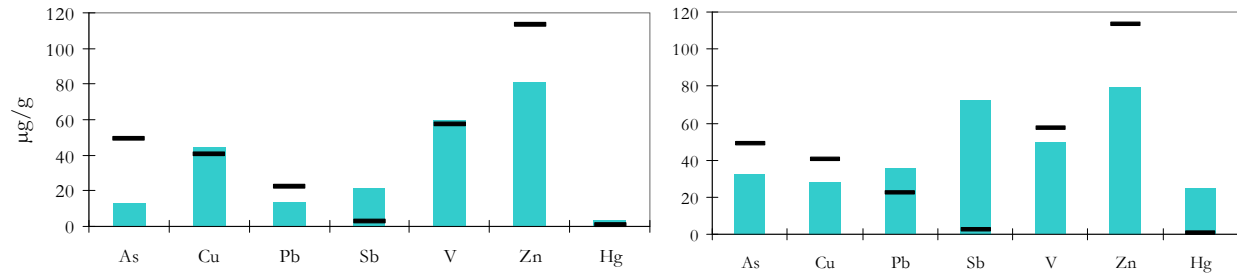


Figure 30 Concentrations of selected heavy metals in 3 sed down (left) and 4 sed down (right). Sediments sampled in the small tributary streams (2 – and 3 downstream respectively). The black lines represent average background level in the area.

The heavy metal levels in the water sampled in the tributary streams (2 and 3 downstream) is similar to the levels in the stream draining the tailing pond with slightly elevated levels for Cu (10 and 9 $\mu\text{g L}^{-1}$ for 2- and 3 downstream respectively) and Mn (30 and 16 $\mu\text{g L}^{-1}$ for 2- and 3 downstream respectively). The other heavy metals have concentrations below detection limit (see appendix D-4)

The sediment sampled in a large flooding area (Figure 24) right next to the tributary streams downstream from the tailing area have high levels of As, Pb, Sb and Hg, above the background level of the area (Figure 31). The concentration of Hg is the highest concentration measured in the collected samples when disregarding the samples at the waste sites (tailing and 1 sed up). This indicates as previously mentioned that periodic peak flow events are important governing the mobilisation of Hg. The concentration of As is somewhat elevated compared to background levels. The level of Sb is highly elevated from the background level.

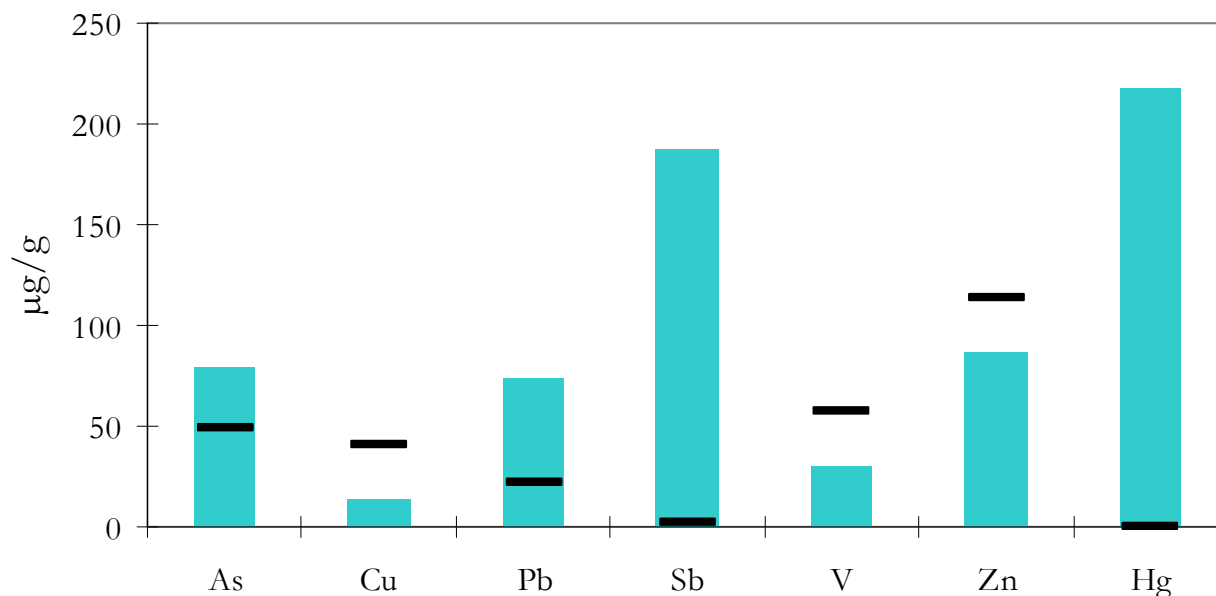


Figure 31 Concentration of selected heavy metals in sediment sampled in the river bed of a dry flooding area (5 sed down). The black lines represent average background level in the area.

The sediments sampled in the stream further downstream from the tailing pond (2 sed down, see Figure 24) have high levels of a number of heavy metals. The concentration of As, Pb, Zn, Cd, Ag, Sb and Hg exceed the background level for the area for all the metals (Figure 32). The concentration of As, Pb and Hg are above the PEC (The PEC for Pb is $128 \mu\text{g g}^{-1}$ (MacDonald et al., 2000)). The concentration of Zn is especially high when comparing with the other samples with higher observed concentrations only in the two waste sites (tailing and 1 sed up). The concentration of Pb is high, higher than in the sediments in the small stream draining the slag heaps (which is $66 \mu\text{g g}^{-1}$). Pb form very stable compounds in the soil and little leaching of Pb normally occurs (Davies, 1995). The Pb is most likely of anthropogenic origin, deposited by atmospheric deposition or during peak flow events. It is likely that Kyrgyzstan, being a developing country, still has cars running with lead acetate as an additive. This may explain some of the enhanced level, but since there is limited amount of traffic in the area the anthropogenic burden is probably mainly from the KMP activity. If traffic is a source of Pb in the sediments one should also find high levels of Pb in the other soil and sediment samples, which was not found. Pb and As in the sediments may also be a result of use of lead arsenate as a pesticide in surrounding agricultural areas.

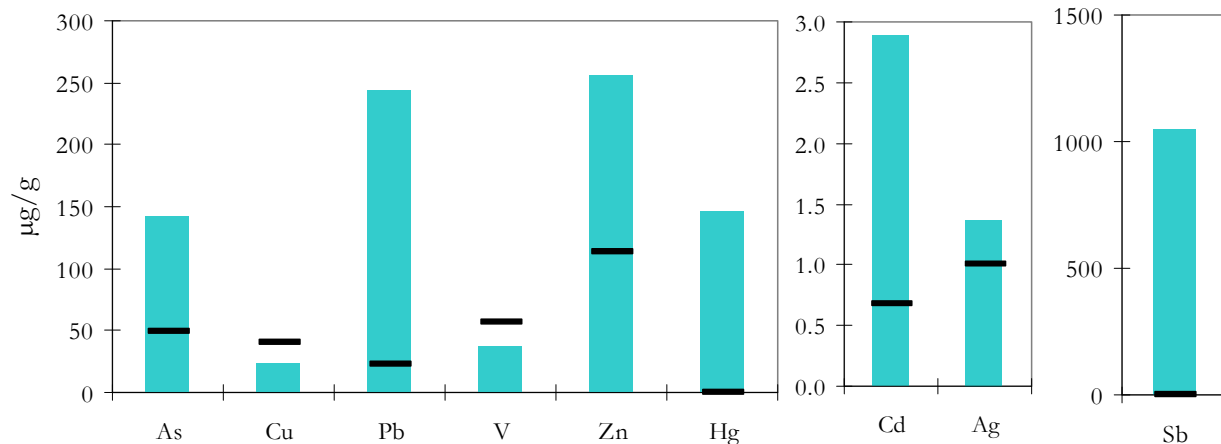


Figure 32 Concentration of selected heavy metals in sediments sampled in a stream used for irrigation of the apple garden (2 sed down). The black lines represent the average background level in the area.

The water sampled in the stream next to the apple garden have heavy metal concentrations below the detection limit of ICP-AES for most of the heavy metals (Appendix D-4) except for Sb, Hg and Cu. The concentration of Sb is higher than the linear range of the method, but by comparing with the signal for the highest standard the signal is somewhat higher than the highest standard of 0.6 mg L^{-1} . Cu has a concentration of $11 \text{ } \mu\text{g L}^{-1}$, slightly above the average natural concentration in streams reported by Bradl (2005) to $7 \text{ } \mu\text{g L}^{-1}$ and the concentration of Hg is as previously stated $0.091 \text{ } \mu\text{g L}^{-1}$, slightly above the average value for streams reported by Bradl (2005) to $0.07 \text{ } \mu\text{g L}^{-1}$.

Soil sampled from a cultivated apple garden downstream from the tailing has high levels of some heavy metals (Figure 33). The levels of As, Pb, Sb, Hg and Cd are all above the background level of the area and the levels of Hg and Sb are high for a cultivated soil. The garden is as previously mentioned irrigated with water from the nearby river (1 downstream). Anthropogenic activity leading to high levels in the water can therefore explain the high level in the agricultural soil. The concentration of Cd in plants is mostly determined by the total concentration in the soil (Alloway, 1995a). A high Cd concentration is therefore of concern in a cultivated area when considering the high toxicity of Cd. The concentration is not, however, alarming. Contamination of Cd from phosphatic fertilisers is often seen in agricultural areas and may be an additional anthropogenic source of the metal in the soil.

The level of As in the soil is very high. Fortunately As has a much lower tendency to bioaccumulate from soil to plants than Cd and the level in plants is often low even for crops grown on

contaminated soil (O'Neill, 1995). The As contamination may be a result of the mining activity. Another explanation of the high levels of As and also Pb in the cultivated area can be that the use of lead arsenate (PbHAsO_4) as a pesticide have lead to high levels of these metals. Lead arsenate was indeed the most extensively used pesticide in fruit orchards until 1947 (Peryea and Creger, 1994) so it is not unlikely that this pesticide has been applied to the area in question.

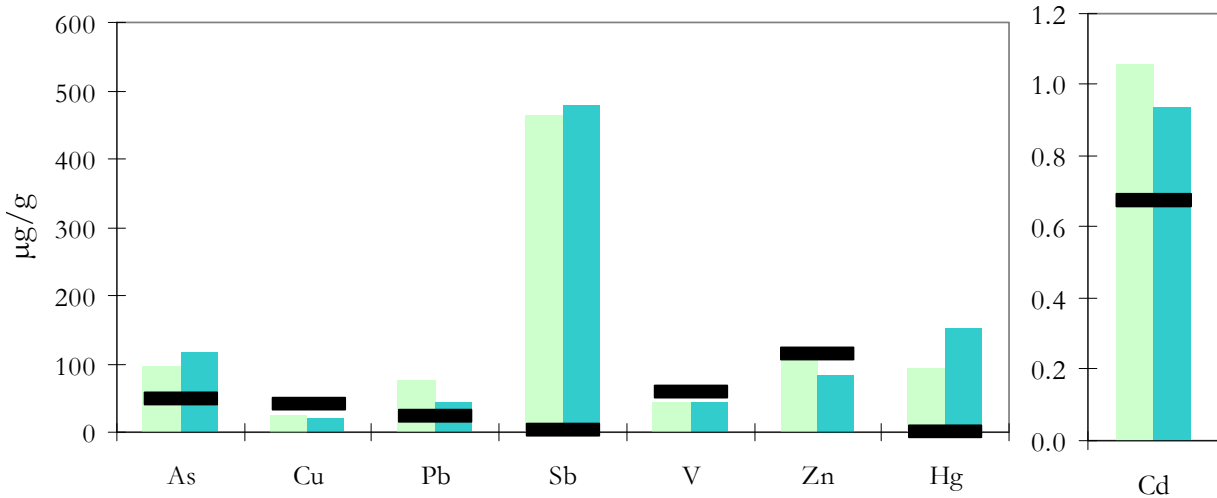


Figure 33 Concentration of selected metals in horizon A_p (light green bar) and B_p (dark green bar) in soil sampled from an apple garden downstream from the tailing. The black lines represent the average background level of the area.

Relatively undisturbed soil downstream from the tailing pond (sample 6) has heavy metal levels that are below the background values for the area except for Hg, Sb and Cd (Figure 34). The levels of Sb and Hg are high above background values. All heavy metals have lower concentration in the lower horizon (B). This soil in question was situated in a small pocket of soil in a mountain slide. The levels of heavy metals are therefore most likely a result of natural weathering of the bedrock enriched in these elements and atmospheric deposition. This can explain the reduction in the concentration of heavy metals down the profile together with OM in the topsoil as an adsorbent for heavy metals.

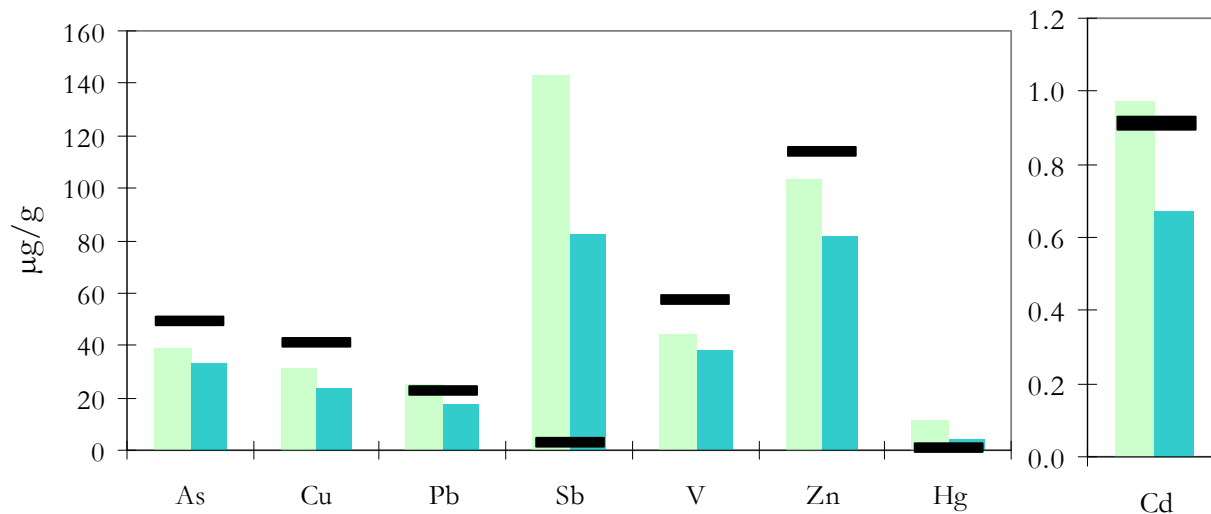


Figure 34 Concentration of selected heavy metals in horizon A (light green bar) and horizon B (dark green bar) in sample 6 downstream. The black lines represent the average background level of the area.

Heavy metal levels upstream from the tailing and slag heaps

Soil was sampled in an elevation gradient up-valley from the slag heaps (see Figure 14 for sample location). The heavy metal levels in these samples are presented in Figure 35 and Figure 36 (upper and lower horizon respectively).

In the upper horizon (Figure 35) there is a trend in increasing concentrations of As, Sb, Hg and Cd towards the slag heaps (Sample 4 is the sample closest to the slag heaps while sample 1 is the sample farthest away up-valley). Sample 1 does, however, have a higher concentration of all the metals except Hg than sample 2. While most of the metals are just slightly above background levels, the concentration of Sb and Hg is highly elevated in all the samples and the concentration of Cd is also somewhat elevated compared to background levels in the area. The levels of As, Pb, V and Zn is below or slightly above the background level in all the samples.

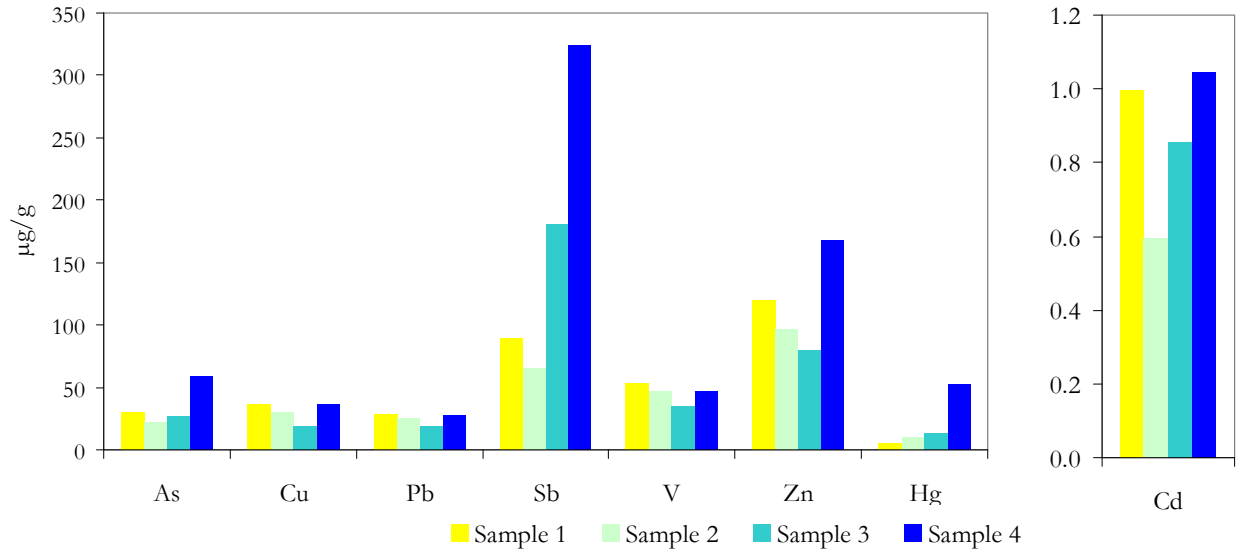


Figure 35 Heavy metal levels in the upper horizon of sample 1, 2, 3 and 4 sampled in an elevation gradient up-valley from the slag heaps

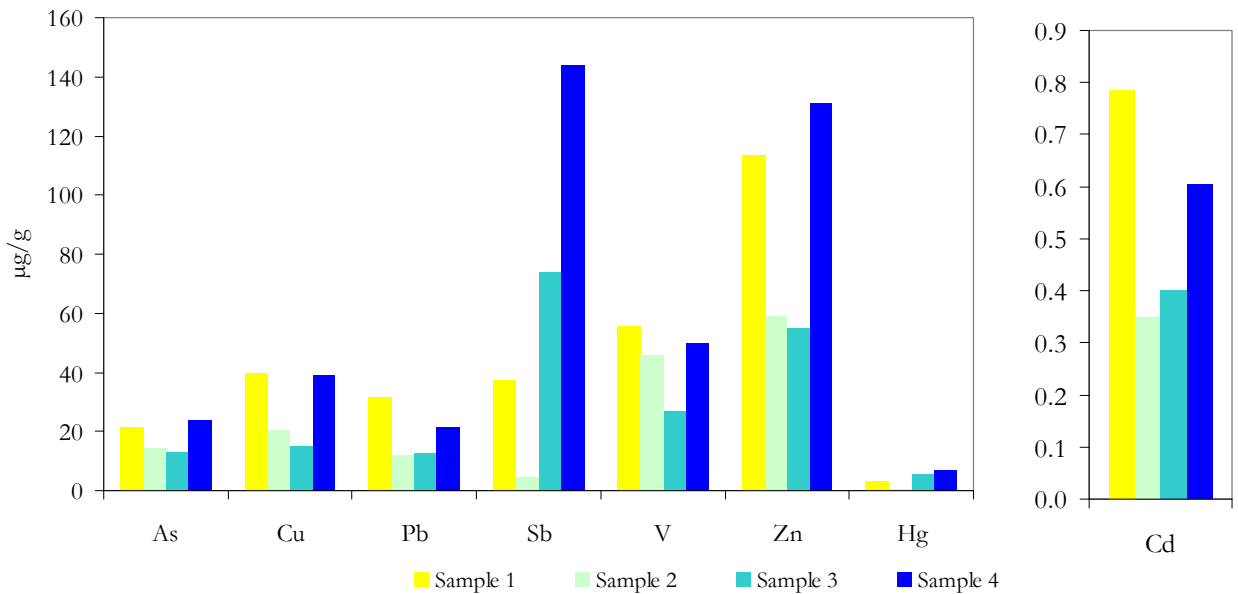


Figure 36 Heavy metal levels in the lower horizon of sample 1, 2, 3 and 4 sampled in an elevation gradient up-valley from the slag heaps

In the lower horizon (Figure 36) of the same samples as discussed above, the same trends as for the upper horizon is seen with an increase in concentration of Sb, Hg and Cd towards the slag heaps and high concentration in sample 1. Sample 2 stands out from the other samples due to it being a C horizon (the other samples are B horizons). That explains the lower level of some of the heavy metals in this horizon. What is interesting is that the levels of As, Cu, Pb, V, Cd and Zn in the C

horizon is not that different from the levels in the B horizon of sample 3. This implies that these metals may be present at a natural enrichment of the soil.

There is a clear trend of enhanced concentrations of Sb and Hg and a small enhancement of Cd and in soil downstream and up-valley of the waste areas. This confirms the hypothesis that the KMP is an anthropogenic source of these metals to the environment due to mobilisation of these heavy metals from the waste areas. There is also some indication that the waste areas are a source of As, Pb and Zn to the environment. Figure 37 is a boxplot presentation of all the samples in Khaidarkan for selected metals. Especially for Sb, but also for As, Cd, Pb and Zn it is clear that some of the samples have high values compared to background values and it is plausible to conclude that KMP is the anthropogenic source of the contamination as the highest values are found near the waste sites. Even though some concentrations of Cu, Mn and V are above the average level in the area, Figure 37 clearly shows that none of the concentrations are higher than the range of background level and are not likely of anthropogenic origin.

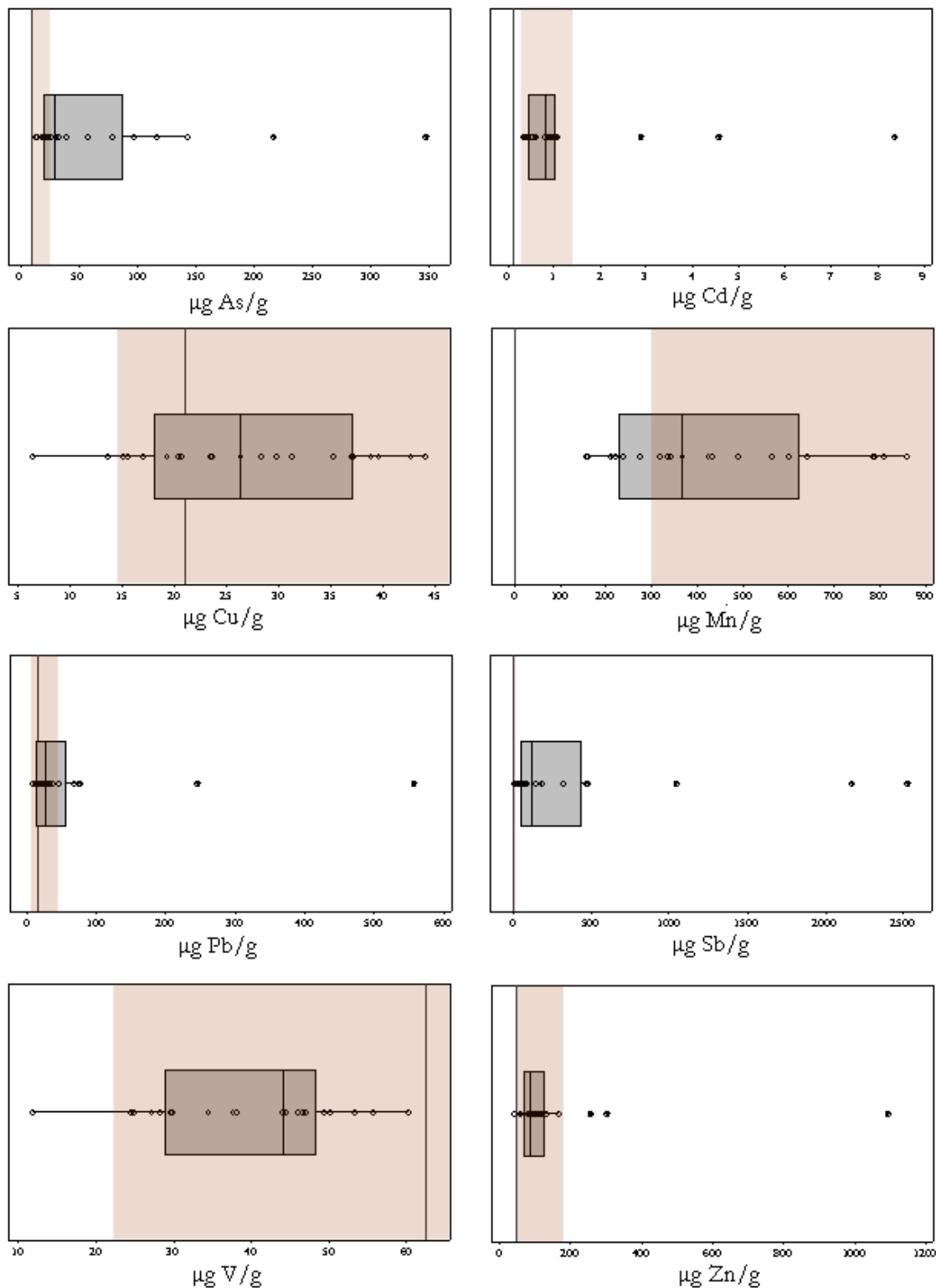


Figure 37 Boxplots showing concentrations of selected heavy metals in soil and sediment sampled in the Khaidarkan area (circles) median value (middle line) and quartiles (box ranges). The vertical black line gives the reference value for uncultivated soil given by (Bradl, 2005) for the respective heavy metals. The brown area represents background values for the area. See appendix N for reference and background values

4.2.5 Sequential extraction

A sequential extraction procedure was performed on the upper horizon of the soil sampled in Khaidarkan as well as the sediment samples with highest level of Hg (2-, 4- and 5 sed down and the tailing pond sediments). The lower horizon of the soil sampled in the apple garden was included due to the high Hg concentration. A reference soil (San Joaquin) was also included as quality control for the procedure's estimate of the total concentration of Hg.

The elementary fraction and the residual fraction were measured with DMA-80. For some unforeseen reason the DMA-80 gave results up to 30 % more than what was to be expected (see section 4.5.1). The sum of the fractions from the sequential extraction procedure exceeded the previously measured total Hg concentrations for some of the samples (see table K-1 and table K-2 in appendix K). This may also be due to uncertainty in the procedure. The results in this section in therefore only indicative and are included only to get an impression of the pools of Hg in the area.

The relative abundance of the different defined fractions and the added total of Hg is shown in Figure 38.

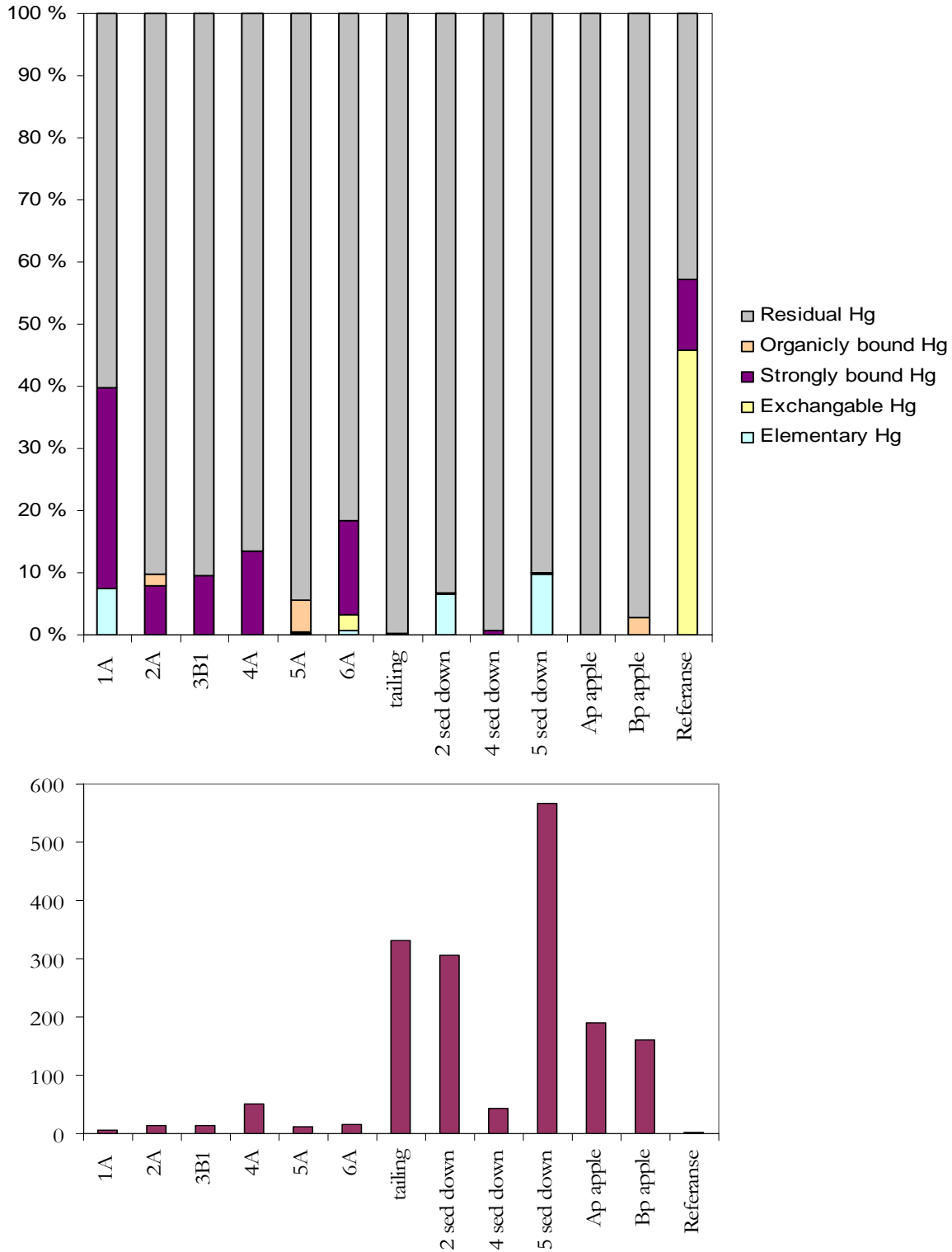


Figure 38 Results from the sequential extraction procedure. In the upper figure, the fractionation of Hg is shown in percentages. The lower figure gives the total Hg concentration (The concentration of all the fractions added up). The letter in the sample names denotes the horizon of the soil sample. The number denotes the sample site (see Figure 14).

Most of the Hg is found in the residual fraction of the soil and sediment (60 – 99.8 %) (see appendix K). In the residual fraction Hg is expected to exist as HgS or buried in the silicate lattice. The residual fraction is not bioavailable and has low mobility. Cinnabar is especially stable in high pH environments as found in Khaidarkan. It therefore seems that Hg is quite stable in the soil and sediments in the area around the KMP. The fact that the residual fraction is high is an indication of that HgS may be mobilised from the waste areas and transported as cinnabar colloids or as suspended particles of cinnabar by the drainage water from slag heap and tailing.

The samples in the elevation gradient have a quite large fraction of the strongly bound Hg (8 – 32 %). Strongly bound Hg reflects Hg from several soil and sediment compartments such as Fe and Mn oxyhydroxides as well as a portion of the organically bound Hg which is exchanged to solution through protonation of organic sites, and exchange from mineral surface sites where Hg is strongly adsorbed (Lechler et al., 1996). Hg has a high affinity for these adsorbents in soil so it is plausible that Hg entering the soil is detained by these complexing agents. A large fraction of the strongly bound Hg is most likely of anthropogenic origin since the naturally present Hg is found mostly in residual form. The highest point in the elevation gradient has also a small fraction of elementary Hg (7 %). This fraction most likely originated from atmospheric transport and is readily available for emission to air and hence long-range atmospheric transport. There is a small fraction of organically bound Hg in the soil sampled in one of the samples sampled up-valley from the slag heaps (2A) and within the city of Khaidarkan (5A) (2 and 5 % respectively), but this is quite small compared with the residual fraction.

In the tailing sample, which had the highest Hg concentration, almost all Hg is estimated to be residual Hg. This seems advantageous for the environment when considering transport and mobility of Hg from the tailing pond. But this does not mean that the Hg in the tailing pond is not at all mobile as has also been shown with the high levels of Hg found in the vicinity of the waste areas. Hg is probably mainly mobilised from the tailing areas as colloids and particles of cinnabar. The transport mechanisms may be atmospheric transportation as wind-blown dust, and as previously mentioned leaching from the pond to the nearby stream is likely as this stream had high concentration of dissolved Hg. Periodic peak flow events has probably also lead to transport of Hg from the tailing to the surrounding environment and may be a potential problem.

The sediment samples with the highest level of Hg (146 and 217 $\mu\text{g g}^{-1}$ for 2- and 5 sed down respectively) have a quite large fraction of elementary Hg (7 and 10 % respectively). This fraction is readily available and may be long-range transported after vaporisation.

The soil samples from the cultivated area consist mostly of residual Hg with 99.8 % residual Hg in A_p apple and 97 % residual Hg in B_p apple. These were possibly the samples of most concern as they have a remarkably high level of Hg for a cultivated soil with 95 and 152 $\mu\text{g g}^{-1}$ for A_p and B_p apple respectively. That most of the Hg in the soil is residual Hg is comforting. Most of the Hg is then relatively unavailable for uptake in plants and is not particularly mobile. But these high values are still of concern and should not be taken light upon. Uptake of Hg from the roots is not the only pathway of uptake in plants. Accumulation of Hg in plants may be a result of volatilization of Hg from the soil and re-adsorption through the stomata (Du and Fang, 1982; Patra and Sharma, 2000). This is, however, not likely mechanisms for the residual Hg in the soil. Dry deposition of reactive Hg-species from the atmosphere through foliar uptake through leafs and stems are also mechanisms of uptake (Lindberg et al., 1992). Sampling and analysis of the apples to check for Hg levels is, nevertheless, recommended.

4.3 Statistical interpretation

4.3.1 Correlation

A correlation matrix was made for the elements and soil parameters analysed in the soil and sediment samples from Khaidarkan. The full correlation matrix is given in table G-1 in appendix G-4. It is found that Fe has a weak correlation with most of the elements and soil parameters except with Al (0,851) and Mn (0,949) which are also strong oxide forming elements in the soil and the heavy metals cobalt (Co) (0,914) and V (0,817). This is quite the opposite of the situation in the background monitoring area, Kara Koi where Fe has a strong correlation with many of the heavy metals and was found to be an important explanatory variable (Vogt, 2008). When a correlation matrix was conducted with only emphasis on the soil samples (i.e. omitting the sediment samples) (see table G-2) the correlation with Fe increased for some of the metals giving a strong correlation

with Cr (0.954), Ni (0.93), V (0.859) and P (0.842). It seems apparent that Fe correlates mostly with hard or borderline metals. The pH shows a weak correlation with all the metals and soil parameters.

The soft heavy metals correlate strongly with each other. Hg has a strong correlation with Cd (0.874) and Sb (0.732) and also with the hard metal Ba (0.914). Sb correlates also strongly with the hard metal As (0.927) which is also the case for Pb (0.874). The correlation between As and Pb strengthens the hypothesis of the use of lead arsenate as a pesticide in the area and hence contamination of the metals. If also here the sediment samples are removed from the correlation analysis, an even stronger correlation between the soft metals is found. Hg has a stronger correlation with Sb (0.929), As (0.974) and Pb (0.731), but a weaker correlation with Cd (0.496). The trend is the same for the other heavy metals discussed in this section. When a correlation matrix is conducted with only emphasis on the sediment samples (Table G-3) Cd shows a strong correlation with Hg (0.864), Sb (0.958) and As (0.739). Pb shows a strong correlation with Zn (0.952) and As (0.866).

The correlation analysis does in many ways strengthen the hypothesis that the high levels of Hg, Sb, Cd and As is a result of the anthropogenic mining activity in the area.

4.3.2 Cluster analysis

A single linkage dendrogram, based on correlation coefficient distance of the variables are given in Figure 39. The cluster analysis confirms previous findings, showing great similarities between Cd and Sb, linked together with As. Pb and Zn have high similarities while Hg is linked to all the mentioned metals with a similarity of above 90 %. LOI is linked to this cluster with a similarity of slightly less than 90 % and seems to be an explanatory variable for these parameters. All the above-mentioned heavy metals have a high affinity towards OM so this seems plausible. Fe and Mn have a large similarity and also V, CEC, Ni and Cu make a cluster with these metals. CEC seems to be an explanatory variable for these metals. The pH and total C are weakly linked to all the above mentioned metals and soil parameters.

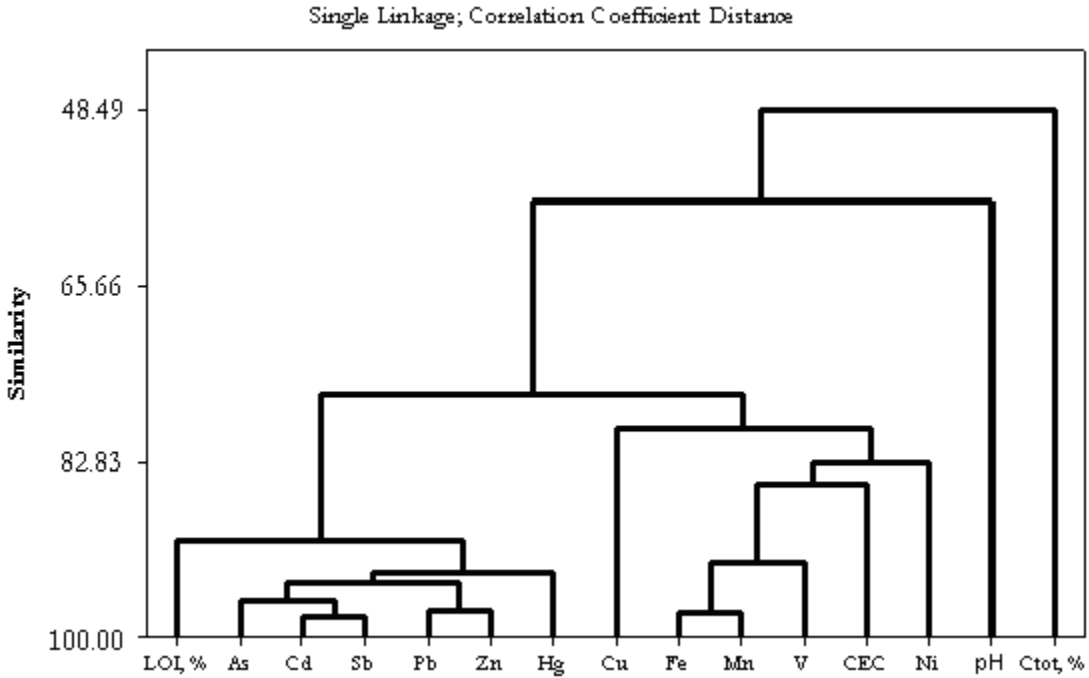


Figure 39 Dendrogram of the soil and sediment samples in Khaidarkan based on the similarities of the heavy metals and some soil parameters.

A single linkage dendrogram made based on Euclidean distances of the samples is given in Figure 40. There is no clear trend in the similarities of the samples. 1 sed up is clearly the sample that differs most from the rest. 1A up and 4B seams to be very alike. 3B₂ and 5B Hid does also show a great similarity. The samples with extreme values of Hg (except 1 sed up) are clustered together with 5A Hid. These are located downstream from the mine tailing and the samples seam to be influenced by the nearby tailing.

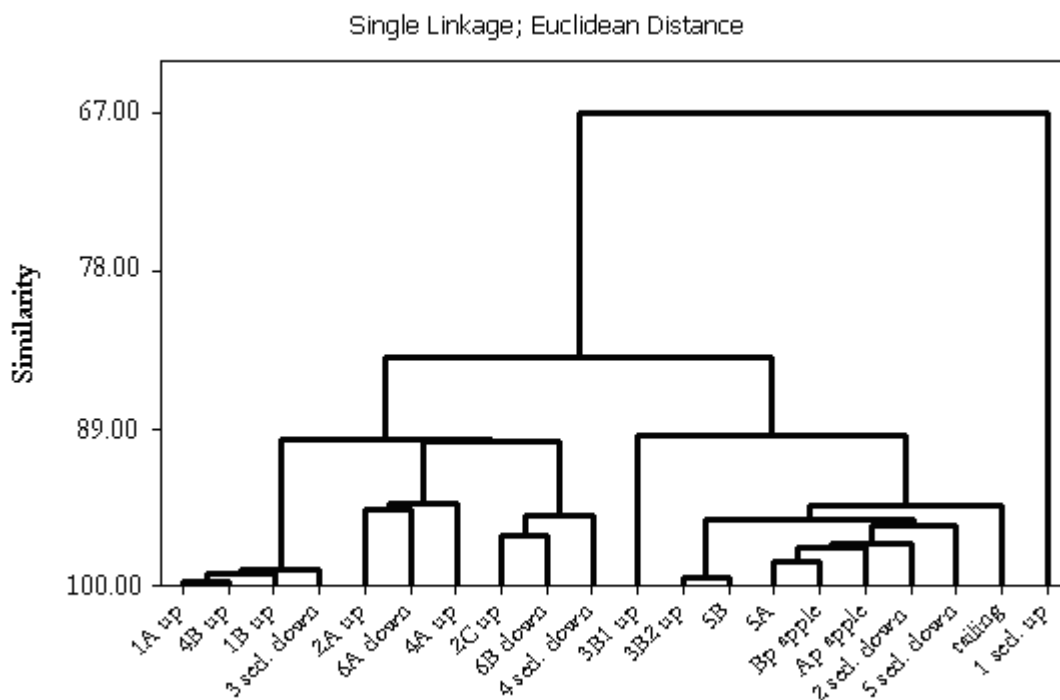


Figure 40 Dendrogram of the soil and sediment samples in Khaidarkan based on the similarities of the different samples.

4.3.3 Principal Component Analysis

A principal component analysis was performed by analysing the heavy metals together with soil parameters of the soil and sediment samples. The resulting loading plot is given in Figure 41. PC1 describe 41.9 % of the variation while PC2 describe 24.3 % of the variation. Since PC1 and PC2 accounts for 66.2 % of the variation only these two are used to describe the dataset. Eigenvalues and the PC values are given in appendix J.

Of the soil parameters Fe has a high positive loading along PC1 while Ct_{tot} and LOI have high loadings along PC2 (In opposite directions). This strongly indicates that C_{tot} is mainly inorganic carbon and that LOI is a measure of the organic content of the soil. The pH has a weak loading along both PC1 and PC2 and it seems to explain little of the variation in the dataset. The pH of the samples has little variation (Table 6). When PC1 is plotted vs. PC3 for only soil samples pH has a high positive loading along PC3 (see appendix J-2), but PC3 describes only 13.3 % of the variation.

Clustered together with Fe are the other acid cations Mn and Al, and V and Co. The co variation of some hard and borderline metals with Fe was also seen in the correlation and cluster analysis.

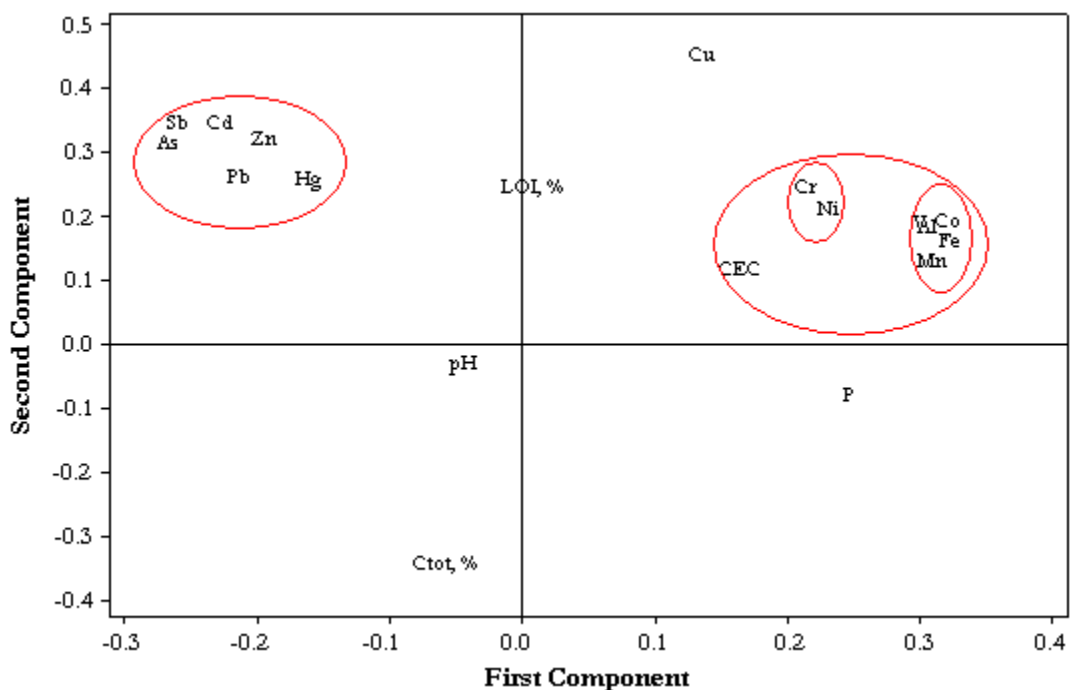


Figure 41 Loading plot of PC1 vs. PC2 for the soil and sediment samples in Khaidarkan with two clear clusters marked in the figure.

The heavy metals Hg, Cd, Sb, As, Zn and Pb are clustered together and have a high positive loading on the PC2 and a large negative loading along PC1. These are all metals that have a high affinity towards OM in the soil. This was not revealed by the correlation matrix were LOI only had a strong correlation with Hg (0.788). As also indicated by the cluster analysis, the LOI seems to be an explaining variable for variables with high loadings along PC2 while C tot is an explanatory variable in the opposite direction. The PC2 seems to reflect the difference in the soils capacity to accumulate contaminants.

The PCA give a good picture of the dataset. The two clusters located in opposite directions along PC1 reflect the different origins for the elements. The PC1 seems to be an anthropogenic vs. natural loading gradient, where a large negative loading along PC1 indicates anthropogenic origin of the element and a large positive loading reflects that the element is naturally present in the soil with Fe as an explanatory variable. This confirms much of what has been hypothesised earlier that the six

elements in the cluster to the left in Figure 41, mainly originate from the Hg mining activity at the KMP.

A score plot of the samples in the dataset show that the tailing sample and 1 sed up have especially high scores along PC2 (Figure 42). This correlates well with the loading plot (Figure 41) in that the heavy metals expected to originate from the waste from KMP also have a high loading along PC2. The samples from the waste area are clearly dominating in the data set.

The additional samples are positioned in a nice gradient in the score plot. There is no obvious explanation for this trend, but the most contaminated samples are positioned with a negative loading along PC1 and many of these samples have high content of inorganic carbon. The samples with highest amount of OM are positioned with positive scores along PC1 and PC2. These are in addition less contaminated (except 4A).

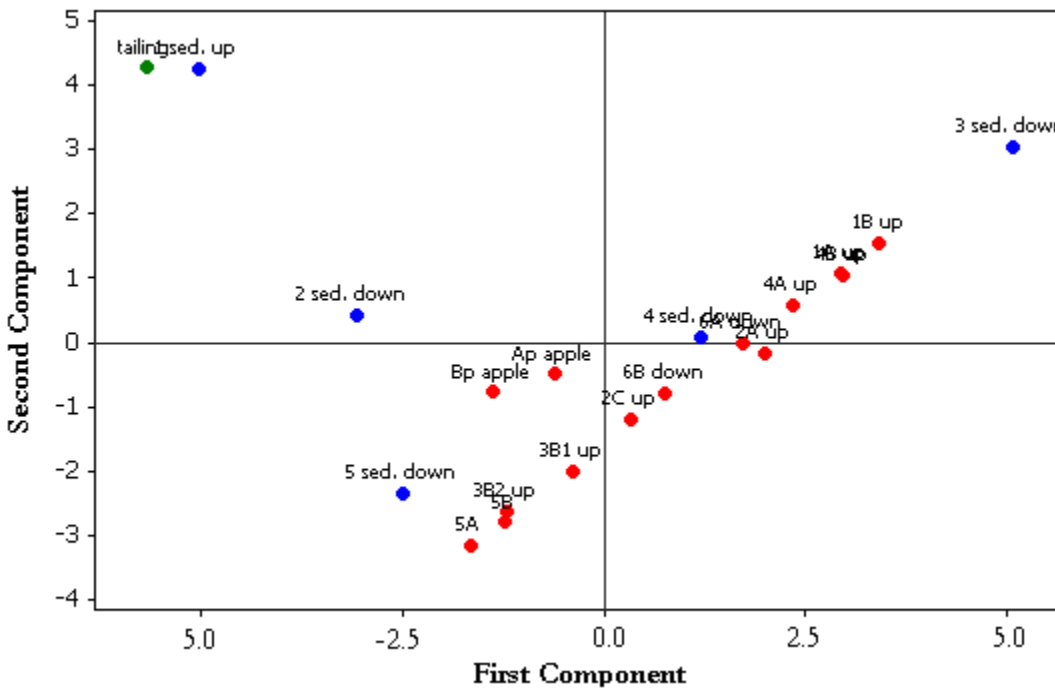


Figure 42 Score plot of PC1 vs. PC2 for the soil and sediment samples in Khaidarkan. Red dots represent soil samples, blue dots represent sediment samples. The green dot represents the tailing sediments.

4.4 Method development of the methods

4.4.1 Development and validation of the homogenisation procedure

Homogenisation only with manual grinding and sieving (with a 2 mm stainless steel sieve) were first performed on all the samples. With this procedure a poor precision of the results for DMA-80 was achieved with relative standard deviation ranging from 2 to 53 % (See appendix C-5). It was attempted to get an improvement by measuring several replicates (up to ten) of each sample with no satisfactory effect.

Preliminary test of the effect of homogenisation using a Retsch Mixer Mill showed a great improvement in the precision. The need for a cooling step (cryogenic grinding) as a part of the homogenisation procedure to avoid losses of Hg during the procedure was tested by measuring the Hg content of a sample that had been homogenised with cryogenic grinding and measuring the Hg content of the same sample homogenised without the cooling step on the DMA-80. The Hg measurements without cryogenic grinding seem to be significantly lower (See appendix C-5). This means that some of the Hg in a sample is lost if the sample is homogenised in a mixer mill without a cooling step, due to heat evolution and vaporisation of Hg during mixing. The sample material was too small to run significance test on the result, but based on the measurement results homogenisation with cryogenic grinding was the homogenisation method of choice and was performed on all the soil samples by three bachelor students, supervised by the candidate.

The samples with highest concentration of Hg were diluted with graphite prior to homogenisation with cryogenic grinding in order to diminish the uncertainty in the balance. The purity of the graphite was checked by analysis with the DMA-80. The content of Hg in graphite (see appendix C-9) was found to be below the method detection limit hence the graphite was found to be a suitable dilution medium.

The improved homogenisation procedure with cryogenic grinding and dilution of samples with high content of Hg lead to a desired improvement in the precision of the method with all except three of the samples having relative standard deviations less than 10 %. (See appendix C-5).

4.4.2 Selection of wavelengths used in the ICP-AES analysis

Several wavelengths for each metal were selected for the analysis with ICP-AES. Only one wavelength for each metal was selected for the presentation of data based on freedom of interferences and the intensity of the line. The lines that were chosen are given in appendix D-4, table D-7.

4.5 Validation and quality control

4.5.1 Validation of the DMA-80 method

Accuracy and precision of the DMA-80 method

DMA-80 analysis provided results with recovery between 104 - 108 % of the certified reference material (San Joaquin soil) measured on three different days (Figure 43). This is an acceptable accuracy. The precision was also good with relative standard deviations from 2.2 to 7.8 % in the same measurements.

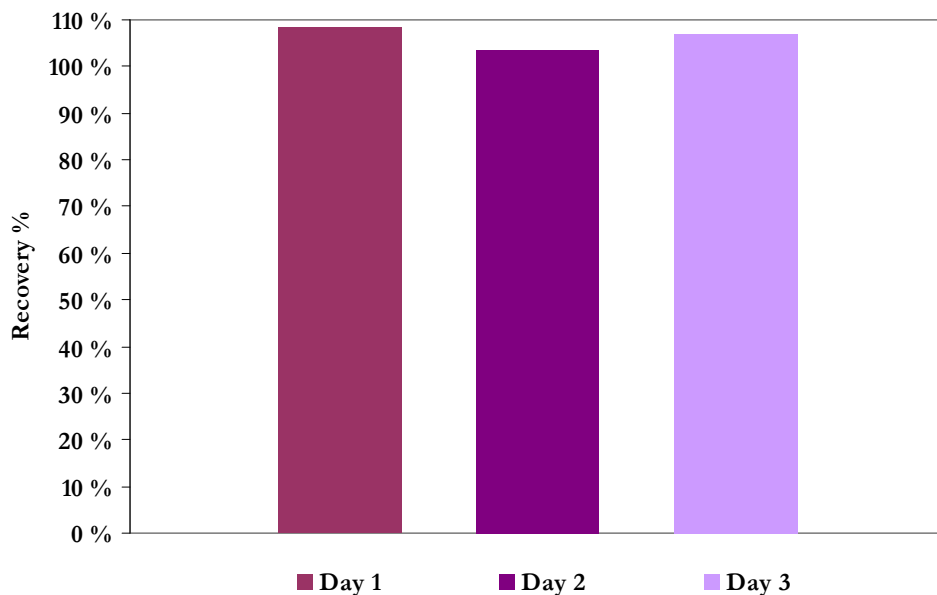


Figure 43 Hg recoveries for San Joaquin soil analyzed by DMA80

An uncertainty test for comparison of the uncertainties of measured values of the CRM and uncertainty of the CRM with the difference between the measured and the certified values are performed as a test of the accuracy of the method. Test results are given in Table 12. See appendix G-3 for equations for calculations and further explanation of the test.

Table 12 Result for uncertainty test when comparing measured values for the certified reference material with given concentrations of the certified reference material (CRM). Mean and STD are given in $\mu\text{g kg}^{-1}$

	Mean _{measured}	u _{measured} ^a	Mean _{CRM}	u _{CRM} ^a	Δ_m ^b	u Δ ^c	U Δ ^d	Remark
Day 1	1516	118	1400	80	116	142	284	No significant difference
Day 2	1451	66	1400	80	51	104	207	No significant difference
Day 3	1498	33	1400	80	98	87	173	No significant difference

^aStandard deviation of the measured value and the value of the CRM respectively

^b $|\text{Mean}_{\text{measured}} - \text{Mean}_{\text{CRM}}|$

^cThe combined uncertainties of the measurements and the CRM

^dThe extended uncertainty, $u_{\Delta} \cdot 2$

Since $\Delta_m \leq U_{\Delta}$ there is no significant difference between the measurement result and the certified value at $P = 0.05$. The accuracy of this method was therefore considered acceptable.

The fractions (elementary Hg and residual Hg) from the sequential extraction were analysed two months later than the total Hg concentrations was determined. During this period the accuracy of the instrument was somewhat poorer than during the analysis of total Hg in the samples. Three different certified reference materials (San Joaquin, 280R and 277R, see also appendix O and P) were run with recoveries of 114, 114 and 120 % (Figure 44). The precision was acceptable with relative standard deviation of 3.3 – 6.1 % in the same measurements.

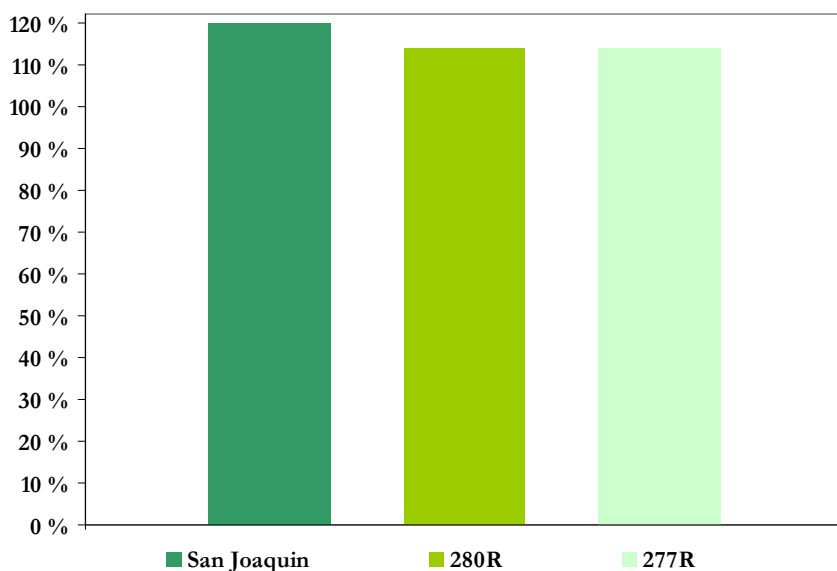


Figure 44 Hg recoveries of San Joaquin, 280R and 277R

These recoveries are in the upper range of what is acceptable for the accuracy of the instrument. It was attempted to improve the accuracy and precision of the instrument by changing the gold amalgamator trap and catalyser of the instrument without much improvement. The uncertainty test for the accuracy was again performed (Table 13).

Table 13 Result for uncertainty test when comparing measured values for three certified reference materials with given concentrations of the certified reference materials (CRM). Mean and STD are given in $\mu\text{g kg}^{-1}$.¹

	Mean _{measured}	u _{measured} ^a	Mean _{CRM}	u _{CRM} ^a	Δ_m ^b	u Δ ^c	U Δ ^d	Remark
San Joaquin	1676	55	1400	80	276	97	194	Significant difference
280R	1663	101	1460	200	203	224	448	No significant difference
277R	146	4.9	128	17	18	18	35	No significant difference

¹For explanation of symbols and abbreviations, see footnotes in Table 12.

It was only the measurement of one of the three CRM's (San Joaquin) that was significantly different than the certified value at $P = 0.05$. The fact that all the CRM's measured gave a higher recovery is, however, an indication on a somewhat higher measured Hg concentration of the sample than what is the real value. There was in addition some indication of poorer accuracy in analysis of samples with high concentration of Hg compared to samples with a low Hg level (Appendix K, table K-2) with an increase in the measured total Hg concentration of up to 30 % for the samples with highest levels of Hg. As a control for the accuracy a CRM was measured in all measurement runs. The results of the analysis of the CRM's indicate that the Hg in the elemental fraction obtained from the

sequential extraction analysis is somewhat underestimated (elemental Hg was determined by measuring the Hg content of the sample after a pyrolysis step (heating the sample at 80 °C for 8 hours) and subtracting the obtained value from the previous measured total content of Hg) and that the residual fraction is somewhat overestimated.

Limit of detection (LOD) and method detection limit (MDL) of the DMA-80 method

The LOD and MDL of the DMA-80 method at the time of the measurement of total Hg and at the time of analysis of the fractions (elemental and residual Hg) from the sequential extraction procedure is given in Table 14 (Two different LOD and MDL are given since the analysis was carried out with a two month time span). See appendix C-6 and C-7 for calculations and raw data.

Table 14 LOD and MDL for the DMA-80 method during total Hg analysis and analysis of fractions of the sequential extraction procedure

	Determined at the same time as the total Hg analysis	Determined at the same time as the sequential extraction analysis
LOD (ng)	0.7	0.2
MLD (ng g ⁻¹)	4	1

The LOD and MLD are actually lower for the sequential extraction analysis. This means that the problem with too high results for the sequential extraction analysis with DMA-80 can not be due to contamination of the instrument or memory effect.

4.5.2 Validation of the IC method

Accuracy of the IC method

IC analysis provided results with recoveries of the main anions in the reference standard solution between 92 - 109 % (Figure 45) implying a satisfactorily accuracy.

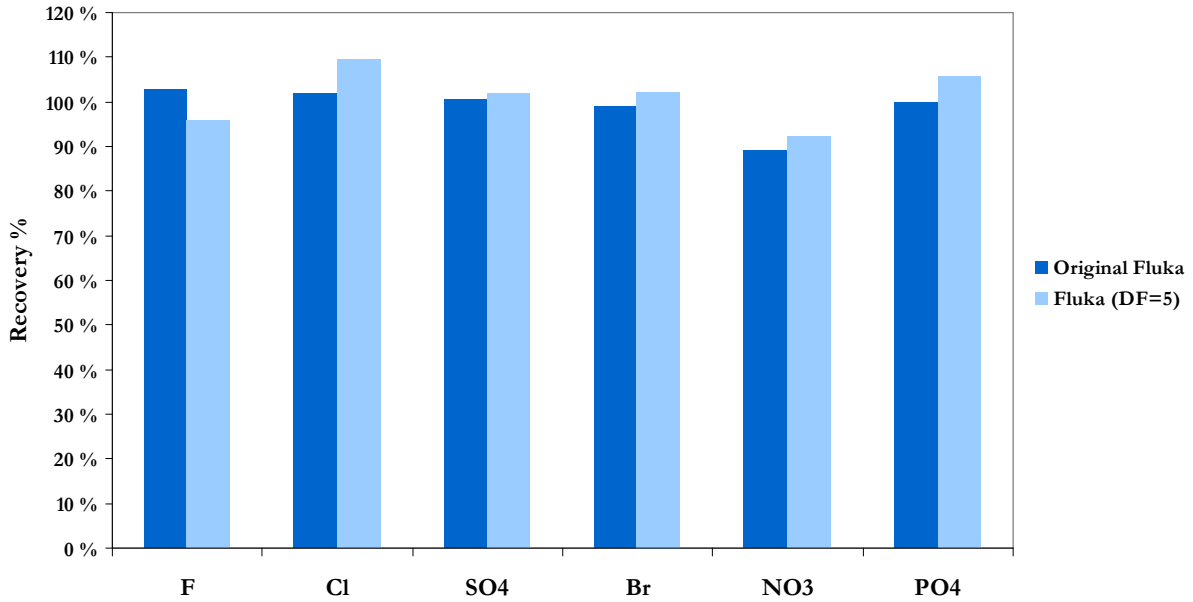


Figure 45 Recovery of the main anions for Fluka reference solution analyzed by IC

4.5.3 Validation of the PSA 1631 method for determination of Hg in water

As a check of the stock standard used to prepare the calibration curve control solutions prepared from an external standard was analysed. The result was within $\pm 10\%$ of the expected value and the accuracy was therefore considered to be acceptable. The recovery is given in Figure 46.

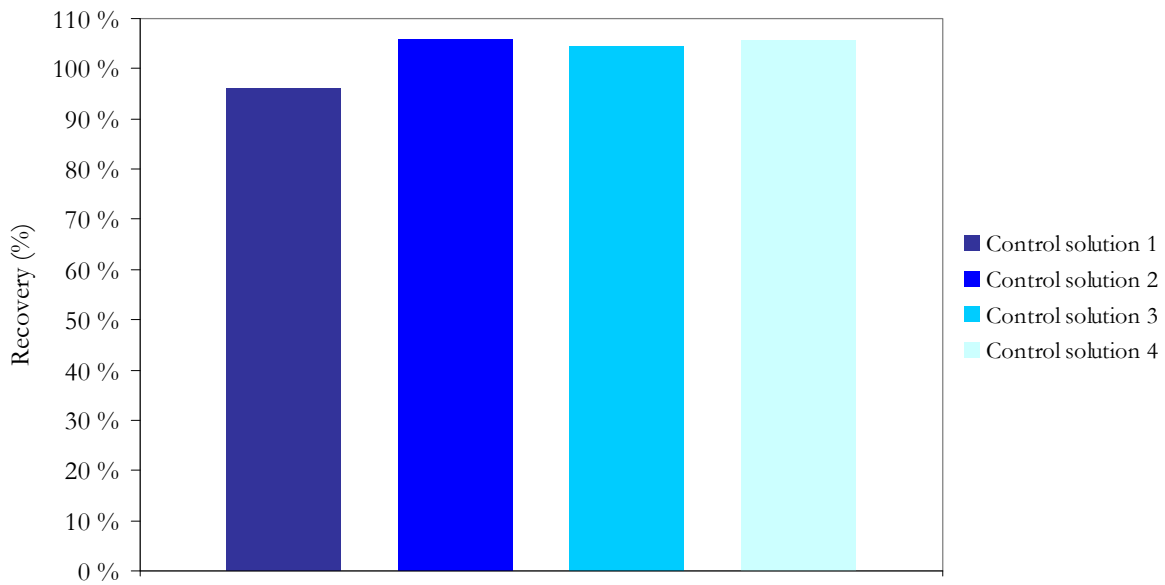


Figure 46 Recovery of Hg in four different control solutions analysed by PSA 1631 Hg analyser

The background equivalent concentration (BEC) was determined as a test of the Millennium Merlin Hg Analyser. See appendix I-4 for further explanation and equations. The BEC should be within the limits of 0.05 – 0.5 ng L⁻¹ given by PSA. It was determined to be 0.1 ng L⁻¹ which was well within the limits.

Limit of detection (LOD) for the determination of Hg in water with the Millennium Merlin Hg Analyser

The LOD for the determination of Hg in water with Millennium Merlin Hg Analyser is given in Table 15. See appendix I-5 for further explanation and calculations.

Table 15 LOD for the PSA 1631 method for Hg determination in water

PSA 1631 method for Hg determination in water	
LOD (ng L ⁻¹)	0.35

4.5.4 Paired t-test for the comparison of Hg measurements with DMA80 and ICP-AES

In order to compare the results for Hg analysed with DMA-80 with the results from ICP-AES conducted at Alex Stewart laboratory in Kara Balta, Kyrgyzstan, a paired t-test for the comparison of methods was conducted. In a paired t-test the difficulty of separating the variation due to method from the variation in samples has been overcome by looking at the difference, *d*, between each pair of results given by the two methods. If there is no difference it is assumed that they come from a population where $\mu_d=0$. The null hypothesis is tested by checking whether \bar{d} differs significantly from 0 by using the statistic *t*. The null hypothesis that there is no difference between the two samples is rejected if the calculated *t* exceeds the critical *t* (Miller and Miller, 2005). The test results are given in Table 16. See appendix G-2 for calculation formulas.

Table 16 Comparison of Hg measurements from analysis with DMA80 and ICP-AES

n	\bar{d}	<i>s_d</i>	<i>t</i>	<i>t</i> ₂₀ ¹⁰
20	11	46	1.05	2.09

Since *t*₂₀ > *t*, the null hypothesis, that the methods give different results for the determination of Hg, is not discarded. The Hg measurements from the two different methods are not significantly

¹⁰ The critical value was received from table A.2 in **Miller J. N. and Miller J. C.** (2005) Statistics and Chemometrics for Analytical Chemistry. 5th edition: Pearson education limited.

different at $P = 0.05$. In this study the results from the DMA-80 were used since the DMA-80 method is easier to perform with no pre-treatment of the sample. The decomposition of the sample includes more steps in the method, hence further risk of contamination and possible loss of analyte. DMA-80 is found to be a highly accurate and suitable method for determination of Hg in solid samples (Milestone, 2003).

5. Conclusions and further work

Khaidarkan is a heavily contaminated area. The levels of Hg and Sb are especially high due to the activity of the Khaidarkan Mercury Plant (KMP). The levels of other heavy metals are also high; Cd and As are found in amounts significantly above background values. Pb and Zn were also found in elevated levels in some of the samples. KMP is likely the main source of these metals as well. This is indicated in a PCA analysis where Cd and As along with Pb and Zn were clustered together with Hg and Sb.

Heavy metals such as Ni and Cr were not found in elevated levels relative to local background values. These metals are clustered together with Fe and other acid metals in the PCA analysis. Fe seem to be an explanatory variable for the heavy metals of natural origin with a high positive loading along PC1, the heavy metals found to be most likely of anthropogenic origin have a strong negative loading along the PC1. PC1 seems therefore to explain anthropogenic versus natural origin of heavy metals. Based on this assessment the statistical analysis confirms that KMP is a large contributor to enhanced levels of Hg, Sb, Cd, As, Pb and Zn in the surrounding environment, relative to local background levels.

The sequential extraction procedure revealed that mercury exists mostly in residual form (as HgS or incorporated in the silicates) in the sampled environments. Hg is then probably mobilised and probably from the waste areas as colloids or particles of residual Hg. High levels of Hg in a flooding area downstream from the tailing pond indicate that much of this Hg is mobilised during periodic peak flow events. High levels of dissolved Hg were found in drainage water from the tailing pond and the slag heaps. Hg is therefore also mobilised in a soluble form from the waste areas.

Studying Hg deposits locally in California, Kim et al. (2000) has found that more soluble secondary Hg compounds (HgSO₄ and Hg-Cl species) were formed during inefficient and incomplete roasting of the sulphide ore (mainly HgS). This may be an important faction understanding the leaching of Hg from slag heaps and mine tailings. The sequential extraction procedure is unsuitable for revealing the exact soluble or colloidal species draining the waste areas since fractions, rather than species is detected. Kim et al (2000) showed that X-ray absorption spectrometry in combination with standard

microanalytical techniques and other speciation techniques will provide useful information on the composition of the mercury mine waste and provide the basis needed to conclude on the compounds determining the mobility and reactivity of Hg. This procedure should be performed on the waste material associated with KMP.

This study shows that Khaidarkan is a heavily contaminated area and the need for further research in the area is urgent. Since this is a pilot study the sampling and analysis scheme is inadequate in order to get a clear picture of the situation in Khaidarkan. A more thorough study is needed in the area in order to make a thorough environmental assessment of the contamination problem. Foremost, samples of soil, water and sediments downstream from the tailing pond should be collected and the levels of Hg and other heavy metals in the samples analysed. In addition, vegetation samples should be sampled in the surrounding area and analysed.

6. References

- Alloway, B. J.** (1995a). Cadmium. In *Heavy metals in soils. 2nd edition.*, (ed. B. J. Alloway): Blackie Academic & Professional.
- Alloway, B. J.** (1995b). The origins of heavy metals in soils. In *Heavy Metals in Soils. 2nd edition.*, (ed. B. J. Alloway): Blackie Academic & Professional.
- Alloway, B. J.** (1995c). Soil processes and the behaviour of metals. In *Heavy Metals in Soils. 2nd edition.*, (ed. B. J. Alloway): Blackie Academic & Professional.
- Appelo, C. A. J. and Postma, D.** (2007). *Geochemistry, groundwater and pollution*, (ed.
- ATSDR.** (1990). Agency for Toxic Substances and Disease Registry. Toxicological Profile for Silver. Available from: <http://www.atsdr.cdc.gov/toxprofiles/tp146.html> Accessed: 24.2.2009.
- ATSDR.** (1992). Agency for Toxic Substances and Disease Registry. Toxicological Profile for Vanadium. Available from: <http://www.atsdr.cdc.gov/toxprofiles/tp58.html> Accessed: 24.2.2009.
- ATSDR.** (1999). Agency for Toxic Substances and Disease Registry. Toxicological Profile for Mercury. Available at: <http://www.atsdr.cdc.gov/toxprofiles/tp46.html> Accessed: 31.1.2009.
- ATSDR.** (2004). Agency for Toxic Substances and Disease Registry. Toxicological Profile for Copper. Available from: <http://www.atsdr.cdc.gov/toxprofiles/tp132.html> Accessed: 3.3.2009.
- ATSDR.** (2005). Agency for Toxic Substances and Disease Registry. Toxicological Profile for Zinc. Available from: <http://www.atsdr.cdc.gov/toxprofiles/tp60.html> Accessed: 3.3.2009.
- ATSDR.** (2008). Agency for Toxic Substances and Disease Registry. Toxicological Profile for Antimony. Available from <http://www.atsdr.cdc.gov/toxprofiles/tp23.html> Accessed 3.5.2009.
- ATSDR.** (2009). Agency for Toxic Substances and Disease Registry. Toxicological Profile for Cadmium. Available at: <http://www.atsdr.cdc.gov/toxprofiles/tp5.html> Accessed: 23.2.2009.
- Baker, D. E. and Senft, J. P.** (1995). Copper. In *Heavy Metals in Soils. 2nd edition.*, (ed. B. J. Alloway): Blackie Academic & Professional.
- Boss, C. B. and Fredeen, K. J.** (2004). *Concepts, Instrumentation and Techniques in Inductively Coupled Plasma Optical Emission Spectrometry*: Perkin Elmer.
- Bradl, H. B.** (2005). Sources and Origins of Heavy Metals. In *Heavy Metals in the Environment; origin, interaction and remediation*, (ed. H. B. Bradl).

- Cancès, B., Ponthieu, M., Castrec-Rouelle, M., Aubry, E. and Benedetti, M. F.** (2003). Metal ions speciation in a soil and its solution: experimental data and model results. *Geoderma* **113**, 341-355.
- Celo, V., Lean, D. R. D. and Scott, S. L.** (2006). Abiotic methylation of mercury in the aquatic environment. *Sci. Total Environ.* **368**, 126-137.
- Clarkson, T. W.** (2002). The Three Modern Faces of Mercury. *Environ. Health Persp.* **110**.
- Clarkson, T. W. and Magos, L.** (2006). The Toxicology of Mercury and Its Chemical Compounds. *Crit. Rev. Toxicol.* **36**, 609-662.
- Davies, B. E.** (1995). Lead. In *Heavy Metals in Soils. 2nd edition.*, (ed. B. J. Alloway): Blackie Academic & Professional.
- Davis, A., Bloom, N. S. and Hee, S. S. Q.** (1997). The Environmental Geochemistry and Bioaccessibility of Mercury in Soils and Sediments: A review. *Risk Anal.* **17**, 557-569.
- Du, S. H. and Fang, S. C.** (1982). Uptake of elemental mercury vapor by C3 and C4 species. *Environ. Exp. Bot.* **22**, 437-443.
- Duffus, J. H.** (2002). "Heavy Metals" - a Meaningless Term? *Pure Appl. Chem.* **74**, 793-807.
- ENVSEC.** (2007). Environment & Security. Transforming risks into cooperation. Central Asia Maps & Images. Available at <http://www.envsec.org/centasia/maps.php> Accessed: 6.5.2009.
- Esbensen, K., Schönkopf, S. and Midtgaard, T.** (1994). Multivariate Analysis - in practice. A Training Package.
- FAO.** (1998). Food and Agriculture Organization. Word reference base for soil resources, (ed. J. A. Deckers O. C. Spaargaren F. O. Nachtergaele L. R. Olderman and R. Brinkman).
- FAO.** (2001). Food and Agriculture Organization. Lecture Notes on the Major Soils of the World. . In *World soil resources reports - 94*, (ed. P. Driessen).
- Fergusson, J. E.** (1990). The Heavy Elements: Chemistry, Environmental Impact and Health Effects: Pergamon Press.
- Frattini, B. and Borroni, A.** (2006). Tranboundary risk assessment on the hazardous waste sites of KANIBADAM (Tajikistan), KHAIDARKEN (KYrgyzstan) KADAMJAI (Kyrgyzstan), in the Ferghana Valley. In *REHRA Regional Synthesis Report 2006*, (ed.
- Fritz, J. F.** (1987). Ion Chromatography. *Anal. Chem.* **59**.
- Gochfeld, M.** (2003). Cases of mercury exposure, bioavailability and absorption. *Ecotox. Environ. Safe.* **56**, 174-179.
- Google Earth.** (2009a). Photo of the Gauyang monitoring site.
- Google Earth.** (2009b). Photo of the Khaidarkan area.

- Gray, J. E., Crock, J. G. and Fey, D. L.** (2002). Environmental geochemistry of abandoned mercury mines in West-Central Nevada, USA. *Appl. Geochem.* **17**, 1069-1079.
- Gray, J. E., Hines, M. E., Higuera, P. L., Adatto, I. and Lasorsa, B. K.** (2004). Mercury Speciation and Microbial Transformations in Mine Wastes, Stream Sediments, and Surface Waters at the Almadén Mining District, Spain. *Environ. Sci. Technol.* **38**, 4285-4292.
- Gustin, M. S., Lindberg, S. E., Austin, K., Coolbaugh, M., Vette, A. and Zhang, H.** (2000). Assessing the contribution of natural sources to regional atmospheric mercury budgets. *Sci. Total Environ.* **259**, 61-71.
- Gustin, M. S., Lindberg, S. E., Marsik, F., Casimir, A., Ebinghaus, R., Edwards, G., Hubble-Fitzgerald, C., Kemp, R., Kock, H., Leonard, T. et al.** (1999). Nevada STORMS project: Measurement of mercury emissions from naturally enriched surfaces. *J. Geophys. Res.* **104**, 21,831-21,844.
- Harris, D. C.** (2003). Quantitative Chemical Analysis: W. H. Freeman and Company.
- Higuera, P. L., Oyarzun, R., Biester, H., Lillo, J. and Lorenzo, S.** (2003). A first insight into mercury distribution and speciation in soils from the Almadén mining district, Spain. *J. Geochem. Explor.* **80**, 95-104.
- Honda, S., Hylander, L. and Sakamoto, M.** (2006). Recent Advances in Evaluation of Health Effects on Mercury with Special Reference to Methylmercury - A Minireview. *Environ. Health Prev. Med.* **11**, 171-176.
- Hylander, L. D. and Meili, M.** (2003). 500 years of mercury production: global annual inventory by region until 2000 and associated emissions. *Sci. Total Environ.* **304**, 13-27.
- IUPAC.** (2000). Guidelines for terms related to chemical speciation and fractionation of elements. Definitions, structural aspects, and methodological approaches. *Pure Appl. Chem.* **72**, 1453-1470.
- Jitaru, P. and Adams, F.** (2004). Toxicity, sources and biogeochemical cycle of mercury. *J. Phys. IV France* **121**, 185-193.
- Järup, L.** (2003). Hazards of heavy metal contamination. *Brit. Med. Bull.* **68**, 167-182.
- Kakareka, S., Gromov, S., Pacyna, J. and Kukharchyk, T.** (2004). Estimation of heavy metal emission fluxes on the territory of the NIS. *Atmos. Environ.* **38**, 7101-7109.
- Kang, B. T. and Tripathi, B. R.** (1992). Technical paper 1: Soil classification and characterization. In *The AFNETA alley farming training manual - Volume 2: Source book for alley farming research*, (ed. B. R. Tripathi and P. J. Psychas).
- Kim, C. S., Brown, G. E. and Rytuba, J. J.** (2000). Characterization and speciation of mercury-bearing mine wastes using X-ray absorption spectroscopy. *Sci. Total Environ.* **261**, 157-168.

Krabbenhoft, D. P., Branfireun, B. A. and Heyes, A. (2005). Biogeochemical cycles affecting the speciation, fate and transport of mercury in the environment. In *Short course series*. Halifax, Nova Scotia: Mineralogical Association of Canada Short Course 34.

Krogstand, T. (1992). Chp. 3 Tørrstoff og glødetap. In *Metoder for jordanalyser*. , (ed. T. Krogstand): Institute of Soil Science, Ås. NLH.

Lechler, P. J., Miller, J. R., Hsu, L. and Desilets, M. O. (1996). Mercury mobility at the Carson River Superfund Site, west-central Nevada, USA: interpretation of mercury speciation data in mill tailings, soils, and sediments. *J. Geochem. Explor.* **58**, 259-267.

Lindberg, S. E., Meyers, T. P., Taylor, G. E., Turner, R. R. and Schroeder, W. H. (1992). Atmosphere-Surface Exchange of Mercury in a Forest: Results of Modeling and Gradient Approaches. *J. Geophys. Res.* **97**, 2519-2528.

Linsinger, T. (2005). Application note 1. Comparison of a measurement result with the certified value. European Reference Materials. Available at http://www.erm-crm.org/html/ERM_products/application_notes/application_note_1/index.htm Accessed: 2.5.2009.

Lottermoser, B. G. (2003). Mine Wastes - characterization, treatment, and environmental impacts: Springer.

MacDonald, D. D., Ingersoll, C. G. and Berger, T. A. (2000). Development and evaluation of consensus-based sediment quality guidelines for freshwater ecosystems. *Arch. Environ. Contam. Toxicol.* **39**, 20-31.

Martino, L., Carlsson, A., Rampolla, G., Kadyrzhanova, I., Svedberg, P., Denisov, N., Novikov, V., Rekacewicz, P., Simonett, O., Skaalvik, J. F. et al. (2005). Environment and Security - Transforming risks into cooperation. Central Asia. Ferghana / Osh / Khujand area, (ed.: UNEP, UNDP, OSCE, NATO).

Mason, R. P. and Benoit, J. M. (2003). Organomercury Compounds in the Environment. In *Organometallics in the Environment. 2nd edition.*, (ed. P. Craig): John Wiley & Sons Ltd.

Mason, R. P., Fitzgerald, W. F. and Morel, F. M. M. (1994). The biogeochemical cycling of elemental mercury: Anthropogenic influences. *Geochem. Cosmochim. Acta* **58**, 3191-3198.

Milestone. (2003). Mercury. DMA-80 Direct Mercury Analyser. Available from: <http://www.milestonesci.com/merc-tech.php> Accessed 28.10.2008.

Miller, J. R. and Miller, J. C. (2005). Statistics and Chemometrics for Analytical Chemistry. 5th edition.: Pearson Education Limited.

Ministry of the Environment. (2007). Regulations on amending the regulation of 1 June 2004, No 922, on restriction on the use of chemical and other products that endanger health and the environment (product regulation) Available from <http://www.regjeringen.no/en/dep/md/press-centre/Press-releases/2007/Bans-mercury-in-products.html?id=495138> Accessed: 9.5.2009.

Ministry of the Environment. (2009). The Swedish Government chemicals policy. Available at: <http://www.sweden.gov.se/sb/d/2023/a/119559> Accessed: 30.3.2009, (ed.: Government Offices of Sweden).

msc-e. (2008a). Meteorological Synthesizing Center - East. Detailed information for Kyrgyzstan. Available at: <http://www.msceast.org/countries/Kyrgyzstan/index.html> Accessed: 30.01.2009.

msc-e. (2008b). Meteorological Synthesizing Center - East. Emissions. Available at: <http://www.msceast.org/hms/emission.html> Accessed: 30.01.2008.

Navarro, A. (2008). Review of characteristics of mercury speciation and mobility from areas of mercury mining in semi-arid environments. *Rev. Environ. Sci. Biotechnol.* **7**, 287-306.

Nriagu, J. O. (1979). Production and uses of mercury. In *The Biogeochemistry of Mercury in the Environment*, (ed. J. O. Nriagu): Elsevier/North-Holland Biomedical Press.

O'Neill, P. G. (1995). Arsenic. In *Heavy Metals in Soils. 2nd edition*, (ed. B. J. Alloway): Blackie Academic & Professional.

Pacyna, E. G. and Pacyna, J. M. (2002). Global emission of mercury from anthropogenic sources in 1995. *Water Air Soil Poll.* **137**, 149-165.

Pacyna, E. G., Pacyna, J. M., Steenhuisen, F. and Wilson, S. (2006). Global anthropogenic mercury emission inventory for 2000. *Atmos. Environ.* **40**, 4048-4063.

Patra, M. and Sharma, A. (2000). Mercury Toxicity in Plants. *Bot. Rev.* **66**, 379-422.

Pearson, R. G. (1963). Hard and Soft Acids and Bases. *J. Am. Chem. Soc.* **85**, 3533-3539.

Peryea, F. J. and Creger, T. L. (1994). Vertical distribution of lead and arsenic in soils contaminated with lead arsenate pesticide residues. *Water Air Soil Poll.* **78**, 297-306.

Piao, H. and Bishop, P. H. (2006). Stabilization of mercury-containing wastes using sulfide. *Environ. Poll.* **139**, 498-506.

Qiu, G., Feng, X., Wang, S. and L., S. (2006). Environmental contamination of mercury from Hg-mining areas in Wuchuan, northeastern Guizhou, China. *Environ. Poll.* **142**, 549-558.

Ravichandran, M. (2004). Interaction between mercury and dissolved organic matter - a review. *Chemosphere* **55**, 319-331.

Rytuba, J. J. (2003). Mercury from mineral deposits and potential environmental impact. *Environ. Geol.* **43**.

Rytuba, J. J. (2005). Geogenic and mining sources of mercury to the environment. In *Mercury, sources, measurements, cycles and effects*, vol. 34 (ed. M. B. Parsons and P. J. B.): Min. Ass. of Canada, Short Course Series.

Schroeder, W. H. and Munthe, J. (1998). Atmospheric Mercury - an Overview. *Atmos. Environ.* **32**, 809-822.

Sharshenova, A. A., Dulatova, G. M., Bezverkhnyaya, Z. A., Kobzar, V. N. and Arzygulova, K. S. (1995). The problem of mercury in the biogeochemical province in Kyrgyzstan. *Toxicology Letters* **78**, 74-75.

Skoog, D. A., Holler, F. J. and Nieman, T. A. (1998). Principles of Instrumental Analysis: Brooks/Cole.

Sladek, C. and Gustin, M. E. (2003). Evaluation of sequential and delective extraction methods for determination of mercury speciation and mobility in mine waste. *Appl. Geochem.* **18**, 567-576.

Stavinskiy, V., Shukurov, E. and Suyunbaev, M. (2001). Mining Industry and Sustainable Development in Kyrgyzstan, (ed. V. Bogdetsky): Mining, Minerals and Sustainable Development.

Steinnes, E. (1995). Mercury. In *Heavy Metals in Soils. 2nd edition*, (ed. B. J. Alloway): Blackie Academic & Professional.

Tan, K. H. (1996). Soil Sampling, Preparation and Analysis. New York: Marcel Dekker, Inc.

UNECE. (1998). To the 1979 Convention on Long-range Transboundary Air Pollution on Heavy Metals. Available from: <http://www.unece.org/env/lrtap/full%20text/1998.Heavy.Metals.e.pdf>. Accessed: 13.01.2008

UNEP Chemicals. (2002). Global Mercury Assessment. *United Nations Environmental Programme - Chemicals*.

UNEP Chemicals. (2006). Summary of supply, trade and demand information on mercury. *United Nations Environmental Programme - Chemicals*.

US EPA. (2005). Method 245.7. Mercury in Water by Cold Vapor Atomic Fluorescence Spectrometry. Available from <http://www.epa.gov/waterscience/methods/method/mercury/> Accessed: 26.3.2009.

US EPA. (2007). Mercury in Solids and Solutions by Thermal Decomposition, Amalgamation, and Atomic Absorption Spectrophotometry. Available from: <http://www.epa.gov/osw/hazard/testmethods/sw846/pdfs/7473.pdf> Accessed: 01.10.2008.

USDA. (1999). Soil Taxonomy - A Basic System of Soil Classification for Making and Interpreting Soil Surveys. *Agricultural Handbook* **436**.

USGS. (2008). 2007 Minerals Yearbook - Mercury, (ed. W. E. Brooks).

vanLoon, G. W. and Duffy, S. J. (2005). Environmental Chemistry - a Global Perspective: Oxford University Press.

Vogt, R. D. (2008). Soil chemistry in Kara Koi. *Internal report*.

Wania, F. and Mackay, D. (1996). Tracking the Distribution of Persistent Organic Pollutants. Control strategies for these contaminants will require a better understanding of how they move around the globe. *Environ. Sci. Technol.* **30**, 390A-396A.

Wehrli, B. and Stumm, W. (1989). Vanadyl in natural waters: Adsorption and hydrolysis promote oxygenation. *Geochem. Cosmochim. Acta* **53**, 69-77.

WHO. (1990). Environmental Health Criteria 101. Methylmercury. *International Programme on Chemical Safety. Geneva.*

WHO. (2000). Mercury. In *Air Quality Guidelines - for Europe*, (ed. F. Theakston).

WHO. (2006). Guidelines for drinking-water quality, Vol 1, 3rd edition incorporating 1st addendum.

Wollast, R., Billen, G. and Mackenzie, F. T. (1975). Behaviour of Mercury in Natural Systems and Its Global Cycle. *Ecol. Toxi.* **7**, 145-166.

Zozulinsky, A. (2007). Kyrgyzstan: Mining Industry Overview, (ed. BISNIS): U.S. Commercial Service.

List of appendices

Appendix A: Reagents, instruments and other equipment.....	117
A-1: Chemicals.....	117
A-2: Gases	117
A-3: Water qualities.....	118
A-4: Certified reference materials	118
A-5: Standard stock solutions.....	118
A-6: Instruments and other equipment	119
Appendix B: Dry content and loss on ignition determination.....	121
B-1: Procedure and equations for the determination of dry content and loss on ignition.....	121
B-2: The results of the determination of dry content, loss on ignition and total carbon... ..	123
Appendix C: DMA-80.....	124
C-1: Technical specifications	124
C-2: Analysis programme.....	124
C-3: Calibration curves for DMA80.....	125
C-4 Results from DMA-80 analysis.....	126
C-5 Comparison of measurements with and without cryogenic grinding.....	128
C-6 Procedure and equations for determining the Limit of detection (LOD) and method detection limit (MDL) for the DMA-80 method	129
C-7 Results for the determination of LOD and MDL for the DMA-80 method.....	130
C-8 Recovery for CRM's with DMA-80.....	131
C-9 Test of the purity of the graphite	131
Appendix D: ICP-AES	132
D-1: Results for soil samples	132
D-2 Results for sediment samples	133
D-3: Results for other solid samples	134
D-4: Results for water samples	135
D-5: Preparation of calibration standards	136
D-6 Calibration curves for ICP-AES.....	137
Appendix E: Determination of total alkalinity	138
E-1: Procedure for determination of total alkalinity.....	138
E-2: Results for the determination of total alkalinity.....	138
Appendix F: IC.....	139
F-1 Preparation of calibration standards	139
F-2 Instrumental conditions	139
F-3 Results.....	140
Appendix G: Statistics.....	141
G-1 General statistics	141
G-2 Paired t-test for the comparison of methods.....	141
G-3 Accuracy test based on uncertainty used to compare recovery values with the certified value of the reference material used in the DMA-80 analysis	142
G-4: Correlation matrixes	143
Appendix H: Water parameters measured in field.....	146
H-1: pH, temperature and conductivity.....	146
Appendix I: PSA 10.035 Millennium Merlin 1631 Hg Analyser.....	147

I-1: Calibration curve.....	147
I-2 Preparation of calibration standards	147
I-3: Results for analysis of water samples.....	148
I-4: Background Equivalent Concentration (BEC).....	148
I-5 Procedure and equations for determining the Limit of detection (LOD) and method detection limit (MDL) for the PSA method for determination of Hg in water.....	149
I-6 Method	150
Appendix J: Principal component analysis.....	151
Appendix J-1: Eigenvalue matrix and PC for the Principal Component Analysis.....	151
Appendix J-2 Loading plot of PC1 vs. PC3 for the PCA	152
Appendix K: Sequential extraction.....	153
Appendix L: Soil parameters	154
Appendix M: Fraction diagram made with Medusa.....	155
Appendix N: Reference values.....	156
N-1 Reference values for uncultivated soil and background levels for selected heavy metals and soil parameters	156
N-2: PEC values for selected heavy metals.....	157
Appendix O: Certificates for Certified Reference Materials.....	158
O-1: Certificate of Analysis for Standard Reference Material 2709.....	158
O-2: Certificate of analysis for Certified Reference Material BCR [®] – 280R.....	164
O-3: Certificate of analysis for Certified Reference Material BCR [®] – 277R.....	164
Appendix P: Flame photometric emission spectroscopy.....	170
P-1: Calibration curve for Na	170
P-2: Calibration curve for K.....	170
P-3: Result for Na and K	172
Appendix Q: Soil colour	173
Q-1: Munsell soil colour.....	173

Appendix A: Reagents, instruments and other equipment

A-1: Chemicals

Listed below are the chemicals used during the experimental work

- Nitric acid (HNO₃), 65 % Suprapure® (Merck, Darmstadt, Germany)
- Hydrochloric acid (HCl), 30 % Suprapure® (Merck, Darmstadt, Germany)
- Magnesium chloride anhydrous (MgCl₂) (Sigma-Aldrich, Steinheim, Germany)
- Sodium hydroxide (NaOH), p.a. (Merck, Darmstadt, Germany)
- Tin(II) Chloride dehydrate (SnCl₂), reagent grade 98 % (Sigma-Aldrich, Steinheim, Germany)
- Fluka 55459 Hydroxylamine hydrochloride (NH₃OH · HCl), p.a. (Sigma-Aldrich, Steinheim, Germany)
- Buffer solution, pH 7.0 (25 °C), CertiPUR® (Merck, Darmstadt, Germany).
- Buffer solution, pH 10.0 (20 °C), CertiPUR® (Merck, Darmstadt, Germany).
- Liquid nitrogen (N)
- Graphite powder ≤0.01 mm (Fluka Chemie AG, Bucks, Switzerland)
- Bromine (bromide-bromate) volumetric standard, 0.1N solution in water (Sigma-Aldrich, Steinheim, Germany)

A-2: Gases

- Oxygen (O₂) gas was used for analyses with DMA-80. The quality of the gas was “Oxygen 5.0” (99.999%) (Yara, Oslo, Norway)
- Argon (Ar) gas was used for analysis with ICP-AES and PSA 10.035 Millennium Merlin 1631 Hg Analyser. The quality if the gas was 99.99 % (AGA, Oslo, Norway)
- Propane (C₃H₁₀) gas was used for analysis with Flame photometer. The quality of the gas was “2.6” (99.6) (AGA, Oslo, Norway)

A-3: Water qualities

Unless stated otherwise, type I water was used.

- Type I water, resistance > 18.0 M Ω cm (at 25 °C) (Millipore, Billerica, USA)
- Type II water, resistance > 1.0 M Ω cm (at 25 °C) (Millipore, Billerica, USA)

A-4: Certified reference materials

- Standard Reference Material[®] 2709, San Joaquin soil (NIST)
- Certified Reference Material BCR[®] – 277R (IRMM)
- Certified Reference Material BCR[®] - 280R (IRMM)

A-5: Standard stock solutions

- Spectrascan[®] Element Standard for Atomic Spectroscopy Mercury(II) stock solution, 1000 \pm 0.5 $\mu\text{g mL}^{-1}$ in 2.5 % HNO₃, (Teknolab AS, Kolbotn, Norway)
- Spectrascan[®] SS-1232 Mercury(II) stock solution 994 \pm 5 $\mu\text{g mL}^{-1}$ in 5 % HNO₃ (Teknolab, Kungsbacka, Sweden)
- Certified standard Mercury(II) stock solution, 1000 \pm 3 $\mu\text{g mL}^{-1}$ in 2.5 % HNO₃ (Spectropure Standards AS, Manglerud, Norway)
- Dionex Seven Anion Standard II (Dionex, Instrument Teknikk A.S, Oslo, Norway) Standardized from SRM 3183, SRM 3182, CRM 0905 NO₂, SRM 3184, SRM 3185, SRM 3186, SRM 3181 (NIST)
- Multielement Ion Chromatography Anion Standard Solution (Fluka, Sigma-Aldrich, Buchs, Switzerland)
- Certified standard Sodium (Na) stock solution, 1000 \pm 3 $\mu\text{g mL}^{-1}$ in 2.5 % HNO₃ (Spectropure Standards AS, Manglerud, Norway)
- Certified standard Potassium (K) stock solution, 1000 \pm 3 $\mu\text{g mL}^{-1}$ in 2.5 % HNO₃ (Spectropure Standards AS, Manglerud, Norway)
- Certified standard Calcium (Ca) stock solution, 1000 \pm 3 $\mu\text{g mL}^{-1}$ in 2.5 % HNO₃ (Spectropure Standards AS, Manglerud, Norway)

- Certified standard Magnesium (Mg) stock solution, $1000 \pm 3 \mu\text{g mL}^{-1}$ in 2.5 % HNO_3 (Teknolab AS, Kolbotn, Norway)
- Multielement standard, $50 \mu\text{g mL}^{-1}$ As, Bi, Ga, Ge, In, Pb, Sb, Se, Sn, Te, Ti, V in 4.9 % (abs) HCl (Teknolab AS, Kolbotn, Norway)
- Multielement standard, $100 \mu\text{g mL}^{-1}$ Cd, Cr³, Co, Cu, Fe, Pb, Mn, Ni, V, Zn in 2.5 % (abs) HNO_3 (Teknolab AS, Kolbotn, Norway)

A-6: Instruments and other equipment

- A Milestone DMA-80 Direct Mercury Analyzer with nickel and quartz sample boats was used in the determination of Hg content in the soil samples.
- A Sartorius CP224S balance was used to weigh the soil samples prior to analysis by the DMA-80.
- A field pH meter was used for the determination of pH in the field
- An EcoScan CON 5 Conductivity Handheld Meter was used for the determination of conductivity and temperature of water in the field.
- A Dionex IC was used for the determination of main anions in selected water samples.
- A Varista Varian ICP-AES with radial view plasma and a V-Groove Nebulizer and CCD Simultaneous detector was used for the determination of selected metals in the water samples.
- A PSA 10.035 Millenium Merlin 1631 Hg Analyser was used for the determination of Hg in the water samples and in the extracts from the sequential extraction.
- A Retsch Mixer Mill MM 2000 equipped with two 10 mL ZrO_2 grinding cups and two 12 mm beads (also of ZrO_2) were used for the homogenisation of the soil samples.
- A Termarks oven was used to dry the soil samples and in the first step in the sequential extraction procedure.
- A 702 SM Titrino was used in the alkalinity measurement of selected water samples.
- A DIONEX 2000 IC with IonPac® AG18 guard and IonPac® AS18 analytical columns with ASRS-Ultra auto-suppressor was used for the determination of anions.

- A Bandelin Sonorex RK100H Ultrasonic bath was used as additional cleaning of ZrO₂ cups and balls.
- A Sherwood Flame Photometer 410 was used for determination of Na and K.

Appendix B: Dry content and loss on ignition determination

B-1: Procedure and equations for the determination of dry content and loss on ignition

The procedure for the determination of dry content and loss on ignition was collected from “Methods for soil analysis” by Krogstad (1992).

An aliquot of the air-dried sample (approximately 3 g) was heated in a crucible in an oven (at $105 \pm 5^\circ\text{C}$) for six hours. The samples were weighed prior to and after the heating (after being cooled down in an exicator for 30 minutes) using an analytical balance and the percentage dry content was calculated from equation B-1 below.

$$\%DryContent = \frac{m_3 - m_1}{m_2} \cdot 100 \quad (B-1)$$

where m_1 = weight of crucible

m_2 = weight of the air-dried soil sample

m_3 = weight of crucible and soil sample after heating

The loss on ignition analysis was performed at the Alex Stuart Laboratory in Kara Balta, Kyrgyzstan.

An aliquot of the air-dried sample (approximately 3 to 5 g) was glowd in a crucible in a Carbolyte Muffle furnace at $550 \pm 25^\circ\text{C}$ for more than 3 hours. The crucible was then cooled down for 30 minutes in an exicator before weighing on an analytical balance. The loss on ignition was then calculated from equation B-2 below.

$$\%LOI = \frac{m_3 - m_4}{m_2} \cdot 100 \quad (B-2)$$

where m_1 , m_2 and m_3 has been explained above and

m_4 = weight of crucible and soil sample after glowing

The procedure for determining total C was conducted according to ISO10694 in air-dried soil passed through a 2.00mm aperture sieve.

The soil samples were oxidized to CO₂ at 940°C on a CuO in a flow of oxygen-containing gas free from CO₂. The released gases were scrubbed and the CO₂ present in the combustion gases were measured with a LECO carbon analyzer with an infrared (IR) detector. The total C was calculated from equation B-3 below

$$w_{C,t} = 1000 \cdot \frac{m_2}{m_1} \cdot 0,2727 \cdot \frac{100 + w_{H_2O}}{100} \quad (\text{B-3})$$

B-2: The results of the determination of dry content, loss on ignition and total carbon

Table B-1 Dry content, loss on ignition and total carbon

	Dry content (%)	LOI (%)	Total C (%)
1-3A	96.6	*	*
1-3B	97.8	*	*
1-3C	97.8	*	*
5-22A	98.5	*	*
5-22B	98.8	*	*
5-22C	99.1	*	*
9-42A	96.1	*	*
9-42B	97.4	*	*
9-42C	98.7	*	*
10-46A	94.5	*	*
10-46B	97.6	*	*
10-46C	98.8	*	*
1A	98.3	9.8	3.2
1B	97.9	13.4	2.5
2A	97.8	11.8	5.7
2C	99.1	8.4	5.0
3B1	98.9	9.2	8.0
3B2	98.5	8.3	7.5
4A	97.6	17.0	5.6
4B	98.6	12.2	3.3
5A	99.3	10.2	9.1
5B	99.3	7.6	8.6
6A	98.5	14.2	5.4
6B	98.6	12.6	5.1
Ap apple	99.2	15.0	5.0
Bp apple	99.5	13.0	4.4
1 sed up	98.0	33.5	5.0
2 sed down	99.8	8.8	2.8
3 sed down	98.4	14.7	2.9
4 sed down	99.4	13.2	5.1
5 sed down	99.8	5.7	6.8
6 sed field	99.9	3.4	6.1
tailing	99.9	2.8	1.4

*LOI and Total C has not been analysed

Appendix C: DMA-80

C-1: Technical specifications

Table C-1 Technical specifications

Instrument Optics	Single beam spectrophotometer with sequential flow through of measurement cells
Light Source	Low-pressure mercury vapor lamp
Detector	Silicon UV photodetector
Wavelength (nm)	253.65
Interference Filter (nm, nm bandwidth)	254, 9
Detection Limit (ng Hg)	0.005
Working Range (ng Hg) (with automatic switch-over)	Low range: 0–35 High range: 35–600
Reproducibility	< 1.5%
Carrier Gas	Oxygen
Input Pressure (bar)	4 bar
Flow Rate (mL min ⁻¹)	~ 165
Power (V)	110

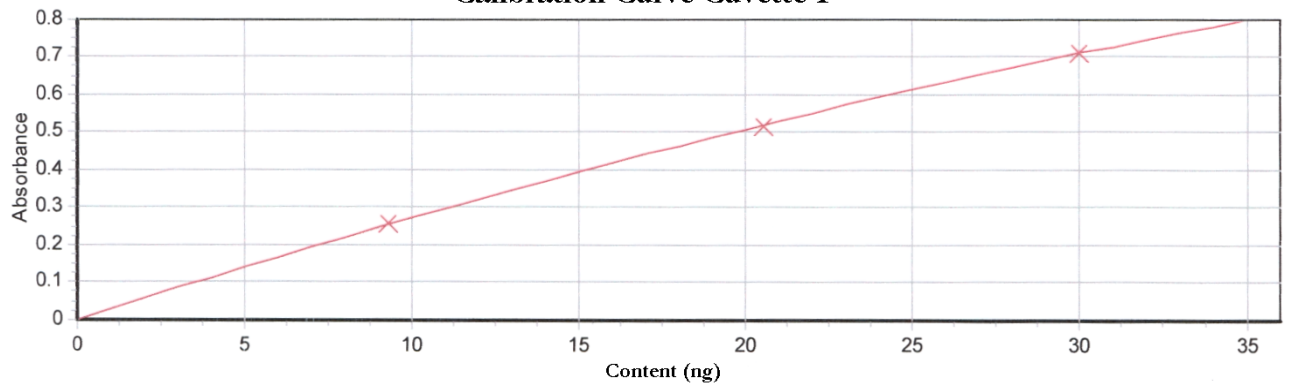
C-2: Analysis programme

Table C-2 Analysis programme

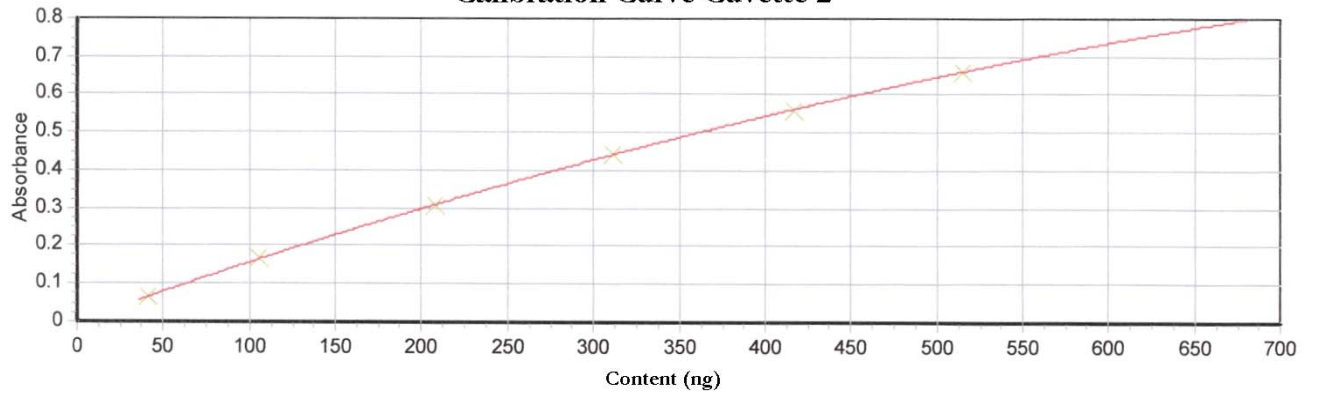
Drying temperature (°C)	300
Drying time (s)	60
Decomposition temperature (°C)	850
Decomposition time (s)	180
Waiting time (s)	60
Amalgamation time (s)	12
Recording time (s)	30

C-3: Calibration curves for DMA80

Calibration Curve Cuvette 1



Calibration Curve Cuvette 2



C-4 Results from DMA-80 analysis

Table C-3 Concentration of Hg in soil sampled in an elevation gradient up- and downstream for the slag heaps and tailing pond

	1A up	1B up	2A up	2C up	3B1 up	3B2 up	4A up	4B up	5A Hid	5B Hid	6A down	6B down
1.replicat ($\mu\text{g Hg kg}^{-1}$)	4791	3284	9963	385	12550	5991	52291	6385	5613	2155	11880	4582
2.replicat ($\mu\text{g Hg kg}^{-1}$)	4917	3254	10301	382	13300	5525	53753	6670	5693	2441	12542	4173
3.replicat ($\mu\text{g Hg kg}^{-1}$)	5333	3270	9735	385	13259	5641	54573	8260	5557	2114	11744	4391
Average ($\mu\text{g Hg kg}^{-1}$)	5014	3269	10000	384	13036	5719	53539	7105	5621	2236	12055	4382
St.dev ($\mu\text{g Hg kg}^{-1}$)	283	15	285	2	422	242	1156	1010	68	178	427	205
Rel st.dev (%)	6	0.5	3	0.4	3	4	2	14	1	8	4	5
Dry weight (DW)	0.98	0.98	0.98	0.99	0.99	0.98	0.98	0.99	0.99	0.99	0.98	0.99
Average ($\mu\text{g Hg kg}^{-1} \text{ DW}^{-1}$)	4928	3201	9781	381	12899	5631	52271	7005	5582	2221	11872	4322
Average ($\mu\text{g Hg g}^{-1} \text{ DW}^{-1}$)	4.9	3.2	9.8	0.4	12.9	5.6	52.3	7.0	5.6	2.2	11.9	4.3

Table C-4 Concentration of Hg in sediments sampled in Khaidarkan and Gauyang

	1 sed up	2 sed down	3 sed down	4 sed down	5 sed down	6 sed field
1.replicat ($\mu\text{g Hg kg}^{-1}$)	7701136	138956	3587.68	25881	242842	891
2.replicat ($\mu\text{g Hg kg}^{-1}$)	8310650	150130	3433.88	23452	190034	877
3.replicat ($\mu\text{g Hg kg}^{-1}$)	10905256	149974	3650.25	26055	220347	889
Average ($\mu\text{g Hg kg}^{-1}$)	8972347	146353	3557	25129	217741	886
St.dev ($\mu\text{g Hg kg}^{-1}$)	1701464	6406	111	1456	26500	7
Rel st.dev (%)	19	4	3	6	12	1
Dry weight (DW)	0.98	1.00	0.98	0.99	1.00	1.00
Average ($\mu\text{g Hg kg}^{-1} \text{ DW}^{-1}$)	8794686	145993	3499	24985	217353	885
Average ($\mu\text{g Hg g}^{-1} \text{ DW}^{-1}$)	8795	146	3	25	217	1

Table C-5 Concentration of Hg in the soil sampled at Gauyang monitoring site

	1-3A	1-3B	1-3C	5-22A	5-22B	5-22C	9-42A	9-42B	9-42C	10-46A	10-46B	10-46C
1.replicat ($\mu\text{g Hg kg}^{-1}$)	475	216	274	261	264	358	920	318	170	799	323	155
2.replicat ($\mu\text{g Hg kg}^{-1}$)	407	220	270	293	269	346	953	322	173	824	318	150
3.replicat ($\mu\text{g Hg kg}^{-1}$)	412	216	272	264	263	353	921	324	180	839	311	148
Average ($\mu\text{g Hg kg}^{-1}$)	431	217	272	273	265	353	931	321	174	821	318	151
St.dev ($\mu\text{g Hg kg}^{-1}$)	38	2	2	18	4	6	19	3	5	20	6	4
Rel st.dev (%)	9	1	1	7	1	2	2	1	3	2	2	2
Dry weight (DW)	0.966	0.9781	0.978	0.985	0.9879	0.991	0.961	0.9743	0.987	0.9455	0.97627	0.9876
Average ($\mu\text{g Hg kg}^{-1} \text{ DW}^{-1}$)	417	213	266	269	262	349	895	313	172	776	310	149
Average ($\mu\text{g Hg g}^{-1} \text{ DW}^{-1}$)	0.4	0.2	0.3	0.3	0.3	0.3	0.9	0.3	0.2	0.8	0.3	0.1

Table C-6 Concentration of Hg in a sample from the tailing pond and soil sampled in an apple garden in Khaidarkan

	Ap-apple	Bp-apple	tailing
1.replicat ($\mu\text{g Hg kg}^{-1}$)	99890	151246	277836
2.replicat ($\mu\text{g Hg kg}^{-1}$)	102028	150762	353044
3.replicat ($\mu\text{g Hg kg}^{-1}$)	84707	155990	392413
4.replicat ($\mu\text{g Hg kg}^{-1}$)			388724
Average ($\mu\text{g Hg kg}^{-1}$)	95542	152666	353004
St.dev ($\mu\text{g Hg kg}^{-1}$)	9444	2889	53164
Rel st.dev (%)	10 %	2 %	15 %
Dry weight (DW)	0.99	0.99	1.00
Average ($\mu\text{g Hg kg}^{-1} \text{ DW}^{-1}$)	94822	151830	352823
Average ($\mu\text{g Hg g}^{-1} \text{ DW}^{-1}$)	95	152	353

C-5 Comparison of measurements with and without cryogenic grinding

Table C-7 Measurement results for a sample homogenised with cryogenic grinding and the results for the same sample with homogenisation without the cooling step

	With cryogenic grinding	Without cryogenic grinding
1. replicate	13338	11775
2. replicate	19144	11799
3. replicate	19481	14399

Table C-8 Relative standard deviation from DMA-80 on soil and sediment samples with and without cryogenic grinding

Sample	Rel. st.dev without cryogenic grinding	Rel. st.dev with cryogenic grinding
1-3A	7 %	9 %
1-3B	3 %	1 %
1-3C	3 %	1 %
5-22A	13 %	7 %
5-22B	17 %	1 %
5-22C	26 %	2 %
9-42A	10 %	2 %
9-42B	13 %	1 %
9-42C	7 %	3 %
10-46A	10 %	2 %
10-46B	8 %	2 %
10-46C	13 %	2 %
1A up	17 %	6 %
1B up	14 %	0 %
2A up	18 %	3 %
2C up	2 %	0 %
3B1 up	6 %	3 %
3B2 up	6 %	4 %
4A up	25 %	2 %
4B up	10 %	14 %
5A Hid	17 %	1 %
5B Hid	11 %	8 %
6A down	42 %	4 %
6B down	8 %	5 %
1 sed up	*	19 %
2 sed down	53 %	4 %
3 sed down	23 %	3 %
4 sed down	7 %	6 %
5 sed down	40 %	12 %
6 sed field	26 %	2 %
Ap-apple	40 %	10 %
Bp-apple	33 %	2 %
tailing	57 %	15 %

* It was not possible to measure the sample without diluting it.

C-6 Procedure and equations for determining the Limit of detection (LOD) and method detection limit (MDL) for the DMA-80 method

The LOD was calculated with the following equation

$$LOD = 3 \cdot s_{blank} \quad (C-1)$$

where s_{blank} is the standard deviation of a blank solution measured n times ($n > 10$)

In this study the MDL was measured by dividing the LOD with the highest mass possible to analyse with the DMA-80 method (Equation C-2). In the application for the instrument it is not recommended to use masses higher than 0.5 g. In the calculations a mass of 0.2 g was used as this is more appropriate for the method.

$$MDL = \frac{LOD}{m_{highest}}$$

C-7 Results for the determination of LOD and MDL for the DMA-80 method

Table C-9 LOD and MDL for total analysis of Hg and sequential extraction procedure with DMA-80 analysis

	Total Hg analysis	Sequential extraction analysis
1. replicate (ng)	0.84	0.12
2. replicate (ng)	0.46	0.12
3. replicate (ng)	0.37	0.12
4. replicate (ng)	0.31	0.11
5. replicate (ng)	0.28	0.11
6. replicate (ng)	0.32	0.09
7. replicate (ng)	1.16	0.11
8. replicate (ng)	0.32	0.1
9. replicate (ng)	0.28	0.1
10. replicate (ng)	0.21	0.09
11. replicate (ng)	0.19	0.09
12. replicate (ng)	0.19	0.09
13. replicate (ng)	0.19	0.09
14. replicate (ng)	0.21	0.11
15. replicate (ng)	0.6	0.13
16. replicate (ng)	0.17	0.44
17. replicate (ng)	0.11	0.14
18. replicate (ng)	0.14	0.09
19. replicate (ng)	0.12	0.14
20. replicate (ng)	0.15	0.07
21. replicate (ng)	0.13	
22. replicate (ng)	0.15	
23. replicate (ng)	0.21	
24. replicate (ng)	0.16	
Mean (ng)	0.30	0.12
St.dev (ng)	0.25	0.08
LOD (ng)	0.74	0.23
Highest possible mass (g)	0.20	0.20
MLD (ng g ⁻¹)	3.72	1.15

C-8 Recovery for CRM's with DMA-80

Table C-10 Recovery of San Joaquin 2709 reference material measured on three different days

	Day 1	Day 2	Day 3
Certified value ($\mu\text{g kg}^{-1}$)	1561.37	1400	1505.76
1. replicate ($\mu\text{g kg}^{-1}$)	1535.58	1521.08	1529.68
2. replicate ($\mu\text{g kg}^{-1}$)	1680	1459.01	1512.39
3. replicate ($\mu\text{g kg}^{-1}$)	1404.56	1460.9	1502.04
4. replicate ($\mu\text{g kg}^{-1}$)	1355.88	1487.22	1441.55
5. replicate ($\mu\text{g kg}^{-1}$)	1557.79	1461.64	
6. replicate ($\mu\text{g kg}^{-1}$)		1463.25	
7. replicate ($\mu\text{g kg}^{-1}$)		1459.9	
8. replicate ($\mu\text{g kg}^{-1}$)		1274.08	
9. replicate ($\mu\text{g kg}^{-1}$)		1440.68	
10. replicate ($\mu\text{g kg}^{-1}$)		1479.38	
Average ($\mu\text{g kg}^{-1}$)	1515.86	1450.71	1498.28
St.dev ($\mu\text{g kg}^{-1}$)	117.59	65.78	33.44
Rel st. dev (%)	7.8	4.5	2.2
Recovery (%)	103.6	108.3	107.0

Table C-11 Recovery of three different certified reference materials measured during sequential extraction analysis

	San Joaquin	280R	277R
Certified value ($\mu\text{g kg}^{-1}$)	1400	1460	128
1. replicate ($\mu\text{g kg}^{-1}$)	1623.81	1520.93	147.6
2. replicate ($\mu\text{g kg}^{-1}$)	1758.3	1678.73	149.2
3. replicate ($\mu\text{g kg}^{-1}$)	1703.14	1697.08	140.01
4. replicate ($\mu\text{g kg}^{-1}$)	1655.05	1757.07	
5. replicate ($\mu\text{g kg}^{-1}$)	1639.07		
Average ($\mu\text{g kg}^{-1}$)	1675.87	1663.45	145.60
St.dev ($\mu\text{g kg}^{-1}$)	54.86	100.73	4.91
Rel st. dev (%)	3.3	6.1	3.4
Recovery (%)	119.7	113.9	113.8

C-9 Test of the purity of the graphite

Table C-12 Concentration of Hg in graphite. Units are given in $\mu\text{g kg}^{-1}$

	Graphite
1. replicate	1.42
2. replicate	1.27
3. replicate	0.77
4. replicate	2.01
5. replicate	1.08
6. replicate	1.13
Average	1.28
St.dev	0.42

Appendix D: ICP-AES

D-1: Results for soil samples

Table D-1 Heavy metal concentration in soil in an elevation gradient in Khaidarkan ($\mu\text{g g}^{-1}$)

	1A	1B	2A	2C	3B1	3B2	4A	4B	5A	5B	6A	6B
Ag	<1.0	<1.0	<1.0	<1.0	<1.0	<1.0	<1.0	<1.0	<1.0	<1.0	<1.0	<1.0
Al	23801	25604	21525	19163	13933	10757	19941	21374	8752	10215	20753	17710
As	29	21	21	14	27	13	58	24	19	20	39	33
Bi	6	4	6	5	<3.5	<3.5	5	6	<3.5	<3.5	<3.5	<3.5
Cd	1	1	1	0.3	1	0.4	1	1	0.4	0.4	1	1
Co	17	17	14	12	9	7	14	16	6	7	14	12
Cr	45	47	39	31	24	19	38	43	21	20	34	28
Cu	37	40	30	21	19	15	37	39	16	17	31	24
Fe	35499	35736	30694	23562	18756	15589	32373	35449	12971	15422	29084	24587
Hg^a	144	48	7	2	139	4	46	7	5	3	12	4
Mn	789	812	602	366	425	335	785	860	273	318	565	490
Mo	<0.5	<0.5	<0.5	<0.5	<0.5	<0.5	<0.5	<0.5	<0.5	1	<0.5	<0.5
Ni	48	50	39	31	26	21	40	43	17	20	40	35
Pb	29	32	24	12	19	13	27	21	12	11	25	18
Sb	89	37	65	4	180	74	324	144	31	20	143	82
Sc	5	5	4	4	3	2	5	5	2	2	4	4
Se	<1.5	<1.5	<1.5	<1.5	<1.5	<1.5	<1.5	<1.5	<1.5	<1.5	<1.5	<1.5
Sn	<2.5	<2.5	<2.5	<2.5	<2.5	<2.5	<2.5	<2.5	<2.5	<2.5	<2.5	<2.5
Sr	63	46	64	345	149	108	50	41	143	150	88	107
Te	<5	<5	<5	<5	<5	<5	<5	<5	<5	<5	<5	<5
Ti	557	543	488	501	354	253	462	493	283	307	391	330
V	53	56	47	46	35	27	47	50	24	28	44	38
W	6	<5	<5	<5	<5	<5	6	<5	<5	<5	<5	<5
Y	13	14	10	9	7	6	10	12	5	6	11	10
Zn	120	114	96	59	79	55	168	131	57	60	103	82
Zr	5	5	4	3	5	4	6	6	2	2	5	4

^aIn this thesis the Hg concentration analysed by the candidate was used

Table D-2 Concentration of main cations of the elevation gradient soil samples in Khaidarkan ($\mu\text{g g}^{-1}$)

	1A	1B	2A	2C	3B1	3B2	4A	4B	5A	5B	6A	6B
Ca	43476	22815	>50000	>50000	>50000	>50000	12814	7950	>50000	>50000	>50000	>50000
K	3881	3688	3898	3138	3275	2212	5669	5845	1859	1927	3473	2952
Mg	16687	13214	22785	13804	27339	22752	8622	8814	47046	50000	12370	8922
Na	166	161	159	237	149	115	140	145	160	149	169	142

D-2 Results for sediment samples

Table D-3 Heavy metal concentration in sediment samples from Khaidarkan ($\mu\text{g g}^{-1}$)

	1 sed. up	2 sed. down	3 sed. down	4 sed. down	5 sed. down	6 sed. field
Ag	1.3	1.4	1.0	1.0	1.0	1.0
Al	10870	14786	23601	15885	10302	3282
As	217	143	13	33	79	19
Bi	<3.5	<3.5	15	11	<3.5	<3.5
Cd	8	3	0.4	0.5	1	0.3
Co	6	4	26	14	5	5
Cr	18	24	149	77	15	5
Cu	43	24	44	28	14	6
Fe	7264	14557	36007	26050	11737	13808
Hg^a	6145	159	23	25	184	3
Mn	161	157	641	433	210	341
Mo	1	<0.5	<0.5	<0.5	<0.5	<0.5
Ni	24	14	193	84	14	8
Pb	67	244	14	35	74	8
Sb	2530	1049	22	73	188	3
Sc	2	2	7	4	2	1
Se	64	<1.5	<1.5	<1.5	<1.5	<1.5
Sn	<2.5	<2.5	<2.5	<2.5	<2.5	<2.5
Sr	382	119	116	148	178	118
Te	<5	<5	<5	<5	<5	<5
Ti	169	154	1383	1065	267	271
V	25	38	60	49	30	12
W	<5	<5	<5	<5	<5	<5
Y	6	7	9	7	5	6
Zn	302	256	81	79	87	40
Zr	14	11	5	6	9	2

^aIn this thesis the Hg concentration analysed by the candidate was used

Table D-4 Concentration of main cations in sediment samples from Khaidarkan ($\mu\text{g g}^{-1}$)

	1 sed. up	2 sed. down	3 sed. down	4 sed. down	5 sed. down	6 sed. field
Ca	>50000	>50000	>50000	>50000	>50000	>50000
K	2627	5150	3002	3003	2993	948
Mg	6078	11475	34890	39221	39856	50000
Na	173	999	167	189	362	106

D-3: Results for other solid samples

Table D-5 Heavy metal concentration in $\mu\text{g g}^{-1}$ in a sample from the mine tailing and in soil samples from a cultivated area

	tailing	Ap apple	Bp apple
Ag	3.8	1.0	1.0
Al	9696	17866	16321
As	347	97	116
Bi	<3.5	<3.5	<3.5
Cd	5	1	1
Co	4	6	6
Cr	39	30	21
Cu	35	26	20
Fe	15407	13948	13141
Hg^a	232	71	110
Mn	211	239	219
Mo	<0.5	<0.5	1
Ni	13	27	17
Pb	557	77	44
Sb	2172	465	479
Sc	2	3	3
Se	3	<1.5	<1.5
Sn	<2.5	<2.5	<2.5
Sr	100	171	197
Te	<5	<5	<5
Ti	21	242	199
V	30	44	44
W	12	<5	<5
Y	5	6	7
Zn	1096	109	85
Zr	9	12	12

^aIn this thesis the Hg concentration analysed by the candidate was used

Table D-6 Heavy metal concentration in $\mu\text{g g}^{-1}$ in a sample from the mine tailing and in soil samples from a cultivated area

	tailing	Ap apple	Bp apple
Ca	>50000	>50000	>50000
K	3207	5523	5298
Mg	797	22481	26352
Na	201	743	705

D-4: Results for water samples

Table D-7 ICP-AES analyses of water samples. Concentrations of metals given in $\mu\text{g L}^{-1}$ unless otherwise stated

	Drinking water	Site 1	1 downstream	2 downstream	3 downstream	Near factory	tailing	Slag heap
Ca 422.673 ^a	53	28	49	76	41	69	44	>
Cd 228.802	<d.l.	<d.l.	<d.l.	<d.l.	<d.l.	<d.l.	<d.l.	14
Co 228.615	<d.l.	<d.l.	<d.l.	<d.l.	<d.l.	<d.l.	<d.l.	<d.l.
Cr 267.716	<d.l.	<d.l.	<d.l.	<d.l.	<d.l.	<d.l.	<d.l.	<d.l.
Cu 324.754	9	6	11	10	9	11	10	341
Fe 238.204	210	<d.l.	> l.r.	> l.r.	> l.r.	145	100	> l.r.
K 766.491 ^a	2	1	2	2	1	1	2	4
Mg 285.213 ^a	48	10	23	55	17	20	19	16
Mn 257.610	<d.l.	<d.l.	36	30	16	8	26	174
Na 588.995 ^a	21	<d.l.	12	22	2	5	11	0
Na 589.592 ^a	20	3	13	21	5	9	12	4
Ni 216.555	<d.l.	<d.l.	<d.l.	<d.l.	<d.l.	<d.l.	<d.l.	<d.l.
Ni 231.604	<d.l.	<d.l.	<d.l.	<d.l.	<d.l.	<d.l.	<d.l.	<d.l.
Pb 283.305	<d.l.	<d.l.	<d.l.	<d.l.	<d.l.	<d.l.	<d.l.	<d.l.
Sb 217.582	<d.l.	<d.l.	> l.r.	<d.l.	<d.l.	<d.l.	> l.r.	> l.r.
V 292.401	<d.l.	<d.l.	<d.l.	<d.l.	<d.l.	<d.l.	<d.l.	<d.l.
V 309.310 ^b	208	100	173	305	145	246	155	639
Zn 213.857	<d.l.	<d.l.	<d.l.	<d.l.	<d.l.	12	<d.l.	466
Zn 202.548	<d.l.	<d.l.	<d.l.	<d.l.	<d.l.	9	<d.l.	538

^a Concentration in mg L^{-1}

^b Signal value is probably due to an interfering line. The vales has not been used in the study

<d.l. = below detection limit

> l.r. = above linear range

D-5: Preparation of calibration standards

In all the calculation the dilution formula in equation D-1 was applied:

$$C_1 \cdot V_1 = C_2 \cdot V_2 \quad (\text{D-1})$$

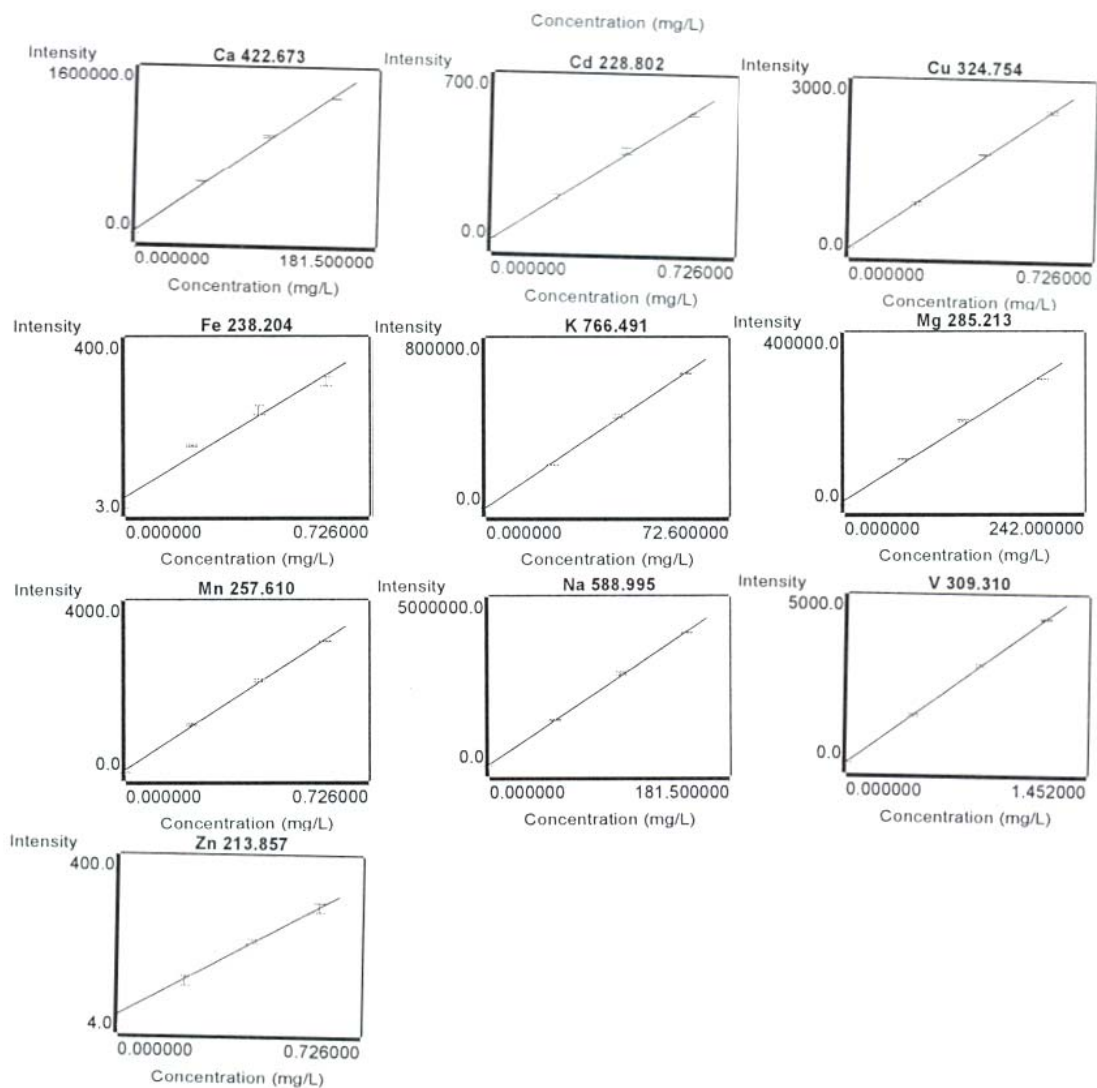
The standards were prepared from the following ICP stock solutions

- Multi-element stock solution 1: 50 $\mu\text{g mL}^{-1}$ As, Bi, Ga, Ge, In, Pb, Sb, Se, Sn, Te, Ti and V in 4.9 % (abs) HCl
- Multi-element stock solution 2: 100 $\mu\text{g mL}^{-1}$ Cd, Cr^{3+} , Co, Cu, Fe, Pb, Mn, Ni, V and Zn in 2.4 % (abs) HNO_3
- Single element stock solutions: 1000 $\mu\text{g mL}^{-1}$ Ca, Mg, Na and K in 2.5 % HNO_3

Table D-8 The amount of ICP standards and acids used to prepare calibration solutions for ICP-AES

Concentration (mg L^{-1})	MS1 (mL)	MS2 (mL)	Ca-std (mL)	Mg-std (mL)	Na-std (mL)	K-std (mL)	HCl (mL)	HNO_3 (mL)	Total volume (mL)
0	0	0	0	0	0	0	0.25	0.7	50
0.2 (As, Sb, Cd,Cu, Fe, Mn, Ni, Zn) 0.4 (Pb and V) 50 (Ca, Na) 60 (Mg) 20 (K)	0.2	0.1	2.5	3	2.5	1	0.48	0.25	50
0.4 (As, Sb, Cd,Cu, Fe, Mn, Ni, Zn) 0.8 (Pb and V) 100 (Ca, Na) 120 (Mg) 40 (K)	0.2	0.1	2.5	3	2.5	1	0.13	0.125	25
0.6 (As, Sb, Cd,Cu, Fe, Mn, Ni, Zn) 1.2 (Pb and V) 150 (Ca, Na) 200 (Mg) 60 (K)	0.3	0.2	3.75	5	3.75	1.5	0.13	0	25

D-6 Calibration curves for ICP-AES



Appendix E: Determination of total alkalinity

E-1: Procedure for determination of total alkalinity

The procedure for the measurement of total alkalinity was according to ISO 9936-1. The sample was titrated with standard acid solution (HCl) to fixed endpoint values of 8.3 and 4.5 (none of the samples had pH values above 8.3) using a 702 SM Titrino. The alkalinity was calculated with equation E-1 below

$$\text{Alkalinity} = \frac{c(\text{HCl}) \cdot V_2 \cdot 1000}{V_1} \quad (\text{E-1})$$

where $c(\text{HCl})$ = the actual concentration of HCl expressed in moles per litre

V_1 = volume (in mL) of the test portion

V_2 = volume (in mL) of HCl consumed to reach pH 4.5

E-2: Results for the determination of total alkalinity

Table E-1 Results for total alkalinity

Sample ID	pH	Alkalinity (mmol L ⁻¹)
Site 1	8.1	2.4*
1 downstream	7.7	2.0
Waste water KMP	8.2	1.6
tailing	7.7	2.3

*Site 1 was measured with a faster titration speed than the others. The alkalinity is probably too high. The value should be around 1.7. It was not measured again due to lack of sample.

Appendix F: IC

F-1 Preparation of calibration standards

In all the calculation the dilution formula in equation F-1 was applied:

$$C_1 \cdot V_1 = C_2 \cdot V_2 \quad (\text{F-1})$$

The calibration standards were prepared from Dionex Seven Anion Standard II (Dionex, Instrument Teknikk A.S, Oslo, Norway) To reference solutions were also prepared from the Multielement Ion Chromatography Anion Standard Solution (Fluka, Sigma-Aldrich, Buchs, Switzerland)

Table F-1 Concentration of reference standard solution and calibration standards for IC in mg L⁻¹

	Fluka Standard (original)	Fluka standard (DF=5)	Dionex standard solution	Standard solution 1	Standard solution 2	Standard solution 3	Standard solution 4
F ⁻	3	0.6	20	0.4	0.8	4	10
Cl ⁻	10	2	100	2	4	20	50
Br ⁻	20	4	100	2	4	20	50
NO ₃ ⁻	20	4	100	2	4	20	50
SO ₄ ²⁻	20	4	100	2	4	20	50
PO ₄ ³⁻	30	6	200	4	8	40	100
NO ₂ ⁻			100	2	4	20	50

F-2 Instrumental conditions

Table F-2 Instrumental conditions

Flow rate (mL min ⁻¹)	1.0
Current (mA)	80
Temperature of column (°C)	30
Temperature of detector (°C)	30
Sample injection	With auto-sampler AS40
Elution with:	32 μM KOH

F-3 Results

Table F-3 Results for anion determination with IC in mg L⁻¹

	F ⁻	Cl ⁻	NO ₂ ⁻	SO ₄ ²⁻	NO ₃ ⁻
Site 1	0.461645	6.744992	3.204681	41.20734	5.542542
1 downstream	0.676319	8.060083	3.63809	54.29827	8.234606
Waste water KMP	1.667169	5.874251	4.24585	56.6448	8.34686
tailing	4.81295	4.4408	3.199544	120.6929	9.640775

Appendix G: Statistics

G-1 General statistics

Mean (\bar{x}), standard deviation (SD) and relative standard deviation (RSD %) were calculated using the formulas in equation G-1, G-2 and G-3 respectively.

$$\bar{x} = \frac{\sum x_i}{n} \quad (\text{G-1})$$

$$SD = \sqrt{\frac{\sum (x_i - \bar{x})^2}{n-1}} \quad (\text{G-2})$$

$$RSD(\%) = \left(\frac{SD}{\bar{x}} \right) \cdot 100 \quad (\text{G-3})$$

where x_i = individual concentration

n = number of samples/replicates

G-2 Paired t-test for the comparison of methods

In order to compare to analytical methods paired t-test can be conducted. A t-value is calculated according to equation G-4. If $t > t_{20}$ at $P = 0.05$ the null hypothesis is discarded and the results are significantly different at $P = 0.05$.

$$t = \bar{d} \cdot \frac{\sqrt{n}}{s_d} \quad (\text{G-4})$$

Where \bar{d} and s_d are mean and standard deviation of the difference between the paired values, d.

The number of degrees of freedom is $n - 1$.

G-3 Accuracy test based on uncertainty used to compare recovery values with the certified value of the reference material used in the DMA-80 analysis

The following method compares the difference between the certified and measured values with its uncertainties. The uncertainties are combined and the expanded uncertainty is compared to the difference between the measured mean and the certified value of the CRM. This difference can be calculated as

$$\Delta_m = | c_m - c_{CRM} | \quad (G-5)$$

where Δ_m is the absolute difference between mean measured value and certified value

c_m is the mean measured value

c_{CRM} is the certified value

Each measurement has an uncertainty u_m . The CRM does also have an uncertainty u_{CRM} stated on the certificate. The uncertainties are often stated as standard deviations, but the variances (the squared standard deviations) are additive. The stated uncertainties can therefore be combined and is the uncertainty of Δ_m

$$u_{\Delta} = \sqrt{u_m^2 + u_{CRM}^2} \quad (G-6)$$

where u_{Δ} is the combined uncertainty of measured and certified value

u_m is the uncertainty of the measurement result

u_{CRM} is the uncertainty of the certified value

The following expanded uncertainty U_{Δ} , correspond to a confidence interval of 95 %

$$U_{\Delta} = 2 \cdot u_{\Delta} \quad (G-7)$$

If $\Delta_m \leq U_{\Delta}$, then there is no difference between the measurement result and the certified value.

G-4: Correlation matrixes

Table G-1 Correlation matrix for all soil and sediment sampled in Khaidarkan and their heavy metal levels and other soil parameters

	LOI (%)	Ctot (%)	pH	Al	As	Ba	Ca	Cd	Co	Cr	Cu	Fe	K	Mg	Mn	Na	Ni	P	Pb	Sb	V	Zn	CEC	Hg	
LOI (%)	1																								
Ctot (%)	-0.089	1																							
pH	-0.092	-0.148	1																						
Al	0.273	-0.508	0.141	1																					
As	0.131	-0.452	0.038	-0.308	1																				
Ba	0.86	-0.109	-0.077	-0.045	0.463	1																			
Ca	-0.158	0.282	0.052	-0.447	0.164	0.009	1																		
Cd	0.574	-0.299	0.018	-0.345	0.795	0.799	0.132	1																	
Co	0.216	-0.364	-0.182	0.807	-0.471	-0.191	-0.397	-0.36	1																
Cr	0.152	-0.431	-0.203	0.551	-0.159	-0.156	-0.088	-0.196	0.825	1															
Cu	0.585	-0.677	-0.104	0.685	0.256	0.39	-0.469	0.399	0.654	0.597	1														
Fe	0.037	-0.417	-0.048	0.851	-0.46	-0.341	-0.576	-0.441	0.914	0.613	0.606	1													
K	0.217	-0.479	0.359	0.593	0.149	0.188	-0.539	-0.057	0.179	0.096	0.446	0.331	1												
Mg	-0.199	0.571	-0.247	-0.228	-0.446	-0.29	0.358	-0.494	0.026	0.232	-0.484	-0.16	-0.361	1											
Mn	0.083	-0.286	-0.133	0.754	-0.504	-0.263	-0.723	-0.404	0.83	0.437	0.555	0.949	0.31	-0.194	1										
Na	-0.021	-0.259	0.602	-0.002	0.318	0.18	0.209	0.096	-0.4	-0.159	-0.147	-0.378	0.541	0.015	-0.482	1									
Ni	0.22	-0.326	-0.229	0.536	-0.283	-0.114	-0.062	-0.221	0.85	0.978	0.543	0.602	0.021	0.273	0.45	0.209	1								
P	0.2	0.172	-0.002	0.582	-0.558	-0.142	-0.526	-0.54	0.481	0.144	0.238	0.588	0.447	0.017	0.673	-0.18	0.184	1							
Pb	-0.273	-0.514	0.168	-0.246	0.876	0.005	0.137	0.499	-0.371	-0.048	0.166	-0.273	0.118	-0.396	-0.373	0.285	-0.217	-0.532	1						
Sb	0.391	-0.366	0.016	-0.418	0.927	0.686	0.149	0.96	-0.454	-0.166	0.337	-0.5	0.019	-0.494	-0.486	0.196	-0.267	-0.6	0.694	1					
V	0.208	-0.54	0.081	0.956	-0.265	-0.098	-0.4	-0.406	0.814	0.686	0.667	0.817	0.608	-0.052	0.678	0.072	-0.646	0.498	-0.179	-0.431	1				
Zn	-0.122	-0.513	-0.032	-0.203	0.892	0.122	0.032	0.596	-0.264	-0.007	0.322	-0.184	0.067	-0.493	-0.244	0.045	-0.167	-0.46	0.951	0.76	-0.163	1			
CEC	0.38	-0.122	0.106	0.625	-0.2	0.135	-0.497	-0.002	0.452	0.036	0.548	0.583	0.331	-0.489	0.676	-0.329	0.061	0.613	-0.232	-0.14	0.416	-0.092	1		
Hg	0.788	-0.036	-0.154	-0.213	0.456	0.914	0.103	0.874	-0.198	-0.147	0.338	-0.375	-0.139	-0.272	-0.301	-0.064	-0.097	-0.353	0.044	0.732	-0.28	0.187	0.092	1	

Table G-2 Correlation matrix for only soil sampled in Khaidarkan and heir heavy metal levels and other soil parameters

	LOI (%)	Ctot (%)	pH	Al	As	Ba	Ca	Cd	Co	Cr	Cu	Fe	K	Mg	Mn	Na	Ni	P	Pb	Sb	V	Zn	CEC	Hg	
LOI (%)	1																								
Ctot (%)	-0.466	1																							
pH	0.071	-0.019	1																						
Al	0.501	-0.903	0.137	1																					
As	0.586	-0.25	-0.094	0.064	1																				
Ba	0.627	-0.367	-0.052	0.225	0.952	1																			
Ca	-0.466	0.492	0.224	-0.483	0.059	-0.133	1																		
Cd	0.74	-0.476	0.254	0.496	0.639	0.714	-0.16	1																	
Co	0.286	-0.399	0.13	0.866	-0.361	-0.187	-0.623	0.254	1																
Cr	0.426	-0.786	0.032	0.925	-0.159	0.04	-0.651	0.343	0.934	1															
Cu	0.599	-0.794	-0.069	0.895	0.023	0.206	-0.748	0.508	0.886	0.955	1														
Fe	0.331	-0.69	0.086	0.86	-0.326	-0.153	-0.661	0.268	0.994	0.939	0.907	1													
K	0.723	-0.645	-0.122	0.572	0.649	0.785	-0.582	0.618	0.306	0.494	0.634	0.36	1												
Mg	-0.374	0.698	-0.173	-0.727	0.05	-0.043	0.508	-0.34	-0.706	-0.612	0.66	0.703	-0.361	1											
Mn	0.341	-0.617	-0.002	0.763	-0.323	-0.135	-0.778	0.278	0.952	0.9	0.908	0.968	0.31	-0.194	1										
Na	0.34	-0.215	-0.148	-0.01	0.901	0.849	0.248	0.39	-0.489	-0.232	-0.142	-0.477	0.541	0.015	-0.482	1									
Ni	0.389	-0.753	0.141	0.914	-0.251	-0.077	-0.578	0.381	0.977	0.961	0.924	0.971	0.021	0.273	0.45	0.209	1								
P	0.809	-0.18	0.055	0.344	0.237	0.342	-0.552	0.626	0.366	0.452	0.615	0.424	0.447	0.017	0.673	-0.18	0.442	1							
Pb	0.604	-0.414	-0.101	0.305	0.811	0.861	-0.006	0.654	-0.138	0.162	0.262	-0.119	0.118	-0.396	-0.373	0.285	0.041	0.35	1						
Sb	0.625	-0.206	-0.093	0.057	0.953	0.967	-0.079	0.67	-0.318	-0.118	0.083	-0.272	0.019	-0.494	-0.486	0.196	-0.216	0.38	0.805	1					
V	0.509	-0.931	0.058	0.973	0.207	0.378	-0.52	0.507	0.783	0.883	0.873	0.782	0.608	-0.052	0.678	0.072	0.827	0.306	0.401	0.199	1				
Zn	0.77	-0.609	-0.015	0.698	0.288	0.471	-0.771	0.674	0.656	0.752	0.888	0.705	0.067	-0.493	-0.244	0.045	0.703	0.831	0.396	0.409	0.72	1			
CEC	0.339	-0.401	0.073	0.608	-0.356	-0.253	-0.497	0.326	0.794	0.709	0.723	0.513	0.331	-0.489	0.676	-0.329	0.811	0.525	-0.133	-0.273	0.457	0.577	1		
Hg	0.48	-0.184	-0.163	-0.025	0.974	0.92	0.068	0.496	-0.437	-0.241	-0.074	-0.399	-0.139	-0.272	-0.301	-0.064	-0.358	0.105	0.731	0.929	0.14	0.192	-0.451	1	

Table G-3 Correlation matrix for only sediments sampled in Khaidarkan and heir heavy metal levels and other soil parameters

	LOI (%)	Ctot (%)	pH	Al	As	Ba	Cd	Co	Cr	Cu	Fe	K	Mg	Mn	Na	Ni	P	Pb	Sb	V	Zn	CEC	Hg	
LOI (%)	1																							
Ctot (%)	0.096	1																						
pH	-0.114	-0.332	1																					
Al	0.275	-0.42	0.145	1																				
As	0.082	-0.569	0.104	-0.255	1																			
Ba	0.91	0.109	-0.069	-0.068	0.365	1																		
Cd	0.621	-0.171	0.014	-0.531	0.739	0.856	1																	
Co	0.211	-0.197	-0.295	0.835	-0.511	-0.171	-0.494	1																
Cr	0.127	-0.392	-0.215	0.886	-0.347	-0.237	-0.515	0.971	1															
Cu	0.64	-0.603	-0.123	0.658	0.377	0.492	0.457	0.528	0.607	1														
Fe	-0.099	-0.315	-0.174	0.795	-0.498	-0.475	-0.673	0.932	0.954	0.37	1													
K	0.01	-0.538	0.797	0.514	0.294	-0.026	-0.116	-0.03	0.124	0.294	0.066	1												
Mg	-0.175	0.607	-0.3	0.475	-0.904	-0.458	-0.839	0.547	0.461	-0.366	0.551	-0.261	1											
Mn	-0.034	-0.07	-0.406	0.62	-0.642	-0.395	-0.605	0.933	0.881	0.257	0.934	-0.271	0.613	1										
Na	-0.163	-0.256	0.977	0.157	-0.095	-0.109	-0.078	-0.317	-0.234	-0.171	-0.198	0.839	-0.198	-0.443	1									
Ni	0.21	-0.245	-0.253	0.861	-0.476	-0.166	-0.488	0.998	0.979	0.557	0.93	0.024	0.52	0.914	-0.273	1								
P	0.111	0.185	-0.192	0.676	-0.837	-0.296	-0.679	0.865	0.774	0.134	0.842	-0.097	0.797	0.884	-0.2	0.841	1							
Pb	-0.366	-0.732	0.245	-0.16	0.866	-0.134	0.307	-0.417	-0.201	0.189	-0.238	0.416	-0.718	-0.46	0.243	-0.378	-0.704	1						
Sb	0.383	-0.348	0.034	-0.613	0.899	0.677	0.958	-0.577	-0.543	0.402	-0.673	-0.046	-0.934	-0.652	-0.052	-0.565	-0.811	0.564	1					
V	0.138	-0.389	0.073	0.972	-0.295	-0.224	-0.691	0.837	0.903	0.573	0.859	0.474	0.596	0.673	0.096	0.856	0.725	-0.131	-0.731	1				
Zn	-0.186	-0.704	-0.005	-0.185	0.925	0.043	0.467	-0.344	-0.149	0.345	-0.238	0.218	-0.764	-0.396	-0.024	-0.313	-0.703	0.952	0.696	-0.168	1			
CEC	0.788	-0.356	0.123	0.358	0.484	0.812	0.806	0.106	0.133	0.79	-0.154	0.357	-0.59	-0.221	0.105	0.146	-0.219	0.129	0.68	0.174	0.248	1		
Hg	0.891	0.138	-0.147	-0.133	0.371	0.995	0.864	-0.189	-0.261	0.466	-0.493	-0.116	-0.46	-0.388	0.19	-0.188	-0.316	-0.134	0.693	-0.281	0.062	0.774	1	

Appendix H: Water parameters measured in field

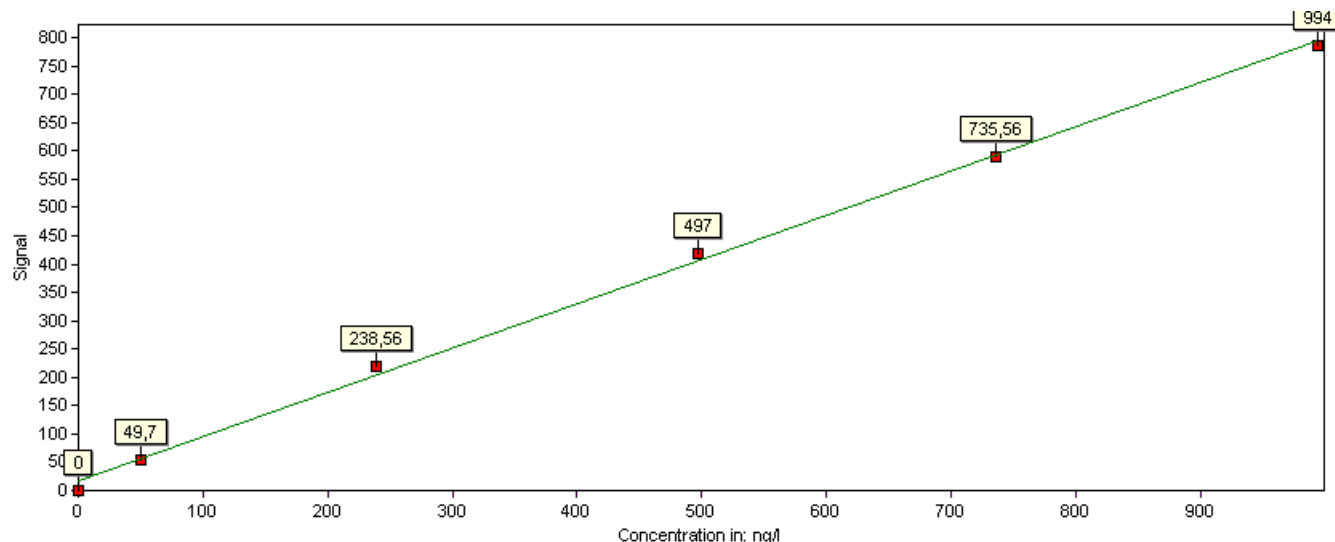
H-1: pH, temperature and conductivity

Table H-1 pH, temperature and conductivity measured in the field

	pH measured in field	Conductivity μS	Temperature $^{\circ}\text{C}$
Slag heap	8.96	568	24.2
1 downstream	8.77	338	18.5
2 downstream	9.1	443	24.4
3 downstream	8.85	771	21.7
Drinking water	8.44	702	19.5
Site 1	8.74	278	N/A
Waste water KMP	8.8	370	18.5
Tailing	8.2	460	19.4

Appendix I: PSA 10.035 Millennium Merlin 1631 Hg Analyser

I-1: Calibration curve



I-2 Preparation of calibration standards

In all the calculation the dilution formula in equation I-1 was applied:

$$C_1 \cdot V_1 = C_2 \cdot V_2 \quad (\text{I-1})$$

First a secondary Hg standard was prepared from the Spectrascan SS-1232 Mercury(II) stock solution $994 \pm 5 \mu\text{g mL}^{-1}$ in 5 % HNO_3 (Teknolab, Kungsbacka, Sweden). This was diluted 1000 times and matrix matched to 0.125 % HCl and 0.5 % bromate/bromide. The concentration of the secondary Hg standard was then $0.994 \mu\text{g L}^{-1}$.

A working Hg standard was prepared from the secondary Hg standard by diluting it 100 times and matrix matching it. The concentration of the working Hg standard was then $9.94 \mu\text{g L}^{-1}$. The calibration solutions were prepared from the working Hg standard according to table I-1 and the following procedure:

1. Add type I water (20-30 mL) followed by correct amount of HCl and KBr/ KBrO_3 .
2. Add correct amount of working Hg standard,

3. Fill up to the mark with type I water, cap the bottle and let stand to oxidize for approximately 30 minutes
4. Add correct amount of $\text{NH}_2\text{OH} \cdot \text{HCl}$ to eliminate excess bromine.

Table I-1 Concentration of calibration standards.

Std #	Hg Concentration (ng L ⁻¹)	Working Hg Std (mL)	HCl (mL)	KBr/KBrO ₃ (mL)	NH ₂ OH · HCl (μL)	Total volume (mL)
0	0	0	2.5	1	50	50
1	49.7	0.25	2.5	1	50	50
2	238.56	1.2	2.5	1	50	50
3	497	2.5	2.5	1	50	50
4	735.56	3.7	2.5	1	50	50
5	994	5	2.5	1	50	50

The same procedure was used to prepare the samples.

I-3: Results for analysis of water samples

Table I-2 Results

	Concentration of Hg in diluted sample (ng L ⁻¹)	Dilution factor	Concentration of Hg in sample (ng L ⁻¹)	Concentration of Hg in sample (μg L ⁻¹)
Site 1	-5.6	2	-11	-0.011
Drinking water	54.665848	2	109	0.109
1 downstream	45.553543	2	91	0.091
2 downstream	35.352455	2	71	0.071
3 downstream	8.003708	2	16	0.016
Waste water KMP	9.997687	2	20	0.020
Tailing	375.928009	2	752	0.752
Slag heap	667.9370725	10000	6679371	6679

I-4: Background Equivalent Concentration (BEC)

The background equivalent concentration is a test of the Millennium Merlin system. A 1 ppb Hg standard in 5 % HNO₃ is analysed with a 5 % HNO₃ blank with the mercury method set to the following condition:

Range: 100

Autozero: No

Mode: Emission.

The BEC is calculated from the following equation:

$$BEC(ppb) = \frac{Baseline_Value_without_reagents \cdot Std_concentration(ppb)}{Std_Peak_Height} \quad (I-1)$$

If BEC is between 0.05 – 0.5 ppb it is within the limits.

Table I-3 BEC test for the PSA 10.035 Millennium Merlin Hg Analyser

Concentration of standard (ppb)	Peak Height Standard	Baseline value without reagents	BEC (ppb)
1.00	767.64	110.10	0.14

I-5 Procedure and equations for determining the Limit of detection (LOD) and method detection limit (MDL) for the PSA method for determination of Hg in water

The LOD was calculated with the following equation

$$LOD = 3 \cdot s_{blank} \quad (C-1)$$

where s_{blank} is the standard deviation of a blank solution measured n times ($n > 10$)

Table I-3 Limit of detection (LOD)

	Concentration
Blank 1	-20.293465
Blank 2	-20.276617
Blank 3	-20.042084
Blank 4	-20.339609
Blank 5	-20.038269
Blank 6	-20.324217
Blank 7	-20.282995
Blank 8	-20.201105
Blank 9	-20.129002
Average	-20.21415144
Std. dev	0.117658682
LOD	0.352976045

I-6 Method

Table I-4 Method settings

Gain	100
Mode	Ratio
Measurement mode	Height
Baseline check type	Units
Baseline check value	5
Filter factor	32
Autozero	no
Valve flush	yes
Delay time (s)	15
Analysis time (s)	40
Memory time (s)	100

Appendix J: Principal component analysis

Appendix J-1: Eigenvalue matrix and PC for the Principal Component Analysis

Eigenvalue	7,9643	4,6133	2,5329	1,7840	1,0367	0,4459	0,3865	0,1176
Proportion	0,419	0,243	0,133	0,094	0,055	0,023	0,020	0,006
Cumulative	0,419	0,662	0,795	0,889	0,944	0,967	0,988	0,994

Eigenvalue	0,0522	0,0217	0,0152	0,0147	0,0061	0,0037	0,0019	0,0019
Proportion	0,003	0,001	0,001	0,001	0,000	0,000	0,000	0,000
Cumulative	0,996	0,998	0,998	0,999	1,000	1,000	1,000	1,000

Eigenvalue	0,0012	0,0003	0,0000
Proportion	0,000	0,000	0,000
Cumulative	1,000	1,000	1,000

Variable	PC1	PC2	PC3	PC4
LOI, %	0,009	0,209	0,525	-0,106
Ctot, %	-0,056	-0,377	0,247	-0,142
pH	-0,044	-0,066	-0,120	0,362
Al	0,306	0,146	-0,017	0,174
As	-0,266	0,278	-0,114	0,073
Cd	-0,227	0,309	0,226	0,029
Co	0,322	0,155	-0,006	-0,135
Cr	0,215	0,210	-0,166	-0,415
Cu	0,137	0,416	0,102	0,048
Fe	0,323	0,124	-0,079	0,143
Mn	0,311	0,093	0,036	0,225
Ni	0,232	0,175	-0,074	-0,444
P	0,248	-0,116	0,171	0,249
Pb	-0,213	0,226	-0,365	0,142
Sb	-0,258	0,309	0,086	0,039
V	0,301	0,152	-0,127	0,005
Zn	-0,194	0,286	-0,263	0,136
CEC	0,166	0,080	0,280	0,471
Hg	-0,160	0,224	0,447	-0,124

Appendix J-2 Loading plot of PC1 vs. PC3 for the PCA

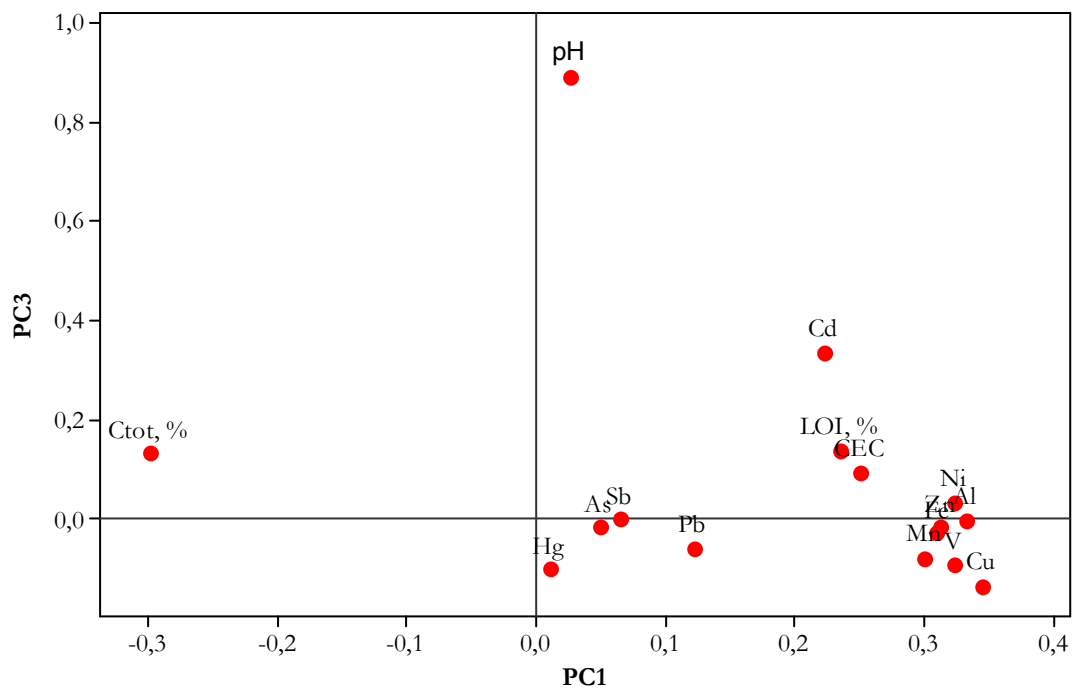


Figure J-1 Loading plot of PC1 vs. PC3 for the soil samples in Khaidarkan

Appendix K: Sequential extraction

Table K-1 Results for the sequential extraction. Results are given in $\mu\text{g kg}^{-1}$ unless otherwise stated.

	1A	2A	3B1	4A	5A	6A	tailing	2 sed down	4 sed down	5 sed down	Ap apple	Bp apple	Reference
Elementary Hg	369	<d.l.	<d.l.	<d.l.	<d.l.	126	<d.l.	19702	<d.l.	55597	<d.l.	<d.l.	<d.l.
% elementary Hg	7	<d.l.	<d.l.	<d.l.	<d.l.	0.8	<d.l.	7	<d.l.	10	<d.l.	<d.l.	<d.l.
Exchangeable Hg	<d.l.	<d.l.	<d.l.	<d.l.	17	387	53	<d.l.	21	<d.l.	102	<d.l.	1232
% exchangeable Hg	<d.l.	<d.l.	<d.l.	<d.l.	0.2	2	<d.l.	<d.l.	<d.l.	<d.l.	0.1	<d.l.	46
Strongly bound Hg	1612	998	1353	6949	39	2390	675	1218	297	565	117	3	309
% strongly bound Hg	32	8	10	14	0.3	15	0.2	0.4	0.7	0.1	0.1	<d.l.	12
Organically bound Hg	1	253	<d.l.	8	596	2	83	<d.l.	<d.l.	<d.l.	<d.l.	4522	<d.l.
% organically bound Hg	<d.l.	2	<d.l.	<d.l.	5	<d.l.	<d.l.	<d.l.	<d.l.	<d.l.	<d.l.	3	<d.l.
Residual Hg	3010	11543	12899	44529	10833	12902	329669	284192	42613	510393	190177	156713	1153
% residual Hg	60	90	91	86	94	82	100	93	99	90	100	97	43
Total Hg sum	4991	12794	14252	51486	11485	15807	330480	305112	42930	566555	190395	161239	2694

< d.l = below detection limit

Elementary and residual Hg were analysed by DMA-80. Exchangeable, strongly bound and organically bound Hg were analysed by PSA 10.035 Millennium Merlin 1631 Hg Analyser.

Table K-2 Total concentration of Hg measured with two months time span. Results are given in $\mu\text{g kg}^{-1}$.

	1A	2A	3B1	4A	5A	6A	tailing	2 sed down	4 sed down	5 sed down	Ap apple	Bp apple	Reference
Total Hg	4928	9781	12899	52271	5582	11872	352823	145993	24985	217353	94822	151830	1400
Total Hg (measured two months later)	5054	11328	14956	54385	6282	12661	456854	166132	30552	238474	122614	153459	1576
% increase in measured value	3 %	16 %	16 %	4 %	13 %	7 %	29 %	14 %	22 %	10 %	29 %	1 %	13 %

Appendix L: Soil parameters

Table L-1 Soil parameters of soil and sediment sampled in Khaidarkan

	pH	LOI (%)	C tot (%)	Fe (%)	CEC (cmol/kg)
1A up	7.72	9.8	3.2	3.5	14.54
1B up	7.59	13.4	2.5	3.6	16.77
2A up	7.67	11.8	5.7	3.1	16.94
2C up	7.90	8.4	5.0	2.4	3.86
3B1 up	7.84	9.2	8.0	1.9	11.40
3B2 up	7.55	8.3	7.5	1.6	9.96
4A up	7.80	17.0	5.6	3.2	14.27
4B up	7.36	12.2	3.3	3.5	15.55
5A Hid	7.62	10.2	9.1	1.3	6.09
5B Hid	7.39	7.6	8.6	1.5	8.51
6A down	7.56	14.2	5.4	2.9	14.99
6B down	8.07	12.6	5.1	2.5	15.39
Ap apple	7.64	15.0	5.0	1.4	6.90
Bp apple	7.50	13.0	4.4	1.3	4.21
1 sed. up	7.32	33.5	5.0	0.7	11.79
2 sed. down	9.38	8.8	2.8	1.5	5.69
3 sed. down	7.25	14.7	2.9	3.6	6.83
4 sed. down	7.29	13.2	5.1	2.6	1.32
5 sed. down	7.35	5.7	6.8	1.2	3.16
6 sed. field	7.23	3.4	6.1	1.4	-0.71
tailing	7.32	2.8	1.4	1.5	5.05

The soil parameters have been analysed at Alex Stuart Laboratory in Kara Balta, Kyrgyzstan.

Appendix M: Fraction diagram made with Medusa

$[\text{Hg}^{2+}]_{\text{TOT}} = 3.75 \text{ nM}$	$[\text{CO}_3^{2-}]_{\text{TOT}} = 2.30 \text{ mM}$
$[\text{Ca}^{2+}]_{\text{TOT}} = 1.10 \text{ mM}$	$[\text{SO}_4^{2-}]_{\text{TOT}} = 1.30 \text{ mM}$
$[\text{Mg}^{2+}]_{\text{TOT}} = 0.79 \text{ mM}$	$[\text{NO}_3^-]_{\text{TOT}} = 0.16 \text{ mM}$
$[\text{K}^+]_{\text{TOT}} = 70.00 \text{ }\mu\text{M}$	$[\text{F}^-]_{\text{TOT}} = 0.25 \text{ mM}$
$[\text{Na}^+]_{\text{TOT}} = 0.59 \text{ mM}$	$[\text{Cl}^-]_{\text{TOT}} = 0.13 \text{ mM}$

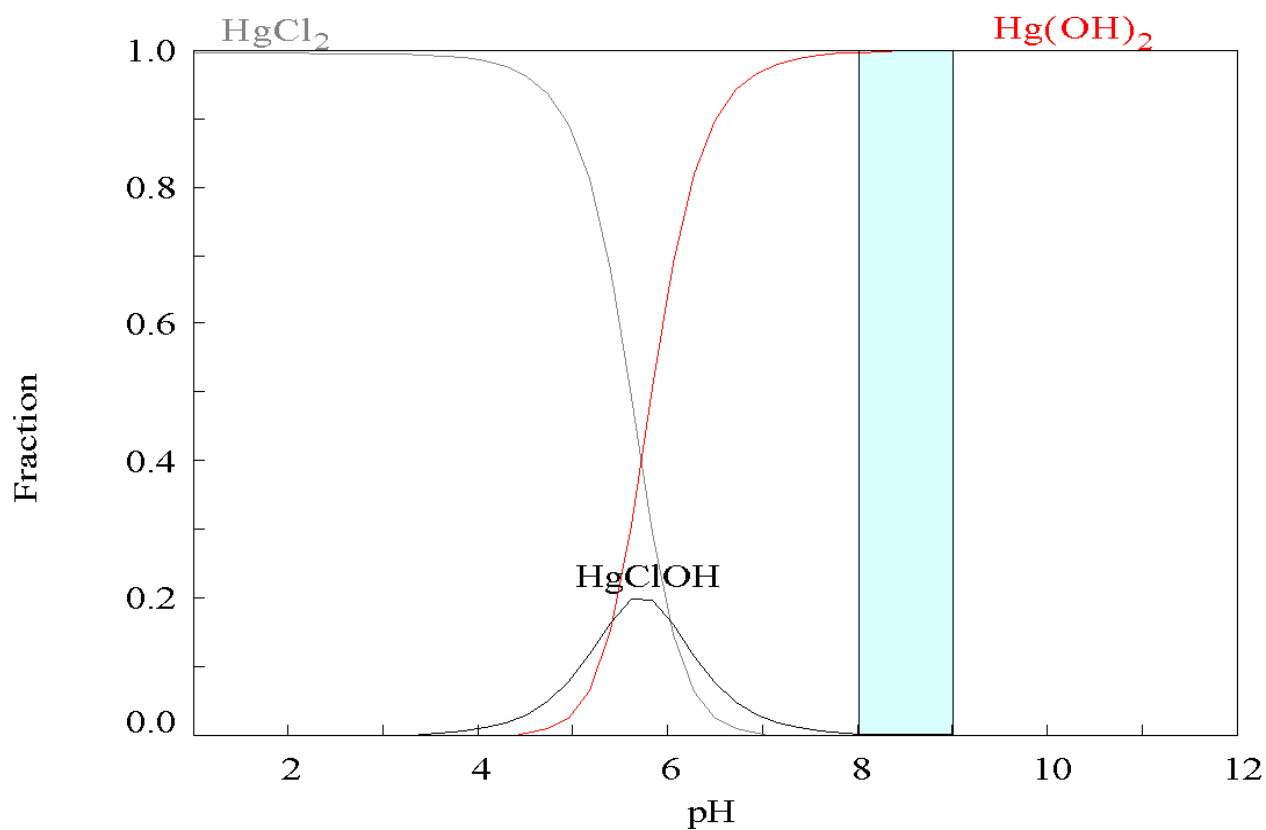


Figure M-1 Fraction diagram of the major Hg species as a function of pH. Conditions are given above. The fraction diagram was made with the speciation program Medusa

Appendix N: Reference values

N-1 Reference values for uncultivated soil and background levels for selected heavy metals and soil parameters

Table N-1 Reference values for uncultivated soil and background levels for selected metals and soil parameters. Values are given in $\mu\text{g g}^{-1}$ unless otherwise noted.

Parameter	Uncultivated soil average ^a	Average values in Kara Koi monitoring field	Range in Kara Koi monitoring field
pH		7.2	6.1 - 8.0
Ctot (%)		5.0	1.5 - 14.7
Dry matter (%)		2.6	0.3 - 6.6
LOI (%)		13.9	5.7 - 35.8
Ctotal (%)		4.8	1.5 - 13.8
Ca		24042.3	5659.3 - 50000
Mg		10890.6	7919 - 13300
Na		302.5	186.8 - 595.4
K		5342.2	1719 - 7519
Al	11000 - 65000	23029.5	8548 - 30220
Fe	4700 - 43000	34760.0	14080 - 49550
Mn	60 - 1100	733.5	289.5 - 1133.0
P		675.9	384.8 - 1140.0
Ba		180.9	58.1 - 255.4
Pb	2.6 - 25.0	22.2	8.0 - 46.7
Cd	0.10 - 0.13	0.7	0.3 - 1.4
Cu	8.7 - 33.0	40.6	14.6 - 90.3
Cr	11.0 - 78.0	48.9	19.0 - 64.3
As	6.7 - 13.0	18.1	9.6 - 27.1
Zn	25.0 - 67.0	113.5	49.1 - 182.0
Ni	4.4 - 23.0	47.8	13.4 - 83.5
Co	1.0 - 14.0	17.9	4.7 - 34.6
V	15 - 110	57.1	21.7 - 77.4
La		22.4	12.9 - 29.9
Be	0.8 - 1.3	1.3	0.3 - 3.0
Mo	0.2 - 5.0	0.8	0.5 - 1.439
Sc	2.1 - 13.0	4.7	1.6 - 6.9
Sr		72.2	31.3 - 228.7
Ti	2000 - 7000	890.8	369 - 1457
Y		12.0	5.2 - 18.3
Zr		2.9	0.6 - 4.736
Hg	0.045-0.160	< 0.5	< 0.5
Sb	2	< 2.5	< 2.5
Se	0.3-0.7	< 1.5	< 1.5
Sn	3.0-10,0	< 2.5	< 2.5
Ag		< 1.0	< 1.0

^a Values from Bradl (2005)

N-2: PEC values for selected heavy metals

Table N-2 PEC values for selected heavy metals

Element	PEC value ^a ($\mu\text{g g}^{-1}$)
Cd	4.98
As	33
Cu	149
Pb	128
Hg	1.06
Zn	459

^a PEC values obtained from MacDonald et al. (2000)

Appendix O: Certificates for Certified Reference Materials

O-1: Certificate of Analysis for Standard Reference Material 2709



National Institute of Standards & Technology

Certificate of Analysis

Standard Reference Material[®] 2709

San Joaquin Soil

Baseline Trace Element Concentrations

This Standard Reference Material (SRM) is intended primarily for use in the analysis of soils, sediments, or other materials of a similar matrix. SRM 2709 is an agricultural soil that was oven-dried, sieved, radiation sterilized, and blended to achieve a high degree of homogeneity. A unit of SRM 2709 consists of 50 g of the dried material.

The certified elements for SRM 2709 are given in Table 1. The values are based on measurements using one definitive method or two or more independent and reliable analytical methods. Noncertified values for a number of elements are given in Table 2 as additional information on the composition. The noncertified values should **NOT** be used for calibration or quality control. Analytical methods used for the characterization of this SRM are given in Table 3 along with analysts and cooperating laboratories. All values (except for carbon) are based on measurements using a sample weight of at least 250 mg. Carbon measurements are based on 100 mg samples.

NOTICE AND WARNINGS TO USERS

Expiration of Certification: This certification of SRM 2709 is valid, within the measurement uncertainties specified, until **31 December 2011**, provided the SRM is handled in accordance with instructions given in this certificate (see *Instructions for Use*). This certification is nullified if the SRM is damaged, contaminated, or otherwise modified.

Maintenance of SRM Certification: NIST will monitor this SRM over the period of its certification. If substantive technical changes occur that affect the certification before the expiration of this certificate, NIST will notify the purchaser. Return of the attached registration card will facilitate notification.

The overall direction and coordination of the analyses were under the chairmanship of M.S. Epstein and R.L. Watters, Jr. of the NIST Inorganic Analytical Research Division.

Statistical consultation was provided by S.B. Schiller of the NIST Statistical Engineering Division.

The technical and support aspects involved in the preparation, certification, and issuance of this SRM were coordinated through the NIST Standard Reference Materials Program by T.E. Gills and J.S. Kane. Revision of this certificate was coordinated through the NIST Standard Reference Materials Program by B.S. MacDonald of the NIST Measurement Services Division.

Willie E. May, Chief
Analytical Chemistry Division

Gaithersburg, MD 20899
Certificate Issue Date: 18 July 2003
See *Certificate Revision History* on Page 6

John Rumble, Jr., Chief
Measurement Services Division

INSTRUCTIONS FOR USE

Use: A minimum sample weight of 250 mg (dry weight - see *Instructions for Drying*) should be used for analytical determinations to be related to the certified values on this Certificate of Analysis.

To obtain the certified values, sample preparation procedures should be designed to effect complete dissolution. If volatile elements (i.e., mercury (Hg), arsenic (As), selenium (Se)) are to be determined, precautions should be taken in the dissolution of SRM 2709 to avoid volatilization losses.

Instructions for Drying: When nonvolatile elements are to be determined, samples should be dried for 2 h at 110 °C. Volatile elements (i.e., Hg, As, Se) should be determined on samples as received; separate samples should be dried as previously described, to obtain a correction factor for moisture. Correction for moisture is to be made to the data for volatile elements before comparing to the certified values. This procedure ensures that these elements are not lost during drying. The weight loss on drying has been found to be in the range of 1.8 % to 2.5 %.

PREPARATION AND ANALYSIS

Source and Preparation of Material: The U.S. Geological Survey (USGS), under contract to NIST, collected and processed the material for SRM 2709. The soil was collected from a plowed field, in the central California San Joaquin Valley, at Longitude 120° 15' and Latitude 36° 30'. The collection site is in the Panoche fan between the Panoche and Cantu creek beds. The top 7.5 to 13 cm (3 to 5 in) of soil containing sticks and plant debris was removed, and the soil was collected from the 13 cm level down to a depth of 46 cm (18 in) below the original surface. The material was shoveled into 0.114 m³ (30 gal) plastic buckets and shipped to the USGS laboratory for processing.

The material was spread on 30.5 cm × 61 cm (1 ft × 2 ft) polyethylene-lined drying trays in an air drying oven and dried for three days at room temperature. The material was then passed over a vibrating 2 mm screen to remove plant material, rocks, and large chunks of aggregated soil. Material remaining on the screen was deaggregated and rescreened. The combined material passing the screen was ground in a ball mill to pass a 74 µm screen and blended for 24 h. Twenty grab samples were taken and measured for the major oxides using X-ray fluorescence spectrometry and for several trace elements using inductively coupled plasma atomic emission analysis to provide preliminary assessment of the homogeneity of the material prior to bottling. The material was bottled into 50 g units and randomly selected bottles were taken for the final homogeneity testing.

Analysis: The homogeneity, using selected elements in the bottled material as indicators, was assessed using X-ray fluorescence spectrometry and neutron activation analysis. In a few cases, statistically significant differences were observed, and the variance due to material inhomogeneity is included in the overall uncertainties of the certified values. The estimated relative standard deviation for material inhomogeneity is less than 1 % for those elements for which homogeneity was assessed.

Certified Values and Uncertainties: The certified values are weighted means of results from two or more independent analytical methods, or the mean of results from a single definitive method, except for mercury. Mercury certification is based on cold vapor atomic absorption spectrometry used by two different laboratories employing different methods of sample preparation prior to measurement. The weights for the weighted means were computed according to the iterative procedure of Paule and Mandel [1]. The stated uncertainty includes allowances for measurement imprecision, material variability, and differences among analytical methods. Each uncertainty is the sum of the half-width of a 95 % prediction interval and includes an allowance for systematic error among the methods used. In the absence of systematic error, a 95 % prediction interval predicts where the true concentrations of 95 % of the samples of this SRM lie. The certified values were corroborated by analyses from nine Polish laboratories cooperating on the certification under the direction of T. Plebanski and J. Lipinski, Polish Committee for Standardization Measures and Quality Control. The Polish laboratory work was supported by the Maria Skłodowska-Curie Joint Fund.

Table 1. Certified Values

Element	Mass Fraction (%)	Element	Mass Fraction ($\mu\text{g/g}$)
Aluminum	7.50 \pm 0.06	Antimony	7.9 \pm 0.6
Calcium	1.89 \pm 0.05	Arsenic	17.7 \pm 0.8
Iron	3.50 \pm 0.11	Barium	968 \pm 40
Magnesium	1.51 \pm 0.05	Cadmium	0.38 \pm 0.01
Phosphorus	0.062 \pm 0.005	Chromium	130 \pm 4
Potassium	2.03 \pm 0.06	Cobalt	13.4 \pm 0.7
Silicon	29.66 \pm 0.23	Copper	34.6 \pm 0.7
Sodium	1.16 \pm 0.03	Lead	18.9 \pm 0.5
Sulfur	0.089 \pm 0.002	Manganese	538 \pm 17
Titanium	0.342 \pm 0.024	Mercury	1.40 \pm 0.08
		Nickel	88 \pm 5
		Selenium	1.57 \pm 0.08
		Silver	0.41 \pm 0.03
		Strontium	231 \pm 2
		Thallium	0.74 \pm 0.05
		Vanadium	112 \pm 5
		Zinc	106 \pm 3

Noncertified Values: Noncertified values, shown below, are provided for information only. An element concentration value may not be certified if a bias is suspected in one or more of the methods used for certification, or if two independent methods are not available.

Table 2. Noncertified Values

Element	Mass Fraction (%)	Element	Mass Fraction ($\mu\text{g/g}$)
Carbon	1.2	Cerium	42
		Cesium	5.3
		Dysprosium	3.5
		Europium	0.9
		Gallium	14
		Gold	0.3
		Hafnium	3.7
		Holmium	0.54
		Iodine	5
		Lanthanum	23
		Molybdenum	2.0
		Neodymium	19
		Rubidium	96
		Samarium	3.8
		Scandium	12
		Thorium	11
		Tungsten	2
		Uranium	3
		Ytterbium	1.6
		Yttrium	18
		Zirconium	160

Table 3. Analytical Methods Used for the Analysis of SRM 2709

Element	Certification Methods *	Element	Certification Methods *
Ag	ID ICPMS; RNAA	Mo	ID ICPMS
Al	XRF1; XRF2; INAA; DCP; ICP	Na	INAA; FAES; ICP
As	RNAA; HYD AAS; INAA	Nd	ICP
Au	INAA; FAAS	Ni	ID ICPMS; ETAAS; INAA
Ba	XRF2; FAES	P	DCP; COLOR; XRF2
C	COUL	Pb	ID TIMS
Ca	XRF1; XRF2; DCP	Rb	INAA
Cd	ID ICPMS; RNAA	S	ID TIMS
Ce	INAA; ICP	Sb	INAA; ETAAS
Co	INAA; ETAAS; ICP	Sc	INAA; ICP
Cr	INAA; DCP; ICP	Se	RNAA; HYD AAS
Cs	INAA	Si	XRF1; XRF2; GRAV
Cu	RNAA; FAES; ICP	Sm	INAA
Dy	INAA	Sr	ID TIMS; INAA; ICP
Eu	INAA	Th	ID TIMS; INAA; ICP
Fe	XRF1; XRF2; INAA; DCP	Ti	INAA; XRF1; XRF2; DCP
Ga	INAA; ICP	Tl	ID TIMS; LEAFS
Hf	INAA	U	ID TIMS; INAA
Hg	CVAAS	V	INAA; ICP
Ho	INAA	W	INAA
I	INAA	Y	ICP
K	XRF1; XRF2; FAES; ICP; INAA	Yb	INAA
La	INAA; ICP	Zn	ID TIMS; ICP; INAA; POLAR
Mg	INAA; XRF1; ICP	Zr	INAA
Mn	INAA; ICP		

*Methods in **bold** were used to corroborate certification methods or to provide information values.

COLOR	Colorimetry; lithium metaborate fusion.
COUL	Combustion coulometry.
CVAAS	Cold vapor atomic absorption spectrometry.
DCP	Direct current plasma atomic emission spectrometry; lithium metaborate fusion.
ETAAS	Electrothermal atomic absorption spectrometry; mixed acid digestion.
FAAS	Flame atomic absorption spectrometry; mixed acid digestion except for Au, leached with HBr-Br ₂ .
FAES	Flame atomic emission spectrometry; mixed acid digestion.
GRAV	Gravimetry; sodium carbonate fusion.
HYD AAS	Hydride generation atomic absorption spectrometry.
ICP	Inductively coupled plasma atomic emission spectrometry; mixed acid digestion.
ID ICPMS	Isotope dilution inductively coupled plasma mass spectrometry; mixed acid digestion.
ID TIMS	Isotope dilution thermal ionization mass spectrometry; mixed acid digestion.
INAA	Instrumental neutron activation analysis.
LEAFS	Laser enhanced atomic fluorescence spectrometry; mixed acid digestion.
POLAR	Polarography.
RNAA	Radiochemical neutron activation analysis; mixed acid digestion.
XRF1	Wavelength dispersive X-ray fluorescence on fused borate discs.
XRF2	Wavelength dispersive X-ray fluorescence spectrometry on pressed powder.

Participating NIST Analysts:

M. Adriaens	A. Marlow
E.S. Beary	J.R. Moody
C.A. Beck	P.J. Paulsen
D.S. Braverman	P. Pella
M.S. Epstein	T.A. Rush
J.D. Fassett	J.M. Smeller
K.M. Garrity	G.C. Turk
R.R. Greenberg	T.W. Vetter
W.R. Kelly	R.D. Vocke
R.M. Lindstrom	L.J. Wood
E.A. Mackey	R.L. Watters, Jr.

Participating Laboratories:

P. Briggs, D. Siems, J. Taggart, S. Wilson
U.S. Geological Survey
Branch of Geochemistry
Denver, CO, USA

J.B. Bodkin
College of Earth and Mineral Sciences
The Pennsylvania State University
University Park, PA, USA

S.E. Landsberger, V.G. Vermette
Department of Nuclear Engineering
University of Illinois
Urbana, IL, USA

J. Lipinski, T. Plebanski
Polish Committee for Standardization,
Measures and Quality Control
Warsaw, Poland

M. Bielawska, B. Galczynska,
J. Galczynska, K. Galczynski,
K. Wiacek
Institute of Soil Science and Plant
Cultivation
Pulawy, Poland

I. Matuszczyk
Forest Research Institute
Division in Katowice,
Warsaw, Poland

Z. Jonca
Institute of Environmental Protection
Warsaw, Poland

P. Bienkowski
Institute of Ecology
Dziekanow Lesny, Poland

H. Matusiewicz
Technical University
Poznan, Poland

B. Ksiazek
Geological Enterprise
Warsaw, Poland

G. Szoltyk
Forest Research Institute
Division in Sekocin,
Warsaw, Poland

J. Rojek
District Chemical Agricultural
Station
Bydgoszcz, Poland

E. Gorecka
Polish Geological Institute
Warsaw, Poland

REFERENCE

- [1] Paule, R.C.; Mandel, J.; *NBS Journal of Research*; Vol. 87, pp. 377-385 (1982).

Certificate Revision History: 18 July 2003 (The description of the SRM has been updated to include that this SRM was radiation sterilized, which was previously omitted); 18 January 2002 (This revision reflects a change in the certification expiration date); 23 August 1993 (Addendum added); 30 October 1992 (Original certificate date).

Users of this SRM should ensure that the certificate in their possession is current. This can be accomplished by contacting the SRM Program at: telephone (301) 975-6776; fax (301) 926-4751; e-mail srminfo@nist.gov; or via the Internet <http://www.nist.gov/srm>.

O-2: Certificate of analysis for Certified Reference Material BCR[®] – 280R



EUROPEAN COMMISSION
JOINT RESEARCH CENTRE
Institute for Reference Materials and Measurements



CERTIFIED REFERENCE MATERIAL BCR[®] – 280R

N^o. 38

CERTIFICATE OF ANALYSIS

LAKE SEDIMENT		
	Mass Fraction	
	Certified value ¹⁾ [mg/kg]	Uncertainty ²⁾ [mg/kg]
As	33.4	2.9
Cd	0.85	0.10
Co	16.8	0.9
Cr	126	7
Cu	53	6
Hg	1.46	0.20
Ni	69	5
Zn	224	25

1) Unweighted mean value of the means of accepted sets of data, each set being obtained in a different laboratory and/or with a different method of determination. The certified values are traceable to the SI.
2) Expanded uncertainty with a coverage factor $k = 2$ according to the Guide for the Expression of Uncertainty in Measurement, corresponding to a level of confidence of about 95 %.


This certificate is valid for one year after purchase.

Sales date: **10 MAR 2009**

The minimum amount of sample to be used is 300 mg.

Geel, July 2006
Latest Revision: May 2007

Signed: _____


Prof. Dr. Hendrik Emons
Unit for Reference Materials
EC-JRC-IRMM
Retieseweg 111
2440 Geel, Belgium



Registration No. 268-TEST
ISO Guide 34 for the
production of reference materials

All following pages are an integral part of the certificate.
Page 1 of 3

Indicative Values		
	Mass Fraction	
	Indicative value ¹⁾ [mg/kg]	Uncertainty ²⁾ [mg/kg]
Se	0.46	0.09
Sn	9.5	1.7

1) Unweighted mean value of the means of accepted sets of data, each set being obtained in a different laboratory and/or with a different method of determination. The indicative values are traceable to the SI, while it should be noted that the indicative value for Sn has been obtained using only ICP-MS methods.

2) Expanded uncertainty with a coverage factor $k = 4.30$ (Se) and $k = 3.18$ (Sn) according to the Guide for the Expression of Uncertainty in Measurement, corresponding to a level of confidence of about 95 %.

DESCRIPTION OF THE SAMPLE

The material consists of 30 g of powder, bottled in amber glass bottles, packaged under argon and closed with polyethylene inserts and plastic screw caps.

ANALYTICAL METHOD USED FOR CERTIFICATION

- Atomic fluorescence spectrometry (AFS)
- Cold vapour atomic absorption spectrometry (CVAAS)
- Differential pulse anodic stripping voltammetry (DPASV)
- Electrothermal atomic absorption spectrometry (ETAAS)
- Flame atomic absorption spectrometry (FAAS)
- Inductively coupled plasma atomic emission spectrometry (ICPAES)
- Inductively coupled plasma mass spectrometry (ICPMS)
- Inductively coupled plasma mass spectrometry using isotope dilution (ICPMS-ID)
- Instrumental neutron activation analysis (INAA)
- k_0 -neutron activation analysis (k_0 -NAA)
- Radiochemical neutron activation analysis (RNAA)
- Thermal ionisation mass spectrometry using isotope dilution (IDTIMS)

PARTICIPANTS

- Bundesanstalt für Materialforschung und -prüfung (BAM), Isotopenverdünnungsanalytik, Berlin (DE)
- Centre National de la Recherche Scientifique (CNRS), Service Central d'Analyse, Vernaison (FR)
- European Commission, DG JRC, Institute for Environment and Sustainability (EC-DG JRC-IES), Ispra (IT)
- European Commission, DG JRC, Institute for Reference Materials and Measurements (EC-DG JRC-IRMM), Geel (BE)
- Fraunhofer-Institut für Molekularbiologie und angewandte Ökologie, Schmallenberg (DE)
- Institut Jozef Stefan (IJS), Dept. Environmental Sciences, Ljubljana (SI)
- Laboratoire National d'Essais (LNE), Centre Metrologie et Instrumentation, Paris (FR)
- The Macaulay Institute (MLURI), Analytical Services, Aberdeen (GB)
- Nederlands Meetinstituut (NMI), Afdeling Chemie, Delft (NL)
- NRG Petten, Isotope Specific Analysis, Petten (NL)
- Umweltbundesamt (UBA), Wien (AT)
- University of Pavia, Nuclear Chemistry, Pavia (IT)
- University of Ghent, Laboratory of Analytical Chemistry, Ghent (BE)
- University of Plymouth, Plymouth (GB)
- Vlaamse Instelling voor Technologisch Onderzoek (VITO), Diagnostiek, Mol (BE)
- Wageningen Agricultural University (WEPAL), Wageningen (NL)

SAFETY INFORMATION

Not applicable.

INSTRUCTIONS FOR USE

The certified values refer to dry mass. A dry mass determination should always be carried out on separate subsamples.

The dry mass determination should be carried out by drying a sample of at least 1 g in a ventilated oven at 105 ± 2 °C for at least 3 hours, until constant weight is achieved. Samples should be cooled down in a desiccator.

Bottles should be thoroughly shaken before opening to rehomogenise the material.

The minimum amount of sample to be used is 300 mg.

The main purpose of the material is to assess method performance, i.e. for checking accuracy of analytical results. As any reference material, it can also be used for control charts or validation studies.

STORAGE

Samples can be stored at room temperature. Care should be taken to avoid moisture pick up once the bottles are opened.

However, the European Commission cannot be held responsible for changes that happen during storage of the material at the customer's premises, especially of opened samples.

LEGAL NOTICE

Neither IRMM, its subsidiaries, its contractors nor any person acting on their behalf.

(a) make any warranty or representation, express or implied that the use of any information, material, apparatus, method or process disclosed in this document does not infringe any privately owned intellectual property rights; or

(b) assume any liability with respect to, or for damages resulting from, the use of any information, material, apparatus, method or process disclosed in this document save for loss or damage arising solely and directly from the negligence of IRMM or any of its subsidiaries.

NOTE

A technical report on the production of BCR-280R is supplied on the internet (<http://www.irmm.jrc.be>). A paper copy can be obtained from IRMM on request.

O-3: Certificate of analysis for Certified Reference Material BCR[®] – 277R



EUROPEAN COMMISSION
JOINT RESEARCH CENTRE
Institute for Reference Materials and Measurements



CERTIFIED REFERENCE MATERIAL BCR[®] – 277R

N° . 92

CERTIFICATE OF ANALYSIS

ESTUARINE SEDIMENT		
	Mass Fraction	
	Certified value ¹⁾ [mg/kg]	Uncertainty ²⁾ [mg/kg]
As	18.3	1.8
Cd	0.61	0.07
Co	22.5	1.4
Cr	188	14
Cu	63	7
Hg	0.128	0.017
Ni	130	8
Zn	178	20

1) Unweighted mean value of the means of accepted sets of data, each set being obtained in a different laboratory and/or with a different method of determination. The certified values are traceable to the SI.
2) Expanded uncertainty with a coverage factor $k = 2$ according to the Guide for the Expression of Uncertainty in Measurement, corresponding to a level of confidence of about 95 %.

This certificate is valid for one year after purchase.

Sales date: 10 MAR 2009

The minimum amount of sample to be used is 300 mg.

Geel, July 2006
Latest Revision: May 2007

Signed: _____


Prof. Dr. Hendrik Emons
Unit for Reference Materials
EC-JRC-IRMM
Retieseweg 111
2440 Geel, Belgium



Registration No. 268-TEST
ISO Guide 34 for the
production of reference materials

All following pages are an integral part of the certificate.
Page 1 of 3

Indicative Values		
	Mass Fraction	
	Indicative value ¹⁾ [mg/kg]	Uncertainty ²⁾ [mg/kg]
Se	0.58	0.11
Sn	6.5	1.8

1) Unweighted mean value of the means of accepted sets of data, each set being obtained in a different laboratory and/or with a different method of determination. The indicative values are traceable to the SI, while it should be noted that the indicative value for Sn has been obtained using only ICP-MS methods.

2) Expanded uncertainty with a coverage factor $k = 3.18$ according to the Guide for the Expression of Uncertainty in Measurement, corresponding to a level of confidence of about 95 %.

DESCRIPTION OF THE SAMPLE

The material consists of 40 g of powder, bottled in amber glass bottles, packaged under argon and closed with polyethylene inserts and plastic screw caps.

ANALYTICAL METHOD USED FOR CERTIFICATION

- Atomic fluorescence spectrometry (AFS)
- Cold vapour atomic absorption spectrometry (CVAAS)
- Differential pulse anodic stripping voltammetry (DPASV)
- Electrothermal atomic absorption spectrometry (ETAAS)
- Flame atomic absorption spectrometry (FAAS)
- Inductively coupled plasma atomic emission spectrometry (ICPAES)
- Inductively coupled plasma mass spectrometry (ICPMS)
- Inductively coupled plasma mass spectrometry using isotope dilution (ICPMS-ID)
- Instrumental neutron activation analysis (INAA)
- k_0 -neutron activation analysis (k_0 -NAA)
- Radiochemical neutron activation analysis (RNAA)
- Thermal ionisation mass spectrometry using isotope dilution (IDTIMS)

PARTICIPANTS

- Bundesanstalt für Materialforschung und -prüfung (BAM), Isotopenverdünnungsanalytik, Berlin (DE)
- Centre National de la Recherche Scientifique (CNRS), Service Central d'Analyse, Vernaison (FR)
- European Commission, DG JRC, Institute for Environment and Sustainability (EC-DG JRC-IES), Ispra (IT)
- European Commission, DG JRC, Institute for Reference Materials and Measurements (EC-DG JRC-IRMM), Geel (BE)
- Fraunhofer-Institut für Molekularbiologie und angewandte Ökologie, Schmallenberg (DE)
- Institut Jozef Stefan (IJS), Dept. Environmental Sciences, Ljubljana (SI)
- Laboratoire National d'Essais (LNE), Centre Metrologie et Instrumentation, Paris (FR)
- The Macaulay Institute (MLURI), Analytical Services, Aberdeen (GB)
- Nederlands Meetinstituut (NMI), Afdeling Chemie, Delft (NL)
- NRG Petten, Isotope Specific Analysis, Petten (NL)
- Umweltbundesamt (UBA), Wien (AT)
- University of Pavia, Nuclear Chemistry, Pavia (IT)
- University of Ghent, Laboratory of Analytical Chemistry, Ghent (BE)
- University of Plymouth, Plymouth (GB)
- Vlaamse Instelling voor Technologisch Onderzoek (VITO), Diagnostiek, Mol (BE)
- Wageningen Agricultural University (WEPAL), Wageningen (NL)

SAFETY INFORMATION

Not applicable.

INSTRUCTIONS FOR USE

The certified values refer to dry mass. A dry mass determination should always be carried out on separate subsamples.

The dry mass determination should be carried out by drying a sample of at least 1 g in a ventilated oven at 105 ± 2 °C for at least 3 hours, until constant weight is achieved. Samples should be cooled down in a desiccator.

Bottles should be thoroughly shaken before opening to rehomogenise the material.

The minimum amount of sample to be used is 300 mg.

The main purpose of the material is to assess method performance, i.e. for checking accuracy of analytical results. As any reference material, it can also be used for control charts or validation studies.

STORAGE

Samples can be stored at room temperature. Care should be taken to avoid moisture pick up once the bottles are opened.

However, the European Commission cannot be held responsible for changes that happen during storage of the material at the customer's premises, especially of opened samples.

LEGAL NOTICE

Neither IRMM, its subsidiaries, its contractors nor any person acting on their behalf.

(a) make any warranty or representation, express or implied that the use of any information, material, apparatus, method or process disclosed in this document does not infringe any privately owned intellectual property rights; or

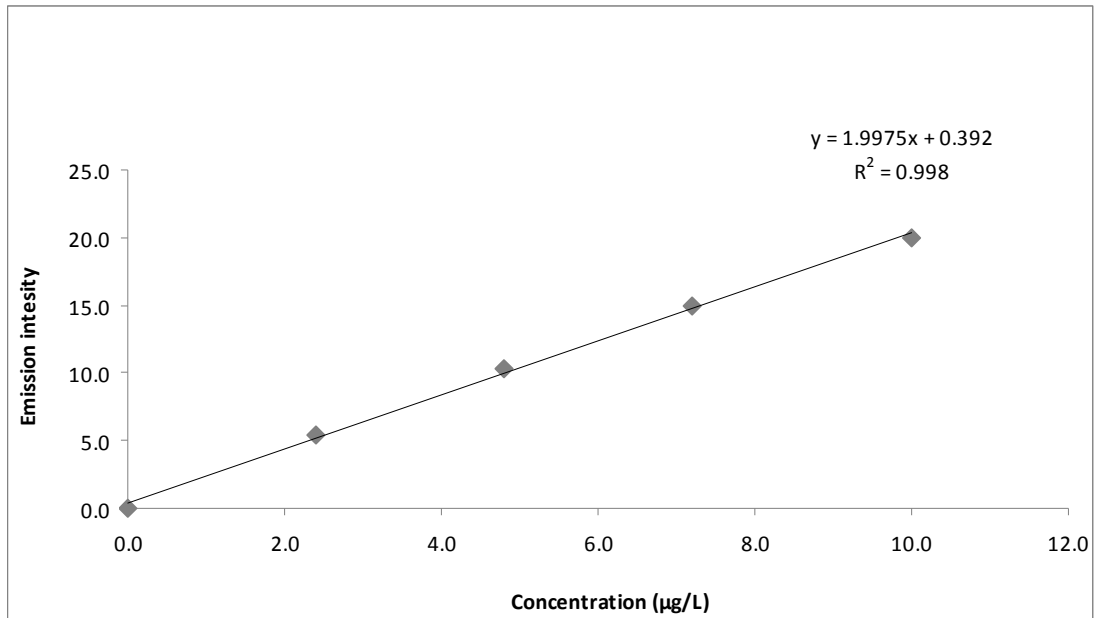
(b) assume any liability with respect to, or for damages resulting from, the use of any information, material, apparatus, method or process disclosed in this document save for loss or damage arising solely and directly from the negligence of IRMM or any of its subsidiaries.

NOTE

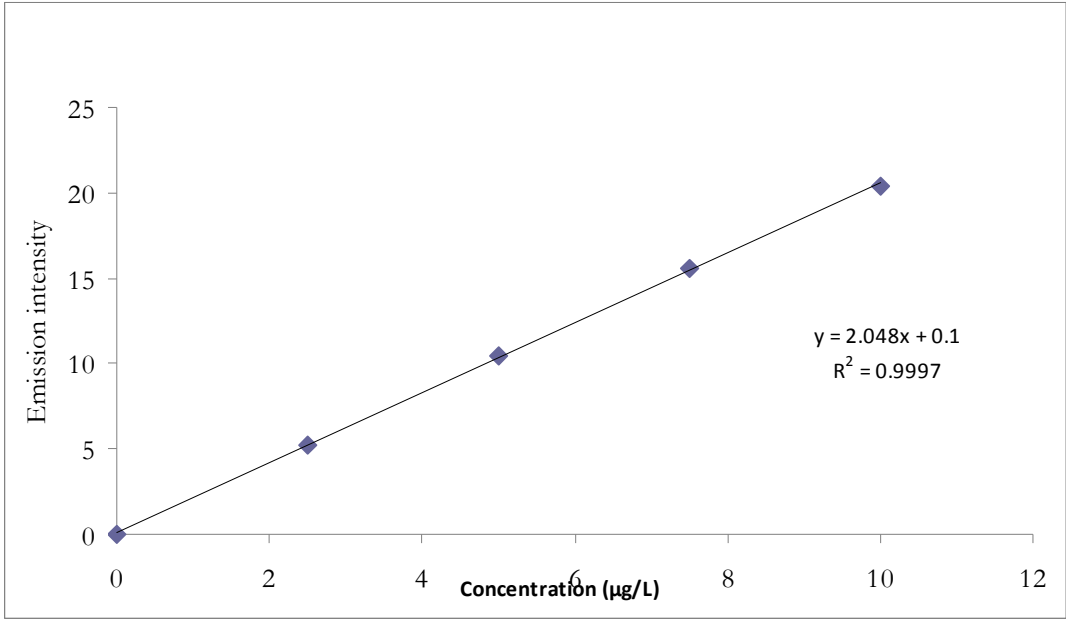
A technical report on the production of BCR-277R is supplied on the internet (<http://www.irmm.jrc.be>). A paper copy can be obtained from IRMM on request.

Appendix P: Flame photometric emission spectroscopy

P-1: Calibration curve for Na



P-2: Calibration curve for K



P-3: Result for Na and K

	K	Na
Site 1	0.8	1.1
1 downstream	3.4	3.1
2 downstream	2.6	4.8
3 downstream	1.0	0.7
Slag heap	6.1	2.2
Waste water from		
KMP	1.8	2.4
Tailing	2.5	2.7
Drinking water	2.5	4.7

Appendix Q: Soil colour

Q-1: Munsell soil colour

Table A-1 Munsell soil colour

Sample ID	Hue	Value	Chroma	Colour
1-3A	10 YR	3	2	very dark greyish brown
1-3B	10 YR	3	2	very dark greyish brown
1-3C	10 YR	6	3	pale brown
5-22A	10 YR	5	3	brown
5-22B	10 YR	6	3	pale brown
5-22C	10 YR	7	2	light gray
9-42A	7,5 YR	3	2	dark brown
9-42B	10 YR	5	4	yellowish brown
9-42C	10 YR	6	4	light yellowish brown
10-46A	10 YR	3	2	very dark greyish brown
10-46B	10 YR	4	3	brown/dark brown
10-46C	10 YR	6	4	light yellowish brown
1A up	10 YR	4	4	dark yellowish brown
1B up	10 YR	4	4	dark yellowish brown
2A up	10 YR	4	3	brown/dark brown
2C up	10 YR	5	4	yellowish brown
3B1 up	10 YR	4	3	dark yellowish brown
3B2 up	10 YR	3	3	dark brown
4A up	10 YR	3	3	dark brown
4B up	10 YR	4	3	dark greyish brown
5A Hid	10 YR	3	3	dark brown
5B Hid	2,5 Y	5	2	greyish brown
6A down	10 YR	3	3	dark brown
6B down	10 YR	4	4	dark yellowish brown
Ap-apple	2,5 Y	4	2	dark greyish brown
Bp-apple	10 YR	4	3	brown/dark brown
1 sed up	10 YR	4	2	dark greyish brown
2 sed down	2,5 Y	4	2	dark greyish brown
3 sed down	2,5 Y	5	2	greyish brown
4 sed down	2,5 Y	5	2	greyish brown
5 sed down	10 YR	6	2	light brownish gray
6 sed field	2,5 Y	5	2	greyish brown
tailing	10 YR	4	1	dark gray

